

University of Louisville

ThinkIR: The University of Louisville's Institutional Repository

Electronic Theses and Dissertations

12-2021

Characterizing the role of macrophages in cisplatin-induced kidney injury and progression to chronic kidney disease.

Sophia M. Sears
University of Louisville

Follow this and additional works at: <https://ir.library.louisville.edu/etd>



Part of the [Pharmacology Commons](#), and the [Toxicology Commons](#)

Recommended Citation

Sears, Sophia M., "Characterizing the role of macrophages in cisplatin-induced kidney injury and progression to chronic kidney disease." (2021). *Electronic Theses and Dissertations*. Paper 3744. Retrieved from <https://ir.library.louisville.edu/etd/3744>

This Doctoral Dissertation is brought to you for free and open access by ThinkIR: The University of Louisville's Institutional Repository. It has been accepted for inclusion in Electronic Theses and Dissertations by an authorized administrator of ThinkIR: The University of Louisville's Institutional Repository. This title appears here courtesy of the author, who has retained all other copyrights. For more information, please contact thinkir@louisville.edu.

CHARACTERIZING THE ROLE OF MACROPHAGES IN CISPLATIN-INDUCED
KIDNEY INJURY AND PROGRESSION TO CHRONIC KIDNEY DISEASE

By

Sophia M. Sears

B.A. Molecular Biology and Biochemistry, Goshen College, 2017

M.S. Pharmacology and Toxicology, University of Louisville, 2019

A Dissertation submitted to the faculty of the School of Medicine of the University
of Louisville in partial fulfillment of the requirements for the degree of

Doctor in Philosophy in Pharmacology and Toxicology

Department of Pharmacology and Toxicology

University of Louisville

Louisville, Kentucky

December 2021

CHARACTERIZING THE ROLE OF MACROPHAGES IN CISPLATIN-INDUCED
KIDNEY INJURY AND PROGRESSION TO CHRONIC KIDNEY DISEASE

By

Sophia M. Sears

B.A. Molecular Biology and Biochemistry, Goshen College, 2017

M.S., Pharmacology and Toxicology, University of Louisville, 2019

A Dissertation approved on

September 9, 2021

By the following Dissertation committee:

Leah Siskind, Ph.D.

Levi Beverly, Ph.D.

Geoff Clark, Ph.D.

Steven Jones, Ph.D.

Kavitha Yaddanapudi, Ph.D.

DEDICATION

This dissertation is dedicated to my husband and family who supported me as a developing scientist and always pushed me to be my best.

ACKNOWLEDGMENTS

I would like to thank my lab mates for helping me through this project. I would also like to thank Drs. Siskind and Beverly for guiding me in my research and providing valuable feedback.

ABSTRACT

CHARACTERIZING THE ROLE OF MACROPHAGES IN CISPLATIN-INDUCED KIDNEY INJURY AND PROGRESSION TO CHRONIC KIDNEY DISEASE

Sophia M. Sears

September 9, 2021

Cisplatin is a commonly used chemotherapeutic for treatment of many solid-organ cancers. Unfortunately, 30% of patients treated with cisplatin develop acute kidney injury (AKI), and even patients who do not develop AKI are at risk for long term declines in kidney function and development of chronic kidney disease (CKD). While traditional rodent toxicity studies have utilized a single, lethal dose of cisplatin, new models of cisplatin-induced kidney injury have revealed that repeated, low doses of cisplatin lead to development of kidney fibrosis. This model can be used to examine AKI-to-CKD transition processes.

C57BL/6 mice are one of the most used mouse strains in research; however, they are resistant to chronic kidney disease-associated pathologies. While repeated 7 mg/kg cisplatin doses induce kidney fibrosis in FVB/n mice, we found that treating C57BL/6 mice with this same dosing regimen does not result in kidney fibrosis. Here, we demonstrate that increasing the dose of cisplatin to 9 mg/kg is sufficient to consistently induce fibrosis in C57BL/6 mice. In addition, we present that cohorts of C57BL/6 mice purchased from Jackson one year apart and mice bred in house display variability in renal outcomes following repeated

low dose cisplatin treatment. This variability revealed CCL2 as a marker of cisplatin-induced kidney injury through correlation studies. In addition, significant myeloid cell infiltration was observed in the kidney after four doses of 9 mg/kg cisplatin, indicating macrophages are present during the AKI-to-CKD transition.

To further evaluate the role of macrophages in cisplatin-induced fibrosis, we used either C57BL/6 mice with *Ccr2* genetic knockout or liposome encapsulated clodronate (Clodrosome) to deplete macrophage populations during repeated, 9 mg/kg cisplatin treatments. We found that *Ccr2*^{-/-} mice had decreased levels of infiltrating macrophages in the kidney following cisplatin treatments. In contrast, Clodrosome treatment depleted resident and M2 macrophages in the kidney following cisplatin treatment. Furthermore, Clodrosome treatment decreased collagen deposition, myofibroblast accumulation, and inflammatory cytokine production, while *Ccr2* genetic knockout had no effect on these markers following cisplatin treatment. These data suggest that Clodrosome depletion of resident and M2 macrophages in the kidney attenuates development of renal fibrosis following repeated, low doses of cisplatin.

TABLE OF CONTENTS

DEDICATION	iii
ACKNOWLEDGMENTS.....	iv
ABSTRACT	v
LIST OF FIGURES	ix
CHAPTER 1: BACKGROUND & INTRODUCTION	1
CISPLATIN.....	1
ACUTE KIDNEY INJURY	3
CHRONIC KIDNEY DISEASE.....	6
MODELING CISPLATIN-INDUCED KIDNEY INJURY	11
Cell Death, Cell Cycle Arrest, and Senescence	13
ER Stress & Autophagy	19
Immune Response	21
Conclusion	26
OVERALL GOALS & SPECIFIC AIMS.....	28
CHAPTER 2: CHARACTERIZATION OF STRAIN DIFFERENCES AND IMMUNE CELL ACTIVITY DURING REPEATED LOW DOSE CISPLATIN TREATMENT.....	31
INTRODUCTION.....	31
MATERIALS & METHODS.....	33
RESULTS.....	37
DISCUSSION.....	60

CHAPTER 3: RESIDENT AND INFILTRATING MACROPHAGES HAVE	
DIFFERENT ROLES IN CISPLAINTN-INDUCED FIBROSIS	67
INTRODUCTION.....	67
MATERIALS & METHODS.....	69
RESULTS.....	76
DISCUSSION.....	104
CHAPTER 4: OVERALL DISCUSSION.....	108
SUMMARY	108
STRENGTHS & LIMITATIONS	110
FUTURE DIRECTIONS.....	112
REFERENCES	116
CURRICULUM VITAE	134

LIST OF FIGURES

Figure 1. Mechanisms of cisplatin-induced AKI following a single high dose (20-30 mg/kg) of cisplatin.....	15
Figure 2. Mechanisms of cisplatin-induced fibrosis following repeated low doses (7-9 mg/kg) cisplatin treatment	18
Figure 3. Immune cell involvement in cisplatin-induced AKI and renal fibrosis...	23
Figure 4. Kidney function and injury in FVB/n and C57BL/6 mice treated with repeated administration of cisplatin	39
Figure 5. Development of renal fibrosis with repeated administration of cisplatin in C57BL/6 and FVB/n mice.	41
Figure 6. Markers of cell stress and cell death with repeated administration of cisplatin in C57BL/6 and FVB/n mice	43
Figure 7. Weight loss, kidney function, and injury in C57BL/6 mice treated with repeated administration of 9 mg/kg cisplatin	46
Figure 8. Pathology scoring of tubular damage in C57BL/6 mice treated with repeated administration of 9 mg/kg cisplatin	48
Figure 9. Inflammatory cytokine production in C57BL/6 mice treated with repeated administration of 9 mg/kg cisplatin	50
Figure 10. Development of renal fibrosis with repeated administration of cisplatin in C57BL/6 mice	52
Figure 11. CCL2 expression in cisplatin-induced kidney injury.....	55

Figure 12. mRNA levels of other inflammatory cytokines measured do not correlate with markers of kidney injury	56
Figure 13. Gating strategy for flow cytometric analysis of renal macrophages and monocytes	58
Figure 14. Flow cytometric analysis of renal macrophages and monocytes	59
Figure 15. Hierarchical gating strategy for flow cytometry.	74
Figure 16. Macrophage infiltration correlates with kidney injury and fibrosis markers but not BUN following RLDC treatment	78
Figure 17. Resident macrophages correlate with kidney injury and fibrosis markers following RLDC treatment.....	79
Figure 18. <i>Ccr2</i> ^{-/-} blocks inflammatory monocyte and macrophage infiltration with no effect on resident or M2 macrophages.	81
Figure 19. Immune cell alterations in <i>Ccr2</i> ^{-/-} kidney.....	83
Figure 20. Immune cell alterations in <i>Ccr2</i> ^{-/-} blood	85
Figure 21. Clodrosome depletes renal resident and M2 macrophages with no effect on infiltrating macrophages.....	87
Figure 22. Immune cell depletion in the kidney following Clodrosome treatment	89
Figure 23. Immune cell depletion in the blood following Clodrosome treatment.	91
Figure 24. Clodrosome reduces inflammatory cytokine and chemokine induction following RLDC while <i>Ccr2</i> ^{-/-} has no effect	93
Figure 25. Clodrosome ameliorates RLDC induced renal fibrosis while <i>Ccr2</i> ^{-/-} has no effect.....	97

Figure 26. Clodrosome blunts RLDC induced fibrotic mRNA markers while *Ccr2*^{-/-} has no effect 99

Figure 27. Clodrosome reduces Kim-1 expression but neither Clodrosome or *Ccr2*^{-/-} altered BUN or NGAL. 102

CHAPTER 1: BACKGROUND & INTRODUCTION

CISPLATIN

Cisplatin (cis-diamminedichloridoplatinum(II)) is an inorganic platinum-based drug that was FDA approved as an anticancer agent in 1978 [1]. It is currently a standard therapy used to treat many solid-organ cancers [2]. The major mechanism of action of cisplatin involves binding DNA and forming adducts, leading to apoptosis or cell-cycle arrest. Unfortunately, the effectiveness of cisplatin is reduced by its dose-limiting nephrotoxicity. Approximately 30% of patients administered cisplatin develop acute kidney injury (AKI) [2]. There are no approved agents to treat AKI and thus its development requires treatment suspension.

To bypass this toxicity, several analogs of cisplatin such as carboplatin and oxaliplatin have been developed. Although these compounds are less nephrotoxic, they are much less effective in killing many types of cancer cells. One study demonstrated that the concentration of carboplatin had to be 20-40 fold higher than that of cisplatin to form the same amount of DNA adducts [3]. Due to its high level of activity, cisplatin is still commonly used in the clinic today.

Patients typically receive cisplatin as either a bolus intravenous injection or slow intravenous infusion [4]. As the kidney receives a large portion of blood flow, it encounters high levels of cisplatin. Cisplatin is filtered from the

blood into the kidney through both glomerular filtration and tubular secretion. As the blood is filtered by the kidney, active accumulation of cisplatin within renal parenchymal cells also occurs. Cisplatin concentrations eventually become greater in the kidney than in the blood [2].

Cisplatin is actively taken up by tubule cells. The high affinity copper transporter (Ctr1) and the organic cation transporter (OCT2) are both highly expressed on the basolateral side of proximal tubule cells and facilitate the uptake of cisplatin [5]. On the apical membrane, multidrug and toxin extrusion 1 (MATE1) is expressed and is capable of transporting cisplatin from tubule cells into the lumen for excretion [6].

Prior to transport, metabolism of cisplatin begins in circulation with glutathione conjugation, possibly by glutathione-S-transferase [2, 5]. These conjugates are then cleaved by gamma glutamyl transpeptidase (GGT) to form cysteinyl-glycine-conjugates [2]. Aminopeptidases further metabolize cisplatin by cleaving it into a cysteine conjugate. The cysteine conjugate is then transported into proximal tubule cells where it is converted to a highly reactive thiol by cysteine-S-conjugate-beta-lyase [2, 7].

As mentioned above, the primary mechanism of cisplatin's anti-cancer activity is thought to be through DNA damage. Several studies have further demonstrated that mitochondrial DNA is the major target of damage [2]. In aqueous environments, cisplatin exchanges its chloride ions for water molecules, forming a positively charged electrophile. This can lead to preferential accumulation in mitochondria as a result of the potential difference across the

mitochondrial membranes [2, 8]. Nevertheless, accumulation of reactive cisplatin metabolites in the cell leads to formation of DNA, RNA, and protein adducts [9]. These adducts contribute to nephrotoxicity via many of the same mechanisms by which cisplatin kills cancer cells.

The nephrotoxicity of cisplatin has been observed in patients since its introduction. Many strategies have been employed to try to prevent this toxicity from occurring. Hydration regimens and use of diuretics such as furosemide and mannitol have been explored. Clinically, however, these regimens do not seem to prevent cisplatin-induced kidney injury (CDDP-KI). Current clinical guidelines recommend pre-hydration with 0.9% saline and avoidance of diuretics [2]. Nevertheless, the nephrotoxicity associated with cisplatin remains a major obstacle in cancer treatment.

ACUTE KIDNEY INJURY

AKI is defined as a rapid decrease in renal function, leading to an increase in retained waste products [10]. Serial measurements of serum creatinine (SCr) and blood urea nitrogen (BUN) are commonly used to assess glomerular filtration rate (GFR) and provide an index of declining kidney function [11]. Clinical diagnosis of AKI is based on either a 0.3 mg/dl increase of serum creatinine within 48 hours or a doubling of serum creatinine from estimated baseline occurring within 7 days [12]. Development of more sensitive biomarkers of AKI such as neutrophil gelatinase-associated lipocalin (NGAL) and kidney injury marker 1 (Kim-1) is also an active area of research in nephrology [13-16].

AKI is one of the most common life-threatening conditions associated with hospital admissions. Since 2002, it has been estimated that 25% of patients admitted to the hospital develop AKI [17, 18]. The most common cause of intrinsic AKI is acute tubular necrosis caused by ischemic or nephrotoxic insults. Furthermore, nephrotoxic side effects of drugs cause around 20% of hospital and community acquired AKI cases [19]. One of the most common class of agents that induce nephrotoxic acute tubular necrosis is nephrotoxic chemotherapies, like cisplatin [20]. It is estimated that 60% of hospital-acquired AKI is caused by nephrotoxicity of chemotherapy [7], and development of AKI increases risk of mortality 5.5-6.5 fold compared to similarly ill patients who do not develop AKI [11]. AKI involves several pathophysiological processes including endothelial damage and vascular impairment, immune response, and tubular cell death [21]. These processes orchestrate AKI development in phases of initiation, extension, maintenance, and recovery [11].

In the initiation phase, the ischemic or nephrotoxic insult causes functional damage to tubule epithelial cells. Renal blood flow decreases as a result of injury, causing a decrease in available cellular ATP. This limited energy supply further damages epithelial and endothelial cells, triggering the release of cytokines and chemokines to initiate the inflammatory cascade [11]. Epithelial cells will also undergo morphological changes, leading to a loss of the brush border membrane and begin undergoing apoptosis or necrosis. After death, these cells often slough off and cause tubular obstruction [11].

The extension phase defines the subsequent continued hypoxia and inflammatory response. Hypoxia is exacerbated by damage to renal vascular endothelial cells [11]. Vascular damage is a major mediator of CDDP-KI. This damage is orchestrated in a variety of ways including alteration of renal blood flow and direct toxicity to endothelial cells [9]. Early vasoconstriction in response to cisplatin has been thought to be an initiator of vascular injury. Although the cause of vasoconstriction is not quite clear, it results in a decrease in GFR and promotes development of a hypoxic environment. Hypoxic conditions triggered in AKI cases further contribute to tubule cell death and renal inflammation. Vascular damage, tubule cell death, and inflammation are all connected and orchestrate the development of AKI. In the extension phase, inflammatory and profibrotic cells begin infiltrating the kidney and proliferating in response to the damage signals being released. Tubule cells continue to die in this phase, leading to a continued decline in GFR [11].

In the maintenance phase, repair processes begin. GFR halts its decline as tubule cells begin dedifferentiation, migration, and proliferation to re-establish structural integrity. Renal blood flow begins to return to normal. Cellular repair and reorganization begin the process of restoring organ function [11].

In the recovery phase, renal function recovers. Epithelial cells re-establish polarity and return to normal function. Inflammatory and profibrotic cells are cleared. The extent to which renal function returns can vary depending on several factors. It is also hypothesized that there may be chronic impairment of vasculature and sublethal changes in tubule epithelial cells making the kidney

more sensitive to additional insults [11]. Regardless of functional recovery, research suggests that a single AKI insult increases risk of chronic kidney disease (CKD) development [22-24].

CHRONIC KIDNEY DISEASE

CKD is defined as a gradual, progressive loss of kidney function. CKD is typically characterized on pathology by interstitial fibrosis, glomerulosclerosis, and chronic inflammation [25]. A diagnosis of CKD encompasses a diverse range of conditions with different causes, severity, and rates of progression. Typically, CKD is diagnosed when patients progress to a 75% reduction in GFR for over 3 months [26]. Since no treatment is available for CKD, patients must be put on dialysis. This can slow the progression of kidney disease, but patients will eventually progress to loss of kidney function (complete loss of function for more than 4 weeks) and then to end stage renal disease (complete loss of function for more than 3 months). Patients at this stage eventually require a renal transplant to survive [12].

CKD prevalence has been steadily increasing over the past 20 years [27]. As of 2017, CKD was estimated to affect 13.4% of people globally [28]. In the United States, there is estimated to be 400 new cases of CKD per million people per year [26]. This increasing prevalence is concerning due to the detrimental impact on patients as well as the high societal cost of CKD. Generally, CKD development is associated with advanced age, hypertension, diabetes, cardiovascular disease, and obesity [26]. Recent studies reveal that AKI also increases the likelihood of CKD development [22, 29].

Although the repair processes following AKI can restore function, in some cases, the kidney undergoes maladaptive repair, leading to development of fibrosis and chronic kidney disease (CKD) [25]. Maladaptive repair results when normal repair processes go awry, causing progressive renal damage. The primary features of maladaptive repair include cell cycle arrest, profibrotic cytokine production, myofibroblast accumulation, chronic immune cell activation, and chronic vascular impairment [25].

Maladaptive repair begins in the maintenance phase of AKI when tubule cells are beginning to respond to renal injury. In this stage, it has been demonstrated that surviving tubule cells are pushed into the cell cycle to proliferate and re-establish the proximal tubule structure [30]. This adaptive proliferation is necessary for healing, but in maladaptive repair, tubule cells can undergo G2/M cell-cycle arrest and senescence [25]. In this arrested state, tubule cells secrete profibrotic factors, such as transforming growth factor beta (TGF β) and connective tissue growth factor (CTGF), downstream of c-Jun N-terminal kinase (JNK) activation [21].

The profibrotic cytokines produced by senesced tubule cells may promote production of activated myofibroblasts [21]. In fact, a major hallmark of maladaptive repair is the appearance of activated myofibroblasts, which are the main contributors of collagen deposition and development of the fibrotic matrix [25]. Myofibroblasts display characteristics of both smooth muscle cells and fibroblasts. In normal wound healing their role is to deposit extracellular matrix (ECM) to maintain the integrity of injured tissue, allowing for proliferation and

healing. In maladaptive repair, myofibroblasts are chronically stimulated leading to overproduction of ECM [31].

Myofibroblasts may differentiate from several different precursors [31]. Although it is still a subject with much controversy, resident fibroblasts and pericytes are thought to be major contributors with mesenchymal stem cells and bone-marrow derived fibrocytes also playing a role [25]. The ECM laid down in renal fibrosis is primarily composed of type I and III collagen cross-linked by fibronectin, although there are likely additional components and not yet described post-translational modifications [32]. The structure and detailed composition of the ECM during the AKI to CKD transition is not well described and is a current knowledge gap in the field.

In addition to profibrotic cytokine production, injured tubule cells also release pro-inflammatory cytokines and chemokines through mechanisms including activation of toll-like receptor (TLR) signaling. TLRs are expressed on tubule epithelial cells. Exogenous and endogenous ligands associated with injury can activate the proinflammatory TLR response leading to production of tumor necrosis factor alpha (TNF α), C-C motif chemokine ligand 2 (CCL2), and interleukin 6 (IL-6) to recruit immune cells to the injured kidney [21]. Neutrophils, monocytes/macrophages, and lymphocytes are among the most responsive infiltrates to the kidney. These immune cells are important in the normal process of recovery to attenuate early injury as well as clear damaged debris; however, chronic immune cell activation can mediate effects of maladaptive repair, particularly through chronically activated macrophages [25].

Macrophages make up a large and diverse population of immune cells. They are a group of phagocytic cells that differentiate from monocytes upon environmental stimulation. In kidney injury, both renal resident and bone-marrow derived infiltrating macrophages respond to injury. Resident macrophages arise from embryonic macrophages that migrate to the kidney during development. These resident cells help maintain renal homeostasis by clearing cellular debris and aiding in tissue remodeling. Infiltrating macrophages are recruited to the kidney following injury. Both resident and infiltrating macrophages can adopt different phenotypes to perform a variety of functions [33]. The detailed nature of the different populations of macrophages active at different stages in the AKI to CKD transition models needs thorough investigation.

Functionally speaking, macrophages display a spectrum of subtypes. For simplicity, we will refer to the extreme ends of the spectrum as M1 and M2. M1 macrophages are thought to appear rapidly in the kidney following injury. These cells are generally considered “pro-inflammatory.” Macrophages are polarized to an M1 phenotype by pro-inflammatory cytokines and danger signals [34]. Upon polarization, they continue to produce proinflammatory cytokines to recruit other immune cells. They also produce reactive oxygen and nitrogen species to destroy pathogenic particles. This is done largely by inducible nitric oxide synthase (iNOS), which is a characteristic marker of M1 function [33]. M1 macrophages play a role in infection clearance, but they are also known to exacerbate acute renal injury [34].

M2 macrophages are thought to appear later in kidney injury and are thought of as having a “pro-repair” phenotype. There are several different subsets of M2 macrophages that differentiate in response to different environmental stimuli. TGF β is one of the major cytokines that drives M2 polarization. M2 macrophages are thought to suppress inflammation and promote tissue repair [34]. Arginase-1 (Arg-1) is characteristically expressed by M2 macrophages and is used to produce building blocks for the ECM. M2 macrophages also secrete TGF β creating a positive feedback signaling loop [33]. Although M1 macrophages may still be present in chronic injury, development of renal fibrosis is associated with an M1 to M2 phenotype transition [34].

The immune cell responses and wound healing processes observed after a renal insult suggests repairing tubule structure is the most immediate response to kidney injury. This repair can unfortunately hinder vascular healing. As mentioned earlier, vascular endothelial damage in AKI leads to renal hypoxia. In the extension phase of AKI, this endothelial injury and dysfunction leads to continued impairment of kidney oxygen delivery. Studies show repeated injury promoting tubule cell proliferation may impede the repair of endothelial cells [25]. Tubule proliferation is associated with high levels of TGF β and low levels of vascular endothelial growth factor (VEGF) in the kidney. Differentiation of pericytes into myofibroblasts triggered by damaged tubule cells also removes vital trophic support of endothelial cells. This suggests that tubular repair may inadvertently impair vasculature repair [25]. Repeated AKI insults and

maladaptive repair therefore also lead to chronically impaired vasculature, further promoting renal fibrosis.

All the above processes demonstrate how maladaptive repair can result from a chronic activation of injury responses. Endothelial damage promotes continued injury leading to tubule G2/M cell-cycle arrest, profibrogenic cytokine production, chronic immune cell activation, and activation of myofibroblasts. These processes promote chronic inflammation, fibrosis, and vascular rarefaction characteristic of CKD [25].

MODELING CISPLATIN-INDUCED KIDNEY INJURY

Cisplatin-induced AKI is commonly modeled in rodents via a single high dose (20-30 mg/kg) of cisplatin. Following treatment, renal function sharply declines, and animals must be euthanized within 3-4 days. This model mirrors the development of AKI in the clinic; however, it does not allow for long term studies of the effects of cisplatin-induced kidney injury (CDDP-KI) and represents only severe cases of AKI [1, 35].

70% of cisplatin-treated patients do not develop AKI by clinical criteria but may still be at risk for long-term renal impairment. Skinner et. al. followed pediatric patients treated with cisplatin that did not develop clinical AKI. Ten years following treatment, 11% had reduced GFR and 15% displayed symptoms of nephrotoxicity [36]. To model this, our lab [37-40] and others [41-46] developed an animal model to study CDDP-KI that involves repeated weekly low doses of cisplatin (7-9 mg/kg) for four weeks. A repeated low dose cisplatin

(RLDC) regimen allows for survival of mice up to 6 months following treatment without showing clinical signs of AKI. Mice develop renal fibrosis during the dosing window and have progressive loss of kidney function following cisplatin treatment [39].

Together, these models facilitate study of renal pathologies on either end of the CDDP-KI spectrum. The acute, high dose model is characterized by high levels of tubular apoptosis and necrosis, a rapid decline in GFR, and increases in BUN and SCr. On the other hand, the chronic, low dose model does not cause dramatic BUN or SCr changes. This model seems to cause subclinical injury that leads to development of fibrosis following the fourth dose. Fibrosis worsens as mice age to 6 months post treatment, accompanied by a chronic infiltration of macrophages. This phenotype is more indicative of CKD development [38].

CDDP-KI models that allow for AKI development and recovery using intermediate doses of cisplatin (10-15 mg/kg) are needed, but optimization is required so that animal survival is not an obstacle [41, 46]. The RLDC and high-dose models of CDDP-KI are well characterized and depict how different biological processes are triggered following acute or chronic cisplatin treatment. Common therapeutic targets of both cisplatin-induced AKI and fibrosis are needed, and potential drug candidates need testing in both models.

Targeting cell death, senescence, ER stress, autophagy, and immune cell activation has different effects on renal outcomes in the high-dose cisplatin model and models of renal fibrosis. As the RLDC model is fairly new, we examine results from studies of fibrosis following ischemia reperfusion (IR) and

unilateral ureteral obstruction (UUO) models. It is important to note that these models of fibrosis may differ from the RLDC model of fibrosis. A discussion of their key similarities and differences may be found elsewhere [47].

Cell Death, Cell Cycle Arrest, and Senescence

In the high-dose cisplatin model, AKI development depends on cell death [2, 5, 9]. Cisplatin induces necrosis as well as intrinsic-, extrinsic-, and endoplasmic reticulum (ER) stress-associated pathways of apoptosis [5, 9]. Intrinsic apoptosis is a key driver of AKI in the high-dose cisplatin model (Figure 1). Global Bcl-2-associated X protein (BAX) knockout confers resistance to cisplatin-induced AKI in mice by decreasing the number of apoptotic cells [48]. Additionally, inhibition and genetic deletion of tumor protein 53 (p53) attenuates cisplatin-induced AKI in mice, demonstrating that DNA damage is a major contributor to intrinsic apoptosis in acute cisplatin nephrotoxicity [49].

The RLDC model does not induce robust apoptotic or necrotic cell death [38], but other forms of cell death have not been examined. A variety of cell death pathways (for example, apoptosis, necrosis, necroptosis, ferroptosis, netosis, and mitophagy [50-53]) have been documented in other models of renal fibrosis and CKD, but the extent to which they drive fibrotic development is unclear. Proximal tubule specific knockout of pro-apoptotic Bcl-2 proteins Bax and Bak protects mice from apoptosis and renal fibrosis in the UUO model [54]. Proximal tubule specific p53 deletion reduces apoptosis and interstitial fibrosis following IR [55]; however, in the UUO model, global deletion of p53 attenuates apoptosis, but does not confer protection from fibrosis 20 days after injury [56]. Attenuation

of fibrosis with p53 inhibition has been observed at earlier timepoints following UUO, but protection was attributed to reduction of G2/M cell cycle arrest rather than apoptosis [57]. These results suggest that apoptosis plays complex and cell type specific roles in renal fibrosis. As with apoptosis, in depth studies of non-apoptotic forms of cell death in fibrosis development are greatly needed.

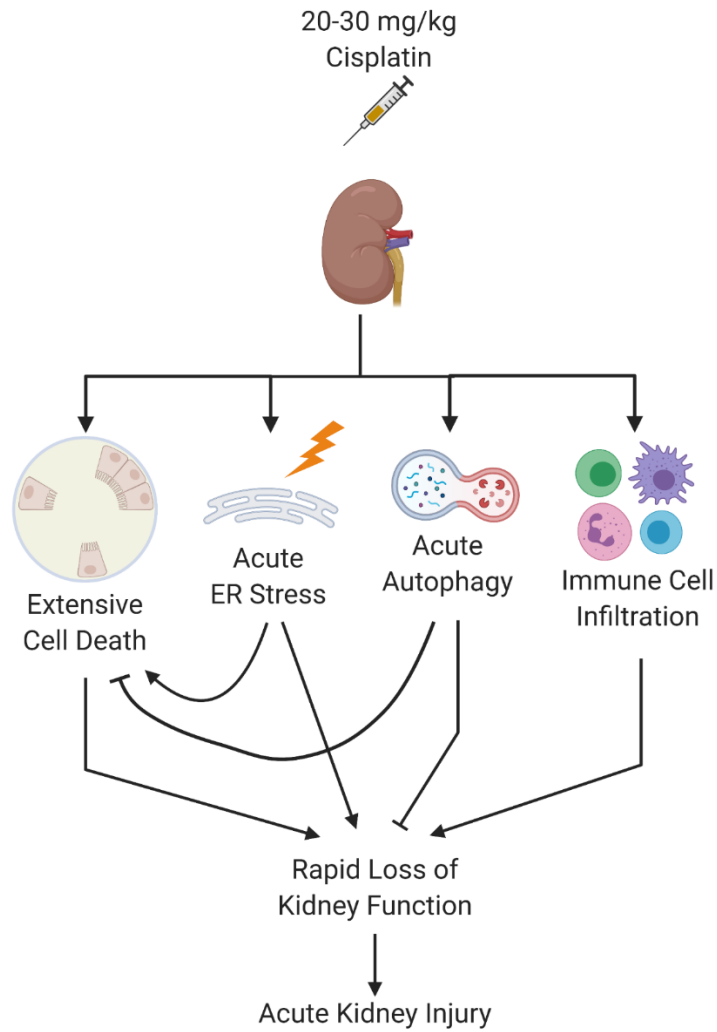


Figure 1. Mechanisms of cisplatin-induced AKI following a single high dose (20-30 mg/kg) of cisplatin. Pointed arrow heads denote promotion of process, solid block lines indicate inhibition of process.

A single high dose of cisplatin induces widespread cell death while RLDC causes very little cell death with surviving cells undergoing sublethal changes, like cell cycle arrest (Figure 2). This may be due to repeated insults to tubule epithelial cells. Administration of diphtheria toxin to transgenic mice expressing proximal tubule specific simian diphtheria toxin receptors directly injures proximal tubules [58]. A single dose of diphtheria toxin allows for replacement of lost tubule cells and recovery of kidney function. Repeated injury to tubules via multiple doses of diphtheria toxin induces either senescence or a prolonged dedifferentiated state of the proximal tubules, inducing maladaptive repair, fibrosis, and glomerulosclerosis [58]. This study suggests that fibrosis is driven by proximal tubule cells that survive injury rather than the loss of proximal tubule cells itself.

Cell cycle G2/M arrest contributes to fibrotic outcomes in renal models of injury. G2/M cell cycle arrest is associated with high levels of JNK signaling and secretion of profibrotic cytokines including TGF β . Pharmacologic inhibition of JNK reduces fibrosis following IR [59]. Data suggest that RLDC causes cell cycle arrest and senescence mediated by JNK signaling [38]. Cisplatin is known to induce JNK phosphorylation and activation [5]. In the high dose model of CDDP-KI, JNK activation promotes apoptosis and inflammation; inhibition of JNK reduces renal damage [60]. JNK activation also promotes G2/M cell cycle arrest when activated by TGF β . This alternative activation identifies JNK signaling as a balancing point between apoptosis and cell cycle arrest with environmental stimuli determining the outcome [61]. In RLDC, p-JNK and TGF β are increased,

accompanying elevated expression of cyclin dependent kinase inhibitor 2a (CDKN2A), a known marker of cellular senescence [38, 39]. Therefore, RLDC-induced fibrosis may be driven by tubule G2/M cell cycle arrest and/or senescence as they attempt repair renal damage. This needs more in-depth investigation.

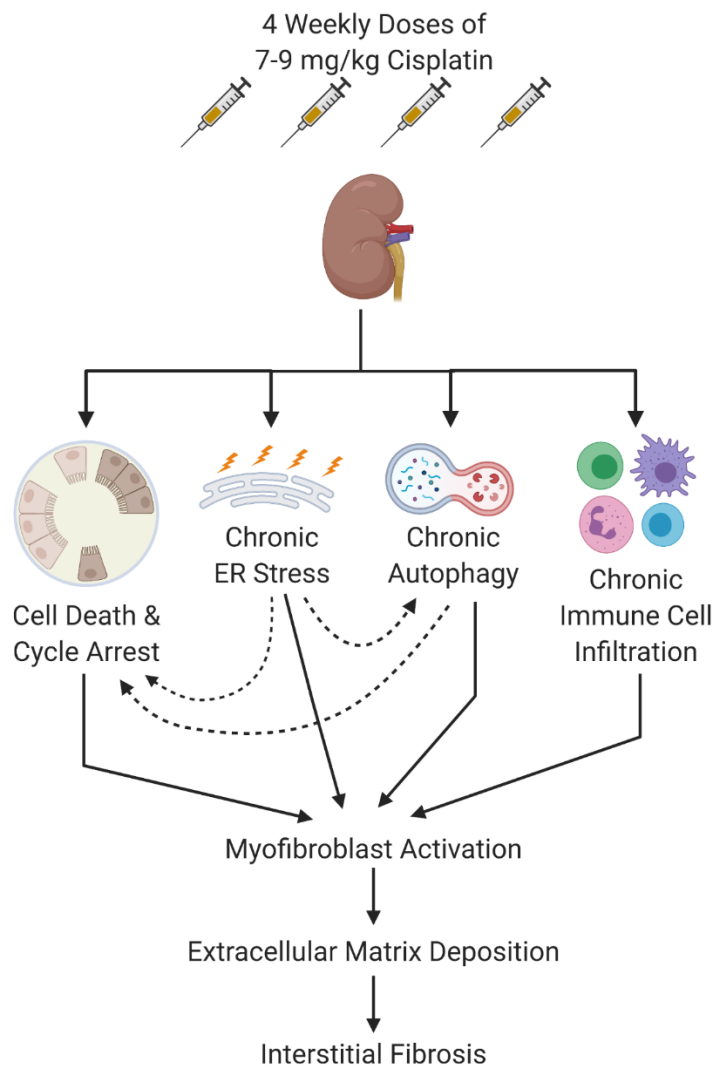


Figure 2. Mechanisms of cisplatin-induced fibrosis following repeated low doses (7-9 mg/kg) cisplatin treatment. Solid line arrows indicate relationships directly examined in the literature. Dotted line arrows represent relationships studied in other models of renal fibrosis that we propose may also be occurring in the RLDC model.

ER Stress & Autophagy

ER stress can lead to outcomes ranging from apoptosis to adaptation. ER stress responses depend on the extent of cellular damage and the insult duration. With acute insults, cells need to withstand stress only for a short period of time. Recovery depends on how quickly the cell can mount the unfolded protein response (UPR) and clear accumulated unfolded proteins. With chronic stress, the cell must undergo a functional change that is more permanent with prolonged UPR allowing cells to adapt and escape cell death [62]. The level and duration of ER stress determines if cells die or adapt and survive. One method of ER stress adaptation is autophagy [63] (discussed below).

ER stress is induced in models of AKI and fibrosis development and its pathologic effects are attributed to apoptotic and autophagic induction [64]. The role of ER stress is studied *in vivo* using many strategies, including pharmacologic intervention and CCAAT/enhancer binding proteins (C/EBP) homologous protein (CHOP) deficient mice. Although CHOP classically is studied as an inducer of proapoptotic genes, it also regulates pro-survival genes [65].

In the high dose cisplatin model, the α_2 adrenergic agonist dexmedetomidine attenuates ER stress via decreased CHOP expression [66], preventing apoptosis and AKI in rats. Similarly, the GPR120 activator TUG891 inhibits ER stress induction, blocks apoptosis, and protects from cisplatin-induced AKI [67]. Although these pharmacologic agents could act through alternative mechanisms, both studies attributed the protective effects to ameliorating ER stress, decreasing CHOP expression, and reducing apoptosis.

In models of renal fibrosis, the role of ER stress may be more complex. In the IR model of injury and fibrosis, both CHOP genetic knockout and pharmacologic inhibition of ER stress are protective, showing reductions in apoptosis, inflammation, and tubule autophagy [68, 69]. CHOP knockout mice have reduced expression of autophagy associated proteins and mitigated fibrosis following UUO as compared to wild type mice [70, 71]. The authors suggest that excessive autophagy can contribute to kidney injury via induction of apoptosis [70]. These studies demonstrate how the ER stress response can lead to both autophagy and apoptosis in kidney disease. These processes may function in opposition or coordination depending on the length and strength of stimuli. In the high-dose model of cisplatin, high levels of ER stress activation accompany apoptosis (Figure 1). In contrast, the RLDC model may lead to sustained, low levels of ER stress, leading to long term upregulation of autophagy that may be maladaptive (Figure 2).

Autophagy is a form of cellular “self-eating” that can be both protective and detrimental [72, 73]. Studies show that cisplatin-induced AKI is associated with induction of autophagy and data suggest that it is protective [9]. Autophagy can help reduce levels of cisplatin-induced apoptosis by ameliorating effects of cellular damage from oxidative stress and mitochondrial dysfunction [72]. In the high-dose cisplatin model, autophagy inhibition exacerbates kidney injury by increasing DNA damage, p53 activation, protein aggregation, and apoptosis [74, 75].

In models of fibrosis, the role of autophagy is still unclear. It has been argued that long-term upregulation of autophagy could actually contribute to renal damage [73]. In a model of IR, mice with specific deletion of autophagy related 5 (Atg5) in proximal tubule cells of the S3 segment have reduced interstitial fibrosis and cellular senescence 30 days after reperfusion. Interestingly, at 2 hours post-reperfusion, autophagy deficient mice have increased levels of cell death. This led to the hypothesis that fibrosis is being driven by proximal tubule cells that survive initial injury via increased autophagy and become senescent later [76].

Mice with distal tubule specific conditional knockout of autophagy related 7 (Atg7) have increased levels of TGF β and renal fibrosis following UUO [77]. In contrast to this study, mice with a proximal tubule specific conditional knockout of Atg7 have decreased levels of renal fibrosis following UUO [78]. Pharmacological inhibitors of autophagy (chloroquine and 3-methyladenine) also prevent UUO-induced fibrosis [78]. Interestingly, TGF β expression was not altered when autophagy was inhibited [78]. These studies indicate that the autophagy in renal fibrosis may play context and cell-type dependent roles [72]. The majority of evidence suggests that elevated autophagy can decrease cell death, providing protection from AKI (Figure 1) [74, 75], but under chronic stress these cells that escape death become sublethally injured and undergo senescence, contributing to fibrosis development (Figure 2) [76, 79, 80].

Immune Response

Renal immune cell infiltration and activation may differ in high dose cisplatin and RLDC models (Figure 3). Inflammation is a major mediator of AKI in the high dose cisplatin model. Inflammation and renal fibrosis are also known to be closely linked [81]. Cisplatin treatment induces upregulation of many different proinflammatory cytokines and chemokines, including TNF α [5, 9, 40].

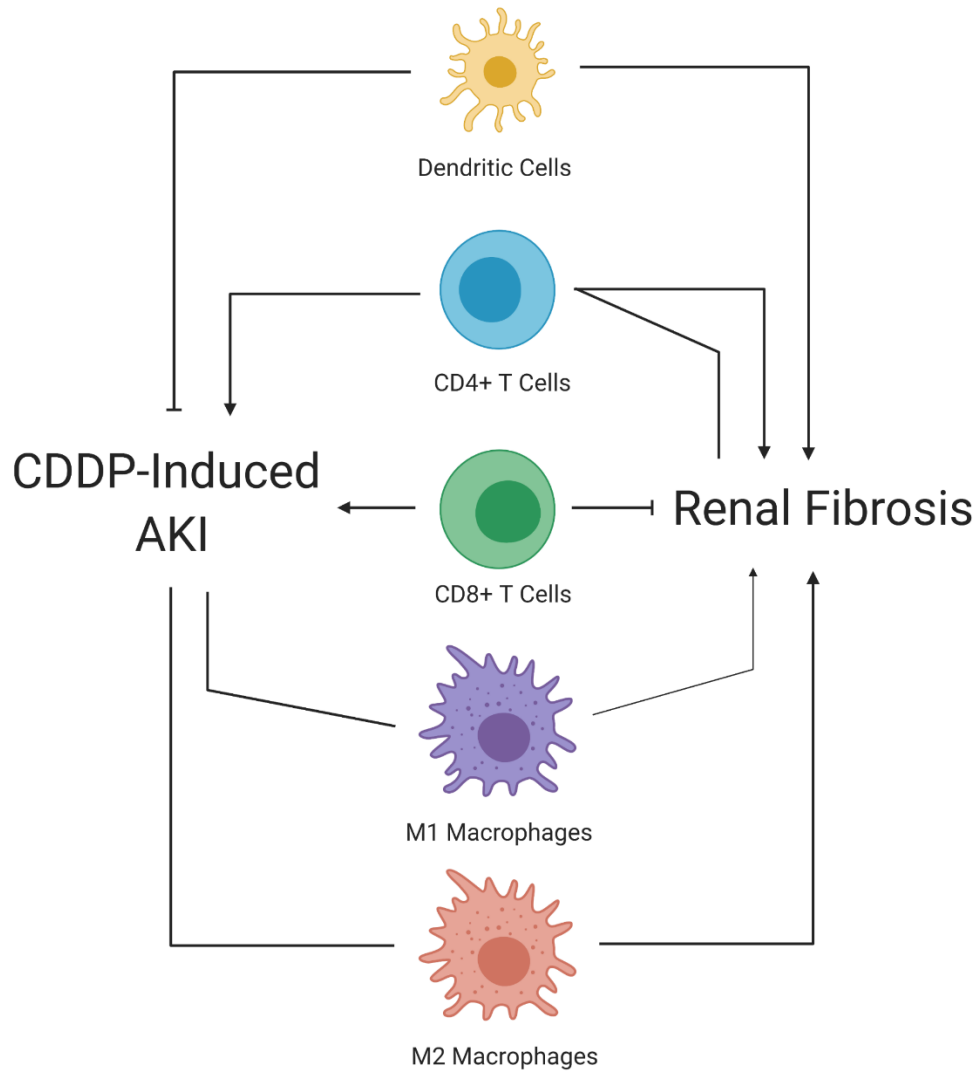


Figure 3. Immune cell involvement in cisplatin-induced AKI and renal fibrosis. Pointed arrow heads denote promotion of process, solid block line endings indicate inhibition of process, lines with no ending denote no effect on process.

Inhibition of TNF α signaling attenuates CDDP-KI in the high dose model and decreases production of other inflammatory mediators, indicating it plays a central role in activation of the cytokine response [82, 83]. In contrast, TNF α deficient mice have worse fibrosis compared to wild type mice 4 weeks after UUO [84]; however, neutralization of TNF α reduces renal fibrosis and improves function up to 1 week after UUO [85]. These conflicting results could be due to the different timepoints observed, indicating that TNF α may be pathogenic in early processes, but may be important for longer term recovery processes. These studies demonstrate the diverse functions the immune response can have at different stages of renal injury and progression to fibrosis, highlighting the importance of more in-depth studies of immune responses in chronic injury models.

We have observed increased expression of TNF α and other inflammatory cytokines in the mouse kidney following RLDC treatment [39, 40]. This cytokine response attracts immune cells to the kidney. Neutrophils, macrophages, T cells, and dendritic cells are the major responders to high dose cisplatin induced injury [2, 9]. Our lab has shown RLDC leads to a significant increase in immune cells in the kidney after four doses [40, 86]. Analysis of myeloid cells revealed a significant increase in M2 macrophages [40]. While further study is needed to evaluate the role of these inflammatory responders in RLDC, studies in other models of both AKI and renal fibrosis can provide some insight on which targets should be examined.

T cell deficient (*nu/nu*) mice are protected from injury following a single high dose of cisplatin [87]. Furthermore, CD4 T cell deficient mice show greater protection than CD8 T cell deficient mice [87]. In contrast, depletion of CD11c dendritic cells using the diphtheria toxin receptor model (CD11c-DTR) sensitizes mice to cisplatin induced AKI, indicating dendritic cells may play a nephroprotective role [88]. Lastly, although macrophages were shown to infiltrate the kidney following cisplatin treatment, depletion of macrophages with liposome encapsulated clodronate (LEC) has no effect on development of AKI [89].

The role of immune cells in renal fibrosis may be more complex. T and B cell deficient RAG-1 mice have less fibrosis development following UUO compared to wild type. Furthermore, reconstitution of CD4 T cells reverses this protection while CD8 T cell reconstitution does not [90]. Additionally, CD8 T cell knockout mice have increased renal fibrosis following UUO, while pharmacologic depletion of CD4 T cells decreases renal fibrosis [91]. These results suggest a pathogenic role for CD4 T cells in renal fibrosis; however, CD4 T cell depletion does not protect mice from RLDC-induced fibrosis [92]. CD4 T cell depletion also hinders the efficacy of cisplatin, accelerating subcutaneous tumor growth [92]. This study indicates that CD4 T cells would not be a viable target in CDDP-KI. It also demonstrates that immune cells may play different roles in the different models.

In IR, global depletion of macrophages via LEC attenuates development of renal fibrosis. Adoptive transfer of M2 macrophages after global depletion reverses this beneficial effect, while M1 transfer does not, suggesting a role for

M2 macrophages in the development of fibrosis post-IRI [93]. The timing and coordination of M1 and M2 responses plays a role in injury and recovery as global depletion of macrophages with LEC after development of IR-induced AKI prevents recovery from injury [94]. Depletion of macrophages and dendritic cells with LEC prior to UUO attenuates renal fibrosis [95, 96]. Altogether, these studies indicate the diverse and complex role of immune cells in renal disease. The role of the immune system in renal fibrosis is made more complex by the transitions that occur from pro-inflammatory to pro-repair phenotypes. Utilizing only the high-dose model of CDDP-KI does not allow for study of immune cell clearance and tissue repair. Further studies are needed to elucidate the role of specific immune cell subtypes in the different phases of RLDC-induced fibrosis.

Conclusion

Nephroprotective agents can have differential success in the high-dose cisplatin model and the RLDC model. This is likely due to the inherent biological differences in these two models in the induction of cell death/senescence, autophagy, ER stress induction and response, and immune cell involvement. While the high-dose CDDP-KI model displays high levels of cell death and ER stress, the RLDC model of injury causes lower levels of ER stress and cell death, leading to more sublethal injury and cellular senescence. The RLDC model is also complicated by chronic immune cell activity in the kidney during recovery. Evaluating the success of different therapeutic strategies in these models may help shed light on the different nephrotoxic mechanisms employed by high-dose cisplatin and RLDC treatment.

Modeling CDDP-KI in rodents is challenging. One challenge is overcoming the differences in pharmacokinetics between rodents and humans. Mice are known to have higher peak plasma concentrations and shorter half-lives of platinum compared to humans [97]. With the differences in cisplatin handling, the best way to model human nephrotoxicity is to match pathologies induced by different dosing regimens. As cisplatin is administered with different dosing regimens depending on the cancer type, it follows that many models of nephrotoxicity should be used in rodent studies.

Another challenge in modeling CDDP-KI is comparing manifestations of kidney injury in mice and humans. Kidney histopathology can be readily evaluated in rodents, but not in humans as kidney biopsies are rarely performed in humans who develop AKI following cisplatin treatment. BUN and SCr are relied on as markers of kidney function for both rodents and humans. Electrolyte disturbances such as hypokalemia and hypomagnesemia are also closely monitored in humans [98], but are largely ignored in rodents even though it is possible to perform these analyses [99]. Finally, humans receiving cisplatin have cancer and the impact of cancer on cisplatin-induced kidney pathologies in rodents has not been well studied. In conclusion, rodent studies largely ignore some key aspects of human cisplatin-induced AKI, which may be essential for understanding this disease.

Despite these challenges, notable similarities in rodent and human AKI development following cisplatin treatment have been observed. Sex differences are noted in both mice and humans, with females being more sensitive than

males to cisplatin-induced AKI [100, 101]. Studies have also been done to identify genetic predictors of cisplatin nephrotoxicity in humans [102, 103], but direct comparisons to rodent models have not been studied in depth. Although controversy exists regarding methods of analysis, some studies have identified a polymorphism in organic cation transporter 2 (OCT2) gene *SLC22A2* rs316019 as a predictor of cisplatin nephrotoxicity [102, 103]. Similarly, OCT2 deletion or inhibition in rodents confers resistance to cisplatin-induced AKI [104-106]. This suggests similar cisplatin handling in rodents and humans.

It is important to consider both acute and chronic renal injury when developing nephroprotective agents. Patients exhibit a wide range of response to cisplatin in the clinic. Some develop AKI after a single low dose while others may receive multiple doses without displaying signs of clinical AKI. Understanding the biological processes occurring in both the high-dose cisplatin and RLDC models will elucidate the pathological processes occurring in all categories of patients, leading to better treatment of AKI and prevention of CKD.

OVERALL GOALS & SPECIFIC AIMS

Despite the high rate of nephrotoxicity associated with cisplatin treatment, 10-20% of all cancer patients are prescribed cisplatin as part of their treatment regimen [107]. In the past, the belief was that as long as renal function recovered (as determined by the return of SCr and BUN to baseline levels) after an AKI incident there would be no long-term consequences [25]. Now, many studies have shown that patients who develop AKI are up to 10 times more likely to develop chronic kidney disease (CKD) [22-24, 108, 109]. Even patients that do

not develop clinical AKI are at risk for long term declines in renal function [36, 110]. As we improve diagnosis and treatment of cancer, the number of cancer survivors is increasing. In 2016, there were 15.5 million cancer survivors in the United States. That number is estimated to increase to 20.3 million by 2026 [111]. As a result of cisplatin-treated patients' extended survival, AKI and CKD incidences have also been increasing [24, 112, 113]. CDDP-KI places a large burden on both patient quality of life and our healthcare system.

There is a great need to develop agents to protect from CDDP-KI to increase cisplatin's therapeutic potential and decrease the rate of CKD development in cancer survivors. We believe research has failed in the past due to a lack of clinically relevant models of injury. We need to use models that allow for long term studies of CDDP-KI to understand the mechanisms of renal repair and recovery following an insult. Our preliminary studies indicate that CKD development following cisplatin treatment involves mechanisms that are very different from AKI development and indicate that we do not understand these processes sufficiently [38]. One example of an area requiring additional understanding is that of the role of macrophages in cisplatin-induced CKD.

The goal of this dissertation is to expand the use of our clinically relevant RLDC model of CDDP-KI to different strains of mice and to evaluate the role of macrophages in RLDC-induced fibrosis and progression to CKD. This goal will be met via two aims. **Aim 1:** Optimize the RLDC model in C57BL/6 mice and identify consistent markers of injury. This aim will also assess macrophage infiltration and polarization following RLDC treatment in C57BL/6 mice. **Aim 2:**

Determine the role of macrophages in RLDC-induced fibrosis and progression to CKD. We will deplete different populations of macrophages during RLDC treatment and assess subsequent development of kidney injury and fibrosis. Understanding the role of macrophages in renal fibrosis and CKD progression will help develop new therapeutic strategies to treat and prevent CDDP-KI.

CHAPTER 2: CHARACTERIZATION OF STRAIN DIFFERENCES AND IMMUNE CELL ACTIVITY DURING REPEATED LOW DOSE CISPLATIN TREATMENT

INTRODUCTION

Cisplatin is a commonly used chemotherapeutic for many types of solid-organ cancers. Although it is effective in killing cancer cells, it is hindered by its dose limiting nephrotoxicity. Thirty percent of patients who receive cisplatin develop acute kidney injury (AKI), characterized by proximal tubule cell death, inflammation, and vascular injury [2, 5, 9]. In the past, cisplatin-induced kidney injury has been modeled in mice by administering a single high dose of cisplatin. This model invokes a high level of tubule cell death and is lethal to mice within 3-4 days. Although this model can be useful for studying the short-term effects of cisplatin and AKI development, it does not allow for study of long-term renal function following treatment [35].

In the last decade, several studies have revealed the interconnectedness of AKI and chronic kidney disease (CKD), identifying AKI as a risk factor for CKD development [22-24]. Studies have also identified a risk of long-term declines in renal function in pediatric patients treated with cisplatin that do not develop clinical AKI [36]. These studies demonstrate the importance of studying the long-term effects of renal insults. Our lab [37-39] and others [41-43] have used a

repeated low dose cisplatin model to observe AKI to CKD transitions following cisplatin treatment. In these studies, mice can survive up to six months after cisplatin treatment and develop progressive renal fibrosis accompanied by declines in kidney function and chronic inflammation [39].

Our lab used FVB/n mice to characterize renal injury following repeated low-dose cisplatin treatment [38, 39]. Mice were given four weekly doses of 7 mg/kg cisplatin. Following the fourth dose, mice developed moderate increases in blood urea nitrogen (BUN) and neutrophil gelatinase associated lipocalin (NGAL), which indicate subclinical kidney injury. Interestingly, mice also developed significant renal fibrosis as measured by collagen deposition and alpha-smooth muscle actin (α SMA) expression. This fibrosis was accompanied by increased inflammatory cytokine mRNA expression and endothelial dysfunction. Kidney function continued to decline and fibrosis progressed up to six months after cisplatin treatment, indicative of progressive CKD [39]. We have since set out to optimize this repeated dosing model in different strains of mice.

C57BL/6 mice are used to generate many transgenic lines and are widely used in studies of kidney injury; however, these mice are resistant to development of interstitial fibrosis and glomerulosclerosis in different models of CKD [114]. When we treated C57BL/6 mice with 7 mg/kg cisplatin once a week for four weeks, we did not observe development of fibrosis. Other studies have also demonstrated that C57BL/6 mice require a higher dose of cisplatin to develop pathologies indicative of CKD; however, this higher dosage can lead to decreased survival [41, 44-46].

The goal of this study was to determine if C57BL/6 mice can be used in our repeated low dose cisplatin model with an increased dose of cisplatin without compromising animal survival and human relevance. In this study, we treated FVB/n and C57BL/6 mice with repeated, weekly doses of 7 and 9 mg/kg cisplatin for four weeks. We observed that while FVB/n mice develop fibrosis and CKD-associated pathology with 7 mg/kg cisplatin, C57BL/6 mice require 9 mg/kg cisplatin to develop similar phenotypes. This increased dosage did not affect survival. Upon repeating studies with C57BL/6 mice, we also found that certain renal outcomes were variable. We observed a difference in structural damage and kidney function loss among C57BL/6 mice bred at and purchased from Jackson Laboratory one year apart as well as C57BL/6 mice bred in house. We analyzed this population variation and identified the C-C Motif Chemokine Ligand 2 (CCL2) as a marker of cisplatin-induced kidney injury. CCL2 is known to play a role in myeloid cell trafficking, and in accordance we also observed an increase in infiltrating renal macrophages and monocytes in C57BL/6 mice following repeated doses of 9 mg/kg cisplatin. This study demonstrates that C57BL/6 mice can be used in the repeated low dose cisplatin model and highlights the importance of using littermate control wild type mice.

MATERIALS & METHODS

Animals. Eight-week-old male FVB/n and C57BL/6 mice were maintained on a 12:12 hour light-dark cycle and provided food and water *ad libitum*. Animals were maintained under standard laboratory conditions. All animal procedures were approved by the Institutional Animal Care and Use Committee of the University of

Louisville (Protocol ID: 16593 and 19568) and followed the guidelines of the American Veterinary Medical Association. Briefly, mice were intraperitoneally (i.p.) injected with either 0.9% N saline vehicle or cisplatin at either 7 or 9 mg/kg at 8:00 AM once a week for four weeks and euthanized at day 24.

Pharmaceutical grade cisplatin purchased directly from the University of Louisville hospital pharmacy (1 mg/ml in 0.9% N saline from either Teva or Intas Pharmaceuticals) was used for all experiments. Mice were monitored for weight loss or evidence of high levels of discomfort/stress. Upon euthanasia, plasma was prepared and stored at -80°C. Kidneys were flash-frozen in liquid nitrogen or fixed in 10% neutral buffered formalin.

Blood urea nitrogen (BUN) determination. BUN was measured in the plasma of mice using a kit from AMS Diagnostics (80146, AMS Diagnostics) per the manufacturer's instructions, and as previously published [39].

ELISAs. ELISA for neutrophil gelatinase associated lipocalin (NGAL; DY1857, R&D Systems) was performed on mouse urine as previously published [39]. ELISA for CCL2 (DY479-05, R&D Systems) was performed on mouse urine according to manufacturer's protocol.

Pathology scoring and analysis. The morphological damage to the kidney was analyzed by light microscopy using hematoxylin and eosin (H&E) and periodic acid-Schiff (PAS) stained sections and evaluating the entire kidney cross section by a semiquantitative method. The following histologic criteria were scored on a 0-4 scale: tubular necrosis, brush border loss, tubular dilatation, tubular cast

formation, distal nephron damage, degeneration, and inflammation.

Degeneration was scored in the proximal tubules that were not necrotic and included cell swelling, the formation of vacuoles, PAS positive granules in the cytoplasm due to the damage to the membranes and disruption of ion transport resulting in the accumulation of intracellular lipids and proteins or lipoproteins.

Regeneration was scored in the tubules that underwent necrosis and were relined by new undifferentiated epithelial cells. The score was given depending on the extent of these changes and the state of differentiation of the epithelium.

Inflammation was determined based on the density and the number of inflammatory cells throughout the kidney. These parameters were evaluated on a scale of 0 to 4: not present (0), mild (1), moderate (2), severe (3), and very severe (4). The scores were given based on the presence and extent of histologic damage using the following findings: 0: damage is not present; 1: damage is present only in and/or around individual tubules; 2: damage is present in and/or around small group of tubules; 3: damage is present confluent in the cortico-medullary junction; and 4: the damage extends to the outer cortex and it can reach the surface of the kidney.

Gene expression. Total RNA was isolated from kidney cortex, and cDNA was made as previously published [39]. The following pre-designed TAQman primers (Life Technologies) were used: *Tnfa* (Mm00443258_m1), *Il-6* (Mm00446190_m1), *Cxcl1* (Mm04207460_m1), *Ccl2* (Mm00441242_m1), *B2m* (Mm00437762_m1), and *Arg-1* (Mm00475988_m1). The following self-designed primers were used: *Kim-1* forward AGATCCACACATGTACCAACATCAA and

reverse CAGTGCCATTCCAGTCTGGTTT; *iNOS* forward

GAGATTGGAGGCCTTGTGTCA and reverse TCAAGCACCTCCAGGAACGT.

Real-time qRT-PCR was performed using iTaq Universal Probes Supermix (172-5134, Bio-Rad) or iTaq Universal SYBR Green Supermix (172-5124, Bio-Rad).

Protein Isolation/Quantification and Western Blot Analysis. Protein isolation, quantification, and western blot analysis was performed on kidney cortex as previously published [39], using 1:5000 dilutions for primary antibodies, except for β -actin (1:10000). 1:20000 dilution was used for secondary antibodies.

Proteins of interest were detected by chemiluminescence substrate. The following antibodies were purchased from Cell Signaling: cleaved caspase-3 (no. 9664), and C/EBP homologous protein (CHOP; no. 2895). β -actin antibody was purchased from Sigma (no. A2228).

Immunohistochemistry and Sirius Red/Fast Green (SR/FG) staining. Alpha smooth muscle actin (α SMA) immunohistochemistry for myofibroblasts and SR/FG stain for total collagen deposition was performed on paraffin embedded kidney sections as previously published [39]. Quantification of positive staining was done using Image J to determine mean intensity of positive staining. Optical density was calculated as: $\text{Log}(255/\text{mean intensity})$, as 255 is the max intensity for 8-bit images.

Flow Cytometry. Whole kidneys were homogenized into single cell suspensions via mechanical disruption and enzymatic digestion with Liberase DL Research Grade (05466202001, Millipore/Sigma). After passing through a 40 μm filter, cells were treated with ACK lysis buffer (A1042-01, Life Technologies) for two minutes

to remove red blood cells. Cells were then suspended in PBS with 0.5% BSA, 0.01% sodium azide, and 2mM EDTA. CD16/32 (101321, Biolegend) was used to block Fc-gamma3 receptors. Cells were then stained with 10 µg/mL of CD45-PerCP (103130, Biolegend), Ly6C-APC-Cy7 (560596, BD Biosciences), and F4/80-BV421 (565411, BD Biosciences), and 7.5 µg/mL of CD11b-BV650 (563402, BD Biosciences). After staining, cells were permeabilized with FoxP3/Transcription Factor Staining Buffer Set (00-5523-00, Invitrogen). Intracellular staining was done with 10 µg/mL CD206-PE. Flow cytometry was done using a BD LSRFortessa, collecting 1 million events per sample.

Statistical analysis. Data are expressed as means ± standard error of the mean (SEM) for all experiments. Comparisons of normally distributed data sets were analyzed by either a one-way or two-way ANOVA, as appropriate, and group means were compared using Tukey post-tests. Nominal data were analyzed with individual chi-square tests. Correlations were determined using a linear regression model. The criteria for statistical differences were: * $p < 0.05$, ** $p < 0.01$, *** $p < 0.001$, and **** $p < 0.0001$.

RESULTS

Loss of kidney function is similar between FVB/n and C57BL/6 mice treated with repeated doses of cisplatin. BUN is commonly used as a measure of kidney function, as levels of urea increase in the blood with loss of kidney function. We have previously shown that loss of kidney function as determined by BUN is minimal with our repeated dosing regimen of cisplatin [38, 39]. When treated with four weekly doses of 7 mg/kg cisplatin, neither FVB/n nor C57BL/6

had a significant increase in BUN ($p=0.99$ and 0.20 respectively). With repeated doses of 9 mg/kg cisplatin, BUN was significantly elevated in FVB/n mice ($p=0.045$) but not in C57BL/6 mice ($p=0.99$) (Figure 4A). We also assessed levels of urinary NGAL, a sensitive kidney injury biomarker. When treated with repeated doses of either 7 or 9 mg/kg cisplatin, NGAL levels increased comparably in both strains, but neither increase was statistically significant (Figure 4B). Taken together, these data indicate that C57BL/6 and FVB/n sustain similar levels of kidney injury when treated with repeated, low doses of cisplatin. Thus, loss of kidney function is minimal and comparable between the two strains of male mice, characteristic of subclinical kidney injury.

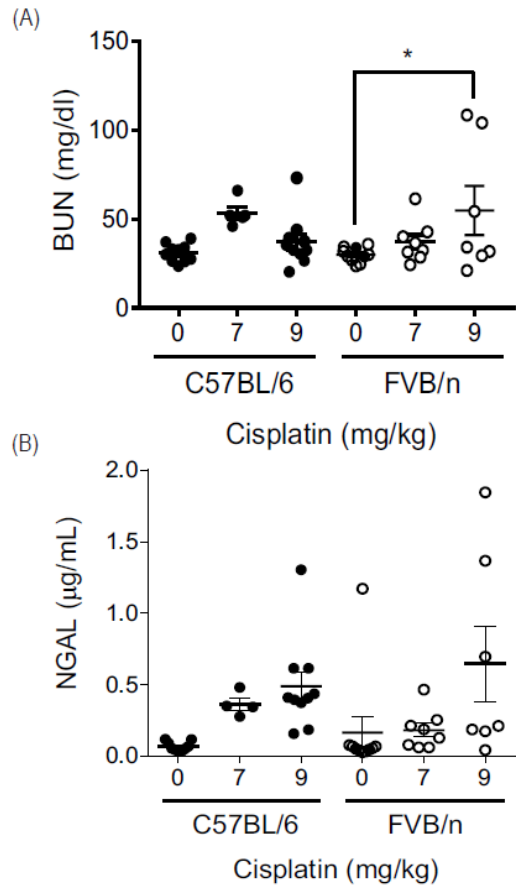


Figure 4. Kidney function and injury in FVB/n and C57BL/6 mice treated with repeated administration of cisplatin. (A) Blood urea nitrogen (BUN) levels were measured in plasma. (B) Neutrophil gelatinase-associated lipocalin (NGAL) levels were measured in urine. Statistical analysis was determined by two-way ANOVA followed by Tukey post-test. * $p < 0.05$.

A higher dose of cisplatin is required for the development of fibrosis in C57BL/6 mice than in FVB/n mice. We have previously published that treating FVB/n mice with 7mg/kg cisplatin once a week for four weeks induces renal fibrosis and myofibroblast accumulation [39]. Myofibroblasts are the main cell type responsible for collagen deposition and are identified by expression of alpha smooth muscle actin (α SMA). Immunohistochemistry staining for α SMA indicated that there were significantly more myofibroblasts present in FVB/n kidneys after repeated treatment with 7 mg/kg cisplatin ($p=0.03$). Myofibroblasts were less present when FVB/n mice were treated with repeated 9 mg/kg doses of cisplatin. In contrast, α SMA levels did not increase in C57BL/6 mice until the dose was increased to 9 mg/kg cisplatin, where levels were significantly elevated compared to both vehicle and 7 mg/kg treated mice ($p=0.004$ and 0.003 respectively) (Figure 5A and 5B). SR/FG staining revealed the same pattern. After repeated 7 mg/kg cisplatin treatment, FVB/n mice had their highest levels of collagen deposition, significantly elevated above both vehicle and 9 mg/kg cisplatin treated mice ($p= <0.0001$ and 0.003 respectively). C57BL/6 mice did not have increased collagen deposition when treated with repeated 7 mg/kg doses of cisplatin ($p>0.99$). When the weekly dose was increased to 9 mg/kg, however, collagen levels significantly increased ($p=0.0006$) (Figure 5C and 5D). Thus, C57BL/6 mice require a higher dose of cisplatin for the development of interstitial fibrosis. In addition, FVB/n mice seem to lose their fibrotic phenotype when treated with a higher dose of cisplatin.

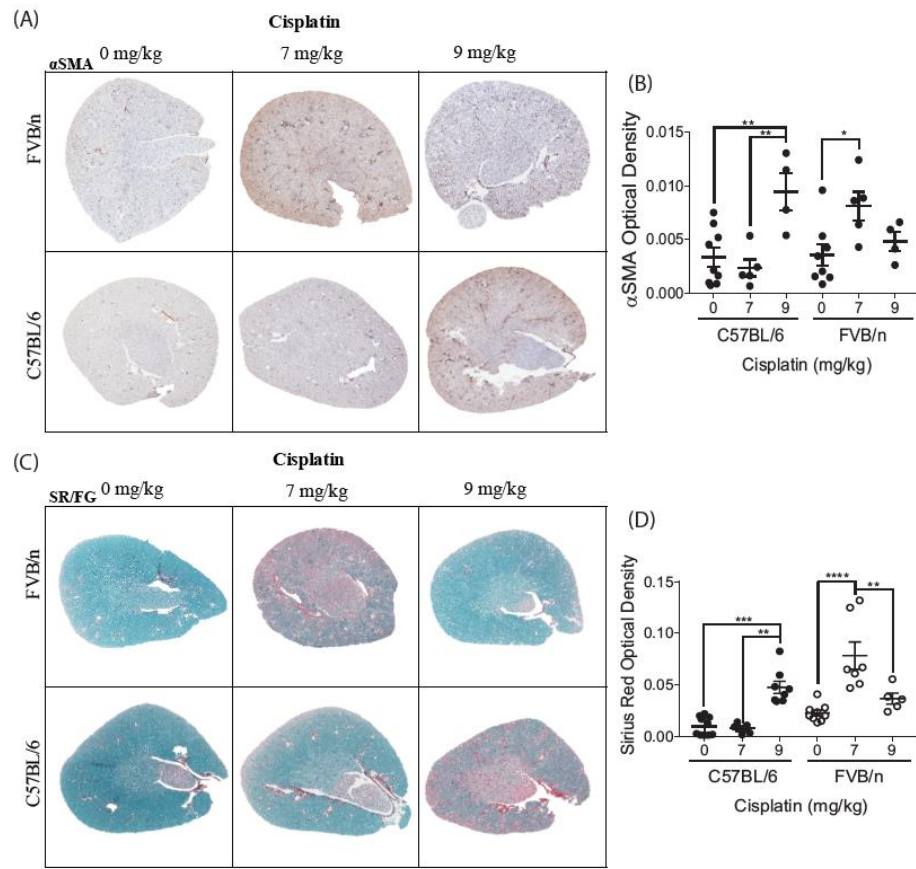


Figure 5. Development of renal fibrosis with repeated administration of cisplatin in C57BL/6 and FVB/n mice. (A) α SMA IHC for myofibroblasts and (B) quantification of optical density of positive staining. (C) SR/FG staining for total collagen deposition and (D) quantification of optical density of positive staining. Statistical analysis was determined by two-way ANOVA followed by Tukey post-test. * $p < 0.05$, ** $p < 0.01$, *** $p < 0.001$, **** $p < 0.0001$.

Differences in apoptosis and ER stress in C57BL/6 and FVB/n mice when treated with cisplatin. The main pathology associated with the single, high dose model of cisplatin induced kidney injury is cell death through both apoptotic and necrotic mechanisms [115, 116]. However, we have previously shown with our repeated, 7 mg/kg dosing regimen of cisplatin that the kidneys of FVB/n mice do not have overt cell death [38]. Thus, we wanted to determine if apoptosis was prevalent in C57BL/6 mice treated with either 7 or 9 mg/kg weekly cisplatin (Figure 6A and 6D). When given repeated doses of 7 mg/kg cisplatin, neither FVB nor C57BL/6 mice displayed an increase in cleaved caspase 3 expression, an indicator of apoptosis. When the weekly dose was increased to 9 mg/kg cisplatin, both FVB/n and C57BL/6 expressed cleaved caspase 3, indicating apoptosis occurs in both strains at this dose (Figure 6C and 6F). Interestingly, we found that CHOP, a marker for endoplasmic reticulum (ER) stress was increased in a dose-dependent manner in C57BL/6 mice, but levels of CHOP were highest with repeated 7 mg/kg cisplatin treatments in FVB/n mice (Figure 6B and 6E).

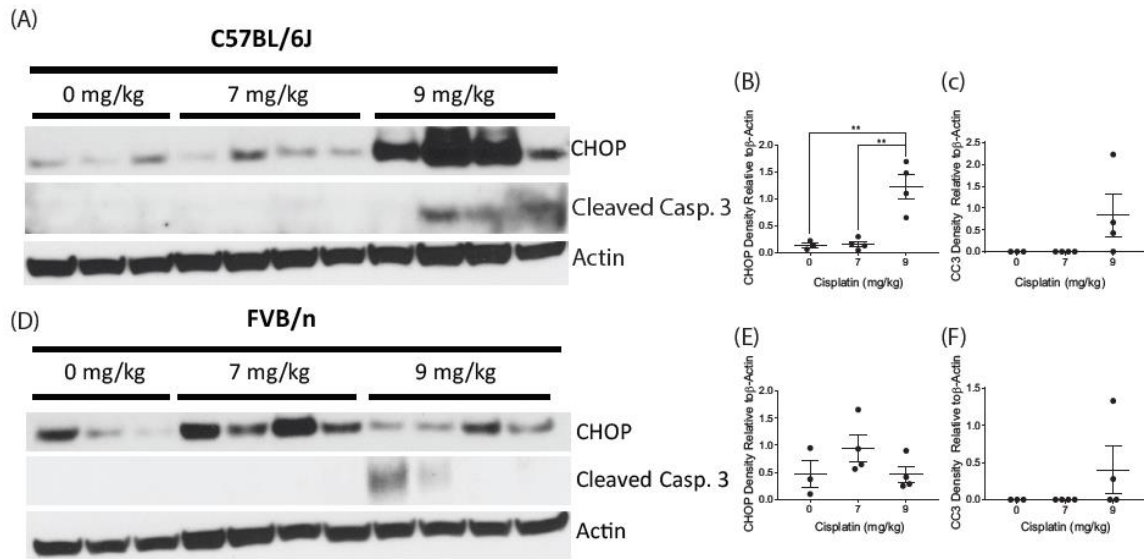


Figure 6. Markers of cell stress and cell death with repeated administration of cisplatin in C57BL/6 and FVB/n mice. CHOP, cleaved caspase 3 (CC3), and β -actin were measured in kidney cortex homogenates via Western blot in (A) C57BL/6 mice with quantification of (B) CHOP and (C) CC3 and (D) FVB/n mice with quantification of (E) CHOP and (F) CC3. Statistical analysis was determined by two-way ANOVA followed by Tukey post-test. ** $p < 0.01$.

C57BL/6 mice display variability in renal injury following repeated low dose (9 mg/kg) cisplatin treatment.

One year after the previous experiments were performed, a second individual in the Siskind laboratory repeated the 9 mg/kg cisplatin dosing regimen of C57BL/6 mice with male mice that again were purchased from Jackson laboratory. Both purchased sets of mice had at least 3 weeks of acclimation before the first dose of cisplatin was administered.

Unexpectedly, the cisplatin treated C57BL/6 mice purchased in 2018 had much greater weight loss than was previously observed (Figure 7A). This presented problems for the use of this model as 25% body weight loss was set as a humane endpoint. We believe dehydration is a major contributor to weight loss, as mice treated with cisplatin become less active and are likely drinking less water. We then treated C57BL/6 male mice bred in house with repeated doses of 9 mg/kg cisplatin. Weight loss appeared to be following a similar trend, so we administered subcutaneous injections of 500 μ L 0.9% N saline one day before dose 3, two days after dose 3, and one day before dose 4. This kept most mice under the 25% body weight loss cutoff. We want to note that while saline reduced body weight loss, we still observed development of kidney injury and fibrosis, indicating these outcomes are not a result of dehydration.

Interestingly, we also observed variability in BUN and NGAL levels among these three cohorts of C57BL/6 mice. Mice purchased from Jackson Laboratory in 2018 and mice bred in house had significantly greater increases in BUN following cisplatin treatment than mice purchased from Jackson Laboratory in 2017 ($p = <0.0001$ and 0.002 respectively), indicating greater loss of renal

function (Figure 7B). Urinary NGAL levels of purchased mice were similarly elevated following treatment; however, in-house bred mice had significantly lower NGAL levels following 9 mg/kg cisplatin treatment compared to 2017 and 2018 purchased groups ($p=0.03$ and 0.009 respectively) (Figure 7C).

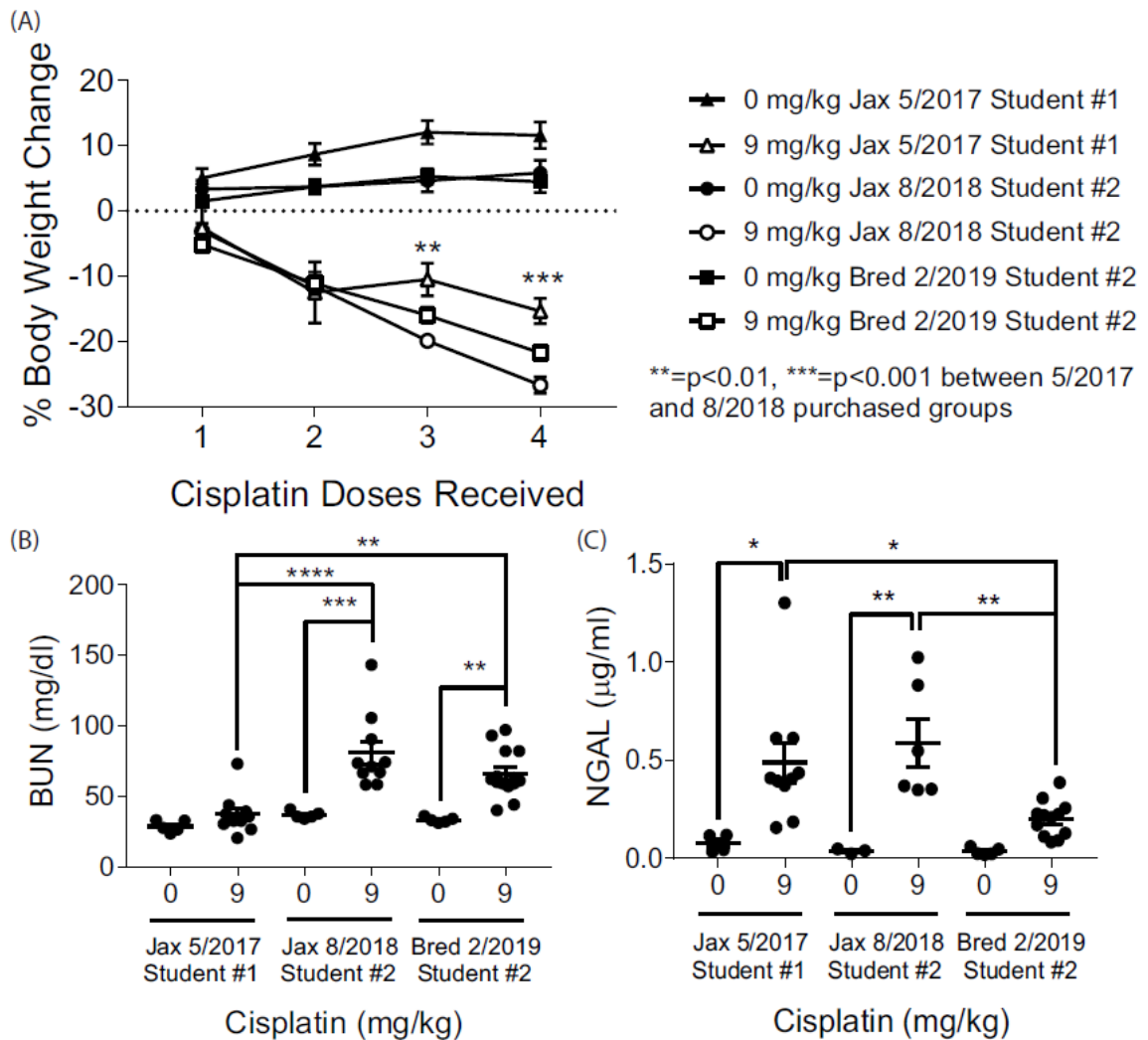


Figure 7. Weight loss, kidney function, and injury in C57BL/6 mice treated with repeated administration of 9 mg/kg cisplatin. (A) Percent body weight loss. (B) Blood urea nitrogen (BUN) levels measured in plasma. (B) Neutrophil gelatinase-associated lipocalin (NGAL) levels measured in urine. Statistical analysis was determined by two-way ANOVA followed by Tukey post-test. * $p < 0.05$, ** $p < 0.01$, *** $p < 0.001$, **** $p < 0.0001$.

C57BL/6 mice have variable structural damage, regeneration, and necrosis following repeated low dose (9 mg/kg) cisplatin treatment. Pathological assessment was performed on H&E and PAS stained sections from all three sets of C57BL/6 mice by the same pathologist in a parallel and blinded manner. Pathology scoring revealed variability in renal damage in C57BL/6 mice following repeated 9 mg/kg cisplatin treatment. Mice purchased in 2018 and in-house bred mice had higher levels of brush border loss, tubular casts, and tubular dilation compared to mice purchased in 2017 (Figures 8A-C). This suggests mice purchased in 2017 had less structural damage when treated with repeated doses of 9 mg/kg cisplatin. On the other hand, widening of the interstitium was similar in mice purchased in 2017 and in-house bred mice, but trended lower in mice purchased in 2018 (Figure 8E). Inflammation was similarly elevated in 2017 and 2018 purchased mice while levels were higher in in-house bred mice (Figure 8F). The greatest differences observed were large increases in tubular necrosis and regeneration displayed in the 2018 purchased mice and in-house bred mice. Mice purchased in 2017 had almost no detectable necrosis or regeneration (Figures 8G and 8H). Representative images of pathology scoring are provided (Figures 8I and 8J).

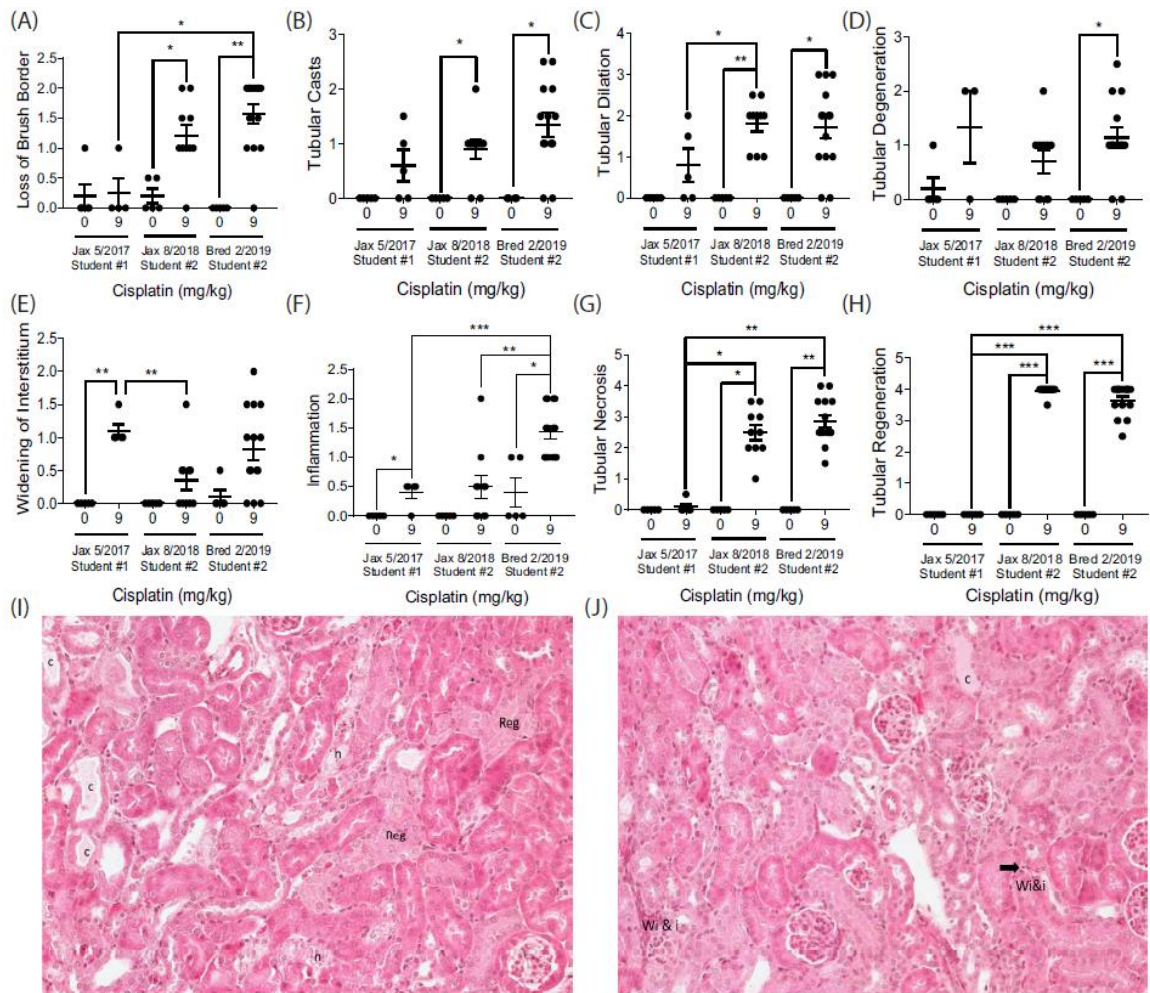


Figure 8. Pathology scoring of tubular damage in C57BL/6 mice treated with repeated administration of 9 mg/kg cisplatin. H&E and PAS-stained sections were scored on a scale of 1-4 for severity of (A) Loss of brush border, (B) Tubular casts, (C) Tubular dilatation, (D) Tubular degeneration, (E) Widening of the interstitium, (F) Inflammation, (G) Tubular necrosis, and (H) Tubular regeneration by a renal pathologist. Statistical analysis was determined by individual chi-squared tests. * $p < 0.05$, ** $p < 0.01$. (I) Representative H&E-stained section with Reg: regeneration; c: cast; i: inflammatory cells; n: necrosis; and (J) Wi&i: widening of the interstitium and inflammatory cells.

C57BL/6 mice have differential inflammatory cytokine responses following repeated low dose (9 mg/kg) cisplatin treatment. Previously, we have characterized an increase in *Tnfa*, *Il6*, *Cxcl1*, and *Ccl2* (also known as monocyte chemoattractant protein-1 (*Mcp-1*)) mRNA following repeated cisplatin treatment in FVB/n mice [38, 39]. We also observed an increase in M2 macrophage marker *Arg-1* accompanied by a decrease in M1 macrophage marker *iNOS* [39]. In this study, we found this response was consistent in C57BL/6 mice but varied in magnitude. C57BL/6 mice purchased in 2017 had a slightly greater increase in *Tnfa* and *IL6* following treatment than those purchased in 2018 or the in-house bred mice, while C57BL/6 mice purchased in 2018 had the largest increase in *Ccl2* levels (Figures 9A-C). In-house bred C57BL/6 mice had the greatest induction of *Cxcl1*, with levels significantly elevated above treated 2017 and 2018 purchased groups ($p=0.0006$ and 0.002 respectively) (Figure 9D). *Arg-1* levels were not elevated in either purchased set of cisplatin treated C57BL/6 mice but showed a significant increase in in-house bred mice. Cisplatin treated in-house bred mice had significantly elevated expression compared to both sets of cisplatin treated purchased mice ($p<0.0001$) (Figure 9E). The decrease in *iNOS* expression was consistent among all treated groups (Figure 9F). Overall, the inflammatory cytokine response was similar in each C57BL/6 group treated, with the exception of *Cxcl1* and *Arg-1* induction.

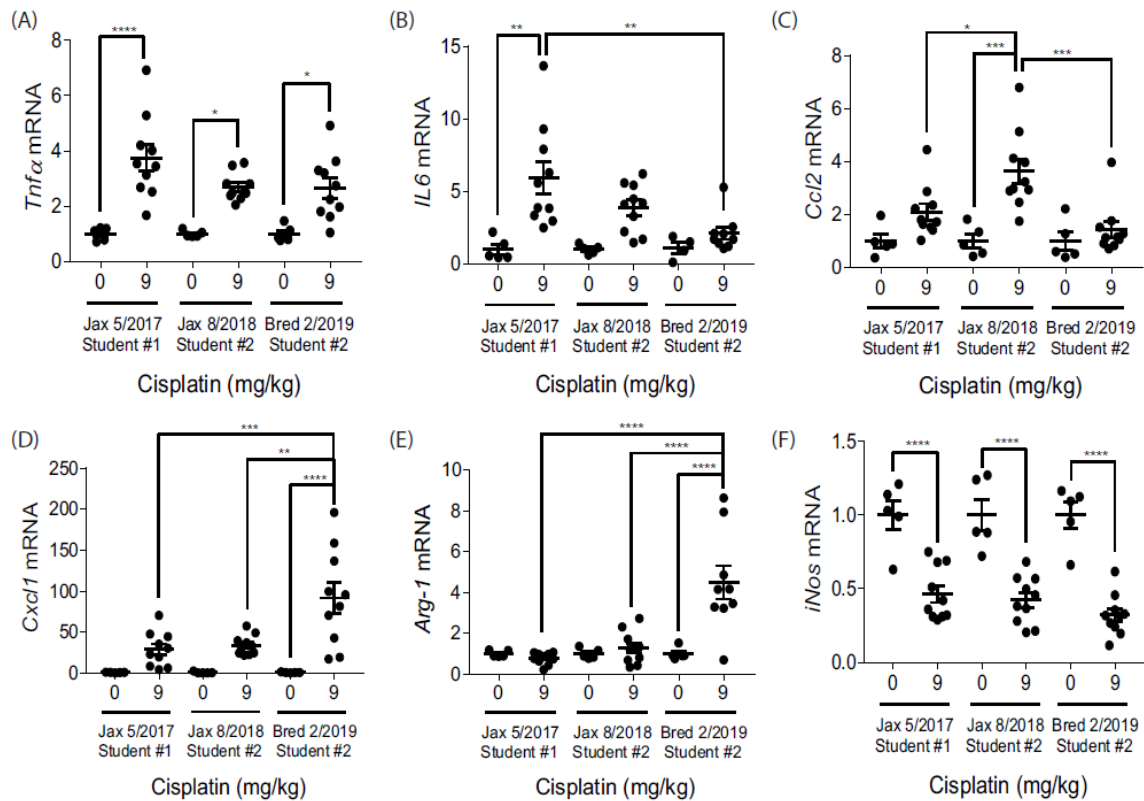


Figure 9. Inflammatory cytokine production in C57BL/6 mice treated with repeated administration of 9 mg/kg cisplatin. mRNA from renal cortex was analyzed with qRT-PCR to determine levels of (A) Tumor necrosis factor alpha (*Tnfa*), (B) Interleukin 6 (*IL6*), (C) C-C motif chemokine ligand 2 (*Ccl2*), (D) C-X-C motif chemokine ligand 1 (*Cxcl1*), (E) Arginase 1 (*Arg-1*), and (F) Inducible nitric oxide synthase (*iNos*). Expression levels were normalized to beta-2-microglobulin. Statistical analysis was determined by two-way ANOVA followed by a Tukey post-test. * $p < 0.05$, ** $p < 0.01$, *** $p < 0.001$, **** $p < 0.0001$.

C57BL/6 populations all develop renal fibrosis following repeated low dose (9 mg/kg) cisplatin treatment. Despite the differences observed in renal function and tubular injury, all C57BL/6 mice treated with 9 mg/kg cisplatin appeared to develop renal fibrosis as assessed by SR/FG staining and α SMA immunohistochemistry. All C57BL/6 mice treated with repeated 9 mg/kg cisplatin had significant increases in collagen deposition in the kidney, as indicated by the increased red color in the SR/FG stains (Figure 10B and 10D). All C57BL/6 mice also had increased α SMA positive cells following repeated 9 mg/kg cisplatin treatment (Figure 10A and 10C). Overall, these results indicate that although variation in renal function and tubular damage may be observed in different populations of C57BL/6 mice, renal collagen deposition and α SMA accumulation appear to be a consistent phenotype associated with the repeated dosing regimen of 9 mg/kg cisplatin in this strain.

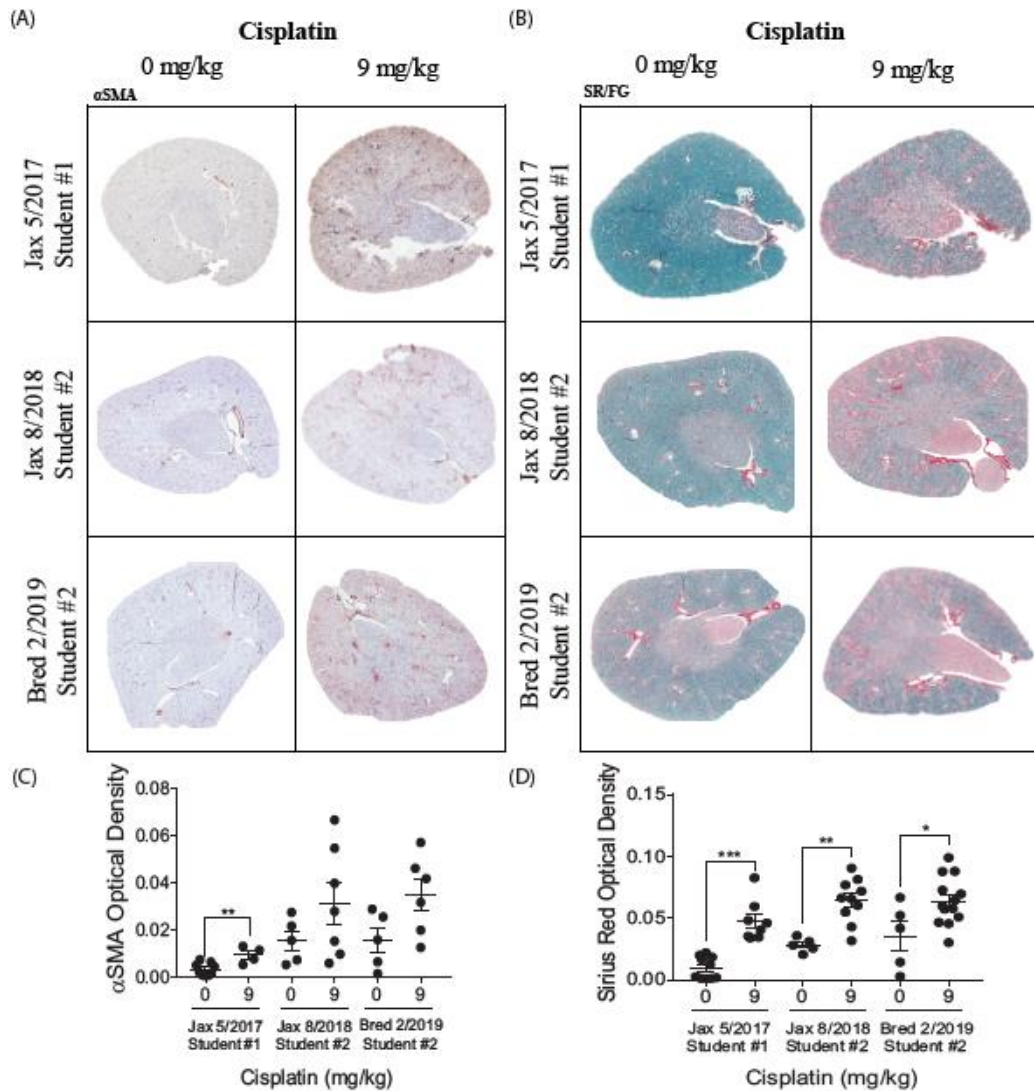


Figure 10. Development of renal fibrosis with repeated administration of cisplatin in C57BL/6 mice. (A) αSMA IHC for myofibroblasts. (B) SR/FG staining for total collagen deposition. Quantification of optical density of (C) αSMA and (D) SR/FG positive staining. Statistical analysis was determined by two-way ANOVA followed by Tukey post-test. *p<0.05, **p<0.01, ***p<0.001.

CCL2 is an indicator of injury following repeated low dose (9 mg/kg)

cisplatin treatment. Due to the variation observed in these studies with C57BL/6 mice, we set out to identify consistent correlations between different kidney injury parameters. We performed linear regressions comparing each quantitative data set collected for cisplatin treated C57BL/6 mice. We found that among treated mice, *Ccl2* mRNA expression in kidney cortex was significantly correlated with body weight loss, BUN, and *kidney injury molecule-1 (Kim-1)* expression ($p=0.003$, 0.02 , and 0.0001 respectively) (Figure 11A-D). Cisplatin treated mice with large increases in *Ccl2* expression also had larger amounts of body weight loss and greater increases in BUN, NGAL, and *Kim-1* expression, indicating worse kidney injury and decreased kidney function. In contrast, *Tnfa*, *Il6*, and *Cxcl1* did not correlate with these markers of injury, indicating that this relationship is specific to *Ccl2* and not general inflammation (Figure 12). These results suggest that *Ccl2* may be useful in identifying cisplatin-induced kidney injury. These correlations also demonstrate that the variation in these experiments is likely due to different susceptibilities of individual mice when treated with cisplatin; mice with high levels of one injury indicator are likely to score high in other measures as well. In addition, urinary CCL2 has recently been identified as a potential biomarker in patients who've developed cisplatin-induced nephrotoxicity [117, 118]. This prompted us to evaluate CCL2 protein levels in the urine of C57BL/6 mice treated with 4 doses of 9 mg/kg cisplatin. While no CCL2 protein was detected in urine of vehicle treated mice, cisplatin treated mice had significantly elevated levels of 7.8 ± 1.8 pg/ml in their urine

($p=0.0012$) (Figure 11E). These results highlight one factor that is similar in the kidney response to cisplatin among mice and humans.

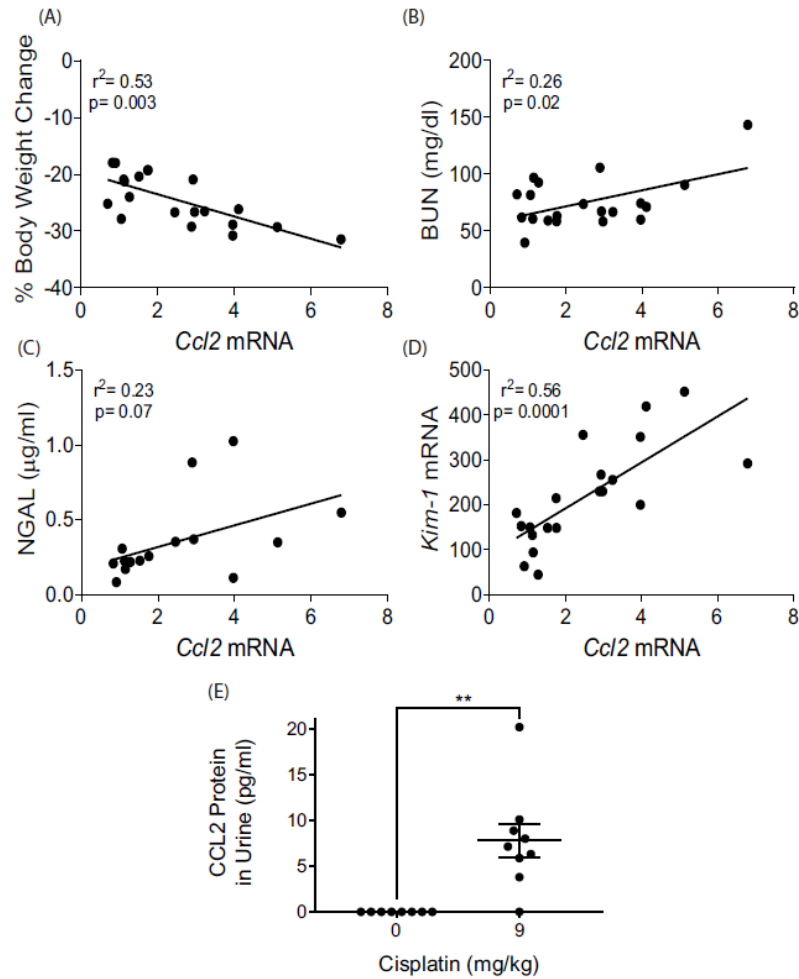


Figure 11. CCL2 expression in cisplatin-induced kidney injury. Correlations of *Ccl2* mRNA expression with (A) body weight loss, (B) BUN, (C) NGAL, and (D) Kim-1 mRNA in C57BL/6 mice treated with repeated administration of 9 mg/kg cisplatin. Correlations were found using a linear regression model with significance determined as $p < 0.05$. (D) Urinary CCL2 in C57BL/6 mice treated with repeated administration of 9 mg/kg cisplatin. An ELISA was performed on 50 μL of undiluted urine from vehicle and cisplatin treated mice. Vehicle treated mice had no detectable signal. Statistical analysis was determined by one-way ANOVA. ** $p < 0.01$.

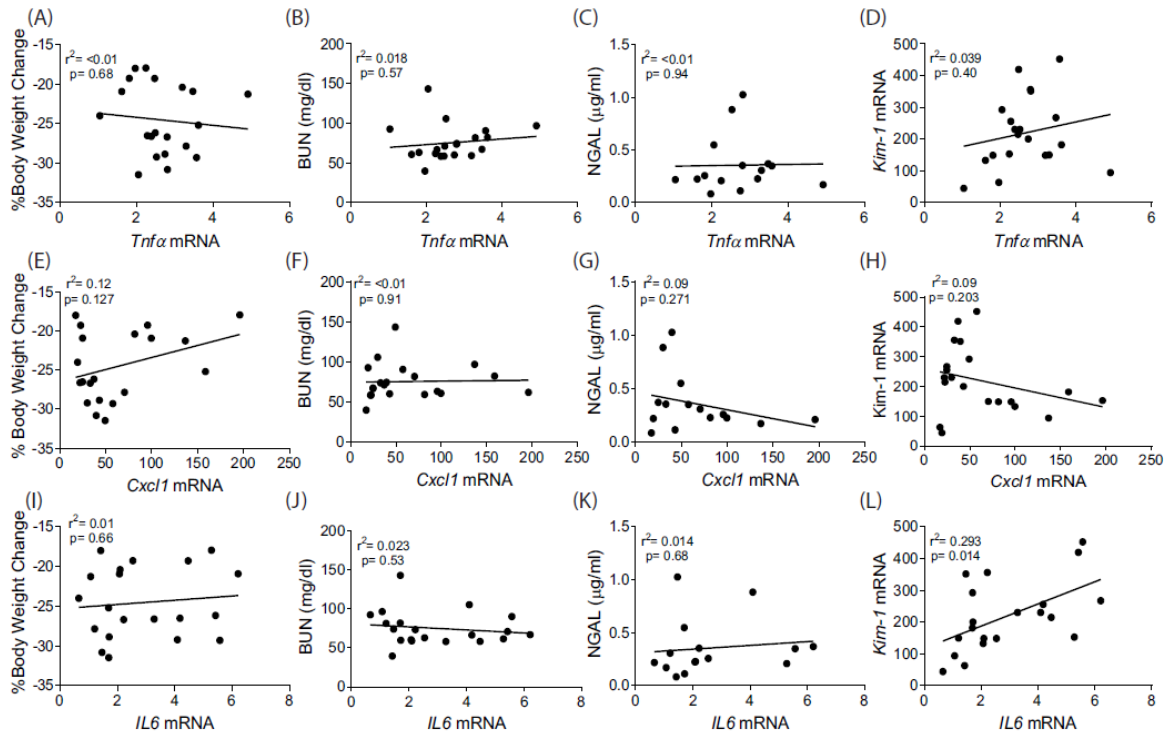


Figure 12. mRNA levels of other inflammatory cytokines measured do not correlate with markers of kidney injury. *Tnfα* mRNA does not correlate with (A) body weight loss, (B) BUN, (C) NGAL, or (D) *Kim-1* mRNA. *Cxcl1* mRNA does not correlate with (E) body weight loss, (F) BUN, (G) NGAL, or (H) *Kim-1* mRNA. *Il6* mRNA does not correlate with (I) body weight loss, (J) BUN, (K) NGAL, or (L) *Kim-1* mRNA. Significant correlations were determined as $p < 0.05$.

Renal immune cell infiltration is observed in C57BL/6 mice following repeated low dose (9 mg/kg) cisplatin treatment. CCL2 is known to play an important role in immune cell trafficking, specifically in myeloid cell recruitment [119]. We hypothesized that the elevation of *Ccl2* mRNA and urinary CCL2 observed in mice treated with cisplatin would be indicative of renal immune cell infiltration. We used the gating strategy shown in Figure 13 to evaluate the immune cells present in the kidney following cisplatin treatment. Contrary to what Black et. al. observed [44], we found a significant increase in the percentage of CD45+ immune cells in the kidney of cisplatin treated mice ($p < 0.0001$) (Figure 14A). We observed significantly increased populations of F4/80^{hi} and F4/80^{lo} macrophages ($p = 0.01$ and < 0.0001 respectively) (Figures 14B and 14C). Further analysis also revealed a significant increase in F4/80+ CD206+ macrophages ($p = 0.002$), indicative of an “M2” phenotype (Figure 14D). Lastly, we observed a significant increase in both Ly6c^{hi} and Ly6c^{lo} monocytes ($p < 0.0001$ for both) (Figure 14E and 14F). These findings suggest that there is a significant immune response to cisplatin-induced renal damage in the repeated low dose model. More studies are needed to assess whether the activity of these immune cells in the kidney plays a major role in promotion of fibrosis.

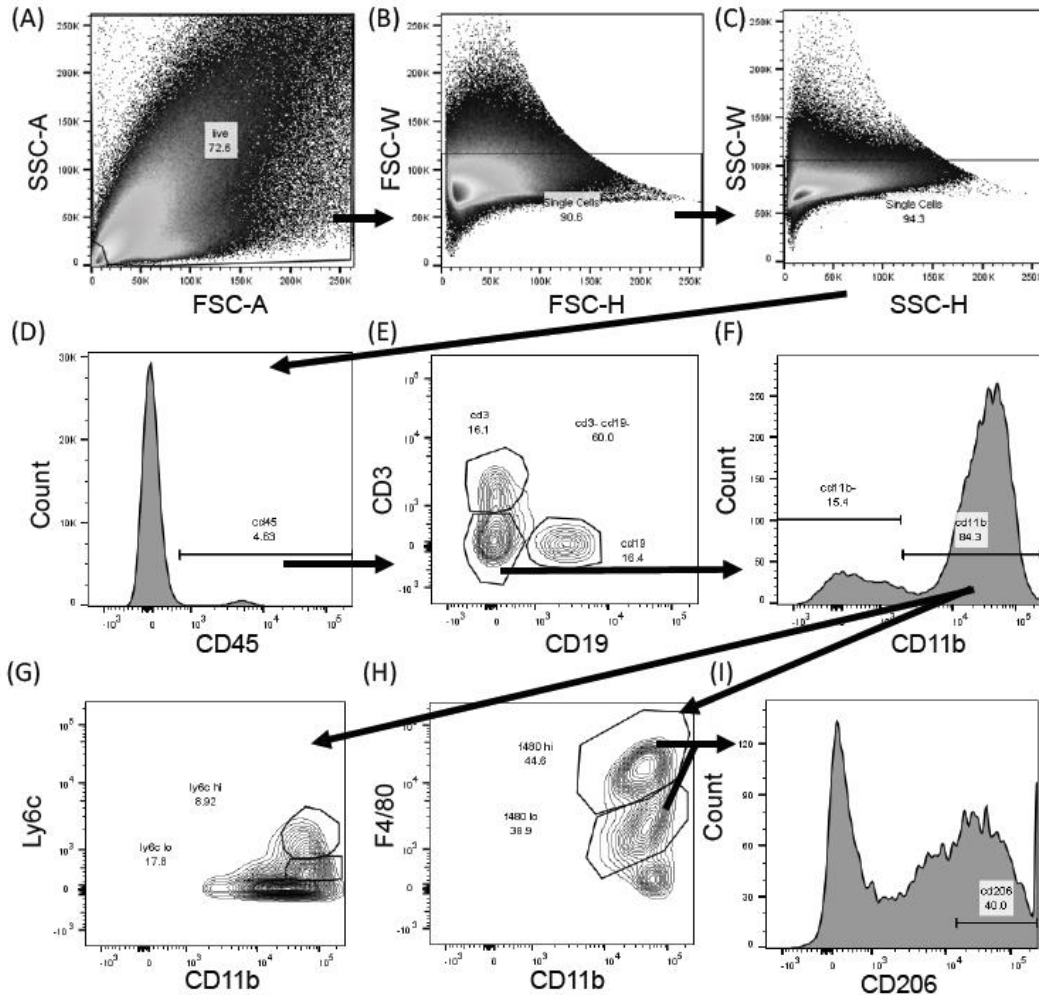


Figure 13. Gating strategy for flow cytometric analysis of renal macrophages and monocytes. (A) Debris was gated out based on FSC-A x SSC-A plot. (B, C) Doublet exclusion was performed. (D) CD45+ Immune cells were selected. (E) CD3+ T cells and CD19+ B cells were excluded. (F) CD11b+ cells were selected. (G) Ly6c hi and Ly6c lo cells were identified from CD11b+ cells. (H) F4/80 hi and F4/80 lo cells were identified from CD11b+ cells. (I) CD206+ cells were selected from all F4/80+ cells.

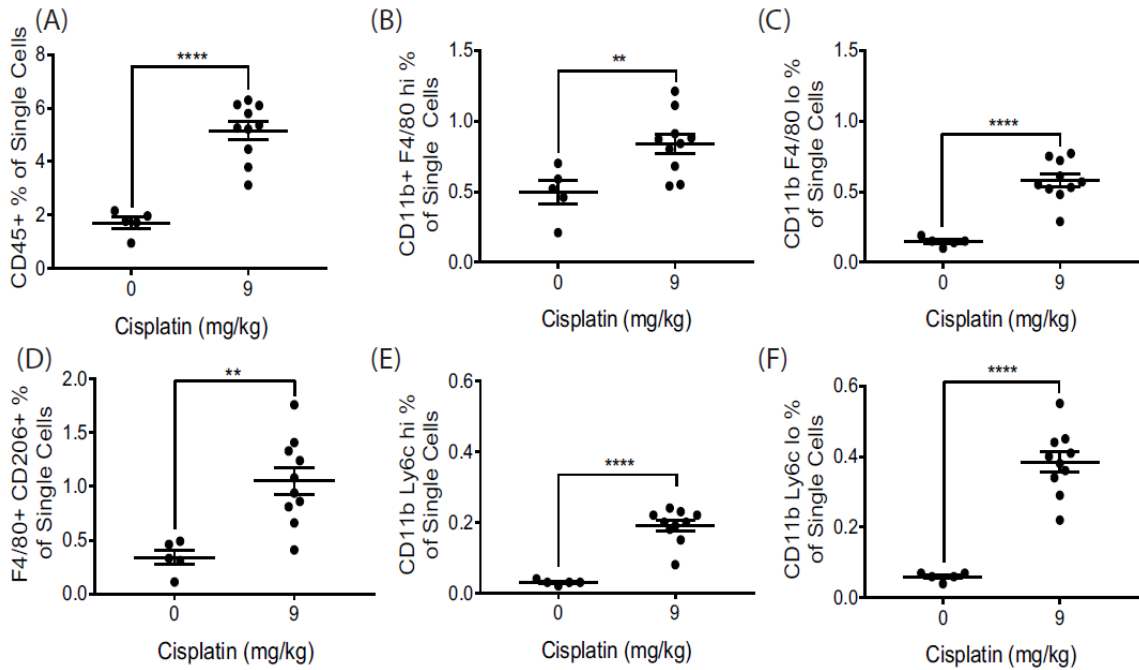


Figure 14. Flow cytometric analysis of renal macrophages and monocytes.

Whole kidneys were homogenized and ~1 million cells were stained. 1 million events were collected from each sample. Analysis identified (A) CD45+ immune cells, (B) CD11b+ F4/80 hi resident macrophages, (C) CD11b+ F4/80 lo infiltrating macrophages, (D) F4/80+ CD206+ M2 macrophages, (E) CD11b+ Ly6c hi inflammatory monocytes, and (F) CD11b+ Ly6c lo resident monocytes. Populations are expressed as a percentage of the number of single cells counted. Statistical analysis was determined by one-way ANOVA. **p<0.01, ****p<0.0001.

DISCUSSION

The development of mouse models of renal fibrosis is important for studying CKD. Previously, we developed a model of fibrosis that results from four weekly treatments of 7 mg/kg cisplatin in FVB/n mice. Fibrosis was characterized by increased collagen deposition via Sirius Red/Fast Green staining and accumulation of myofibroblasts by α SMA immunohistochemistry. We also observed an increase in inflammatory cytokine mRNA expression and markers of endothelial dysfunction [39]. C57BL/6 mice are well known to be resistant to development of fibrosis in other models, limiting their use in studies of CKD development [114]. We observed here that administration of 7 mg/kg cisplatin in C57BL/6 did not result in fibrosis as seen in FVB/n mice. These results highlight that this repeated low dose model of cisplatin-induced kidney injury is in fact a model of renal fibrosis and not AKI. The biological processes induced by the acute, high dose model of cisplatin-induced kidney injury are different than what occurs in this repeated low dose model.

Similar low dosing regimens of cisplatin have indicated that with higher doses of cisplatin (9-15 mg/kg), C57BL/6 mice will develop mild tubulointerstitial fibrosis. Torres et. al. showed that 2 treatments of 15 mg/kg cisplatin two weeks apart leads to slight fibrosis and changes in glomeruli, although glomerulosclerosis was not present [46]. Additionally, Katagiri et al., and Ravichandran et. al. have shown that administration of 10 mg/kg cisplatin once a week for three or four weeks, respectively, results in mild fibrosis [41, 92]. We have found that 10 mg/kg cisplatin administered once a week for four weeks

increases frequency of animal death and leads to unacceptable levels of body weight loss (data not shown). Thus, the goal of our study was to optimize a dose of cisplatin in C57BL/6 mice that would induce the development of fibrosis with minimal animal death and less than 25% body weight loss.

In this study, we found that i.p. administration of 9 mg/kg cisplatin once a week for four weeks is sufficient to cause interstitial fibrosis in C57BL/6 mice. Administration of subcutaneous saline with this dosing regimen may also be used to prevent severe weight loss and does not hinder development of kidney injury or fibrosis. Similar studies by other groups have also indicated that repeated low doses of 8-9 mg/kg cisplatin induces fibrosis in C57BL/6 mice without compromising survival [44, 45]. Additionally, we observed marked differences between FVB/n and C57BL/6 mice in apoptosis induction and CHOP expression. We also observed variation in kidney function and tubular damage in different populations of C57BL/6 mice. Despite this variation, collagen deposition and α SMA accumulation with repeated 9 mg/kg cisplatin treatment was consistent.

It is well established that experimental AKI is met with high levels of inflammation and consequently high levels of both apoptotic and necrotic cell death. We have shown that treating FVB/n mice with 7 mg/kg cisplatin once a week for four weeks results in little to no apoptosis or necrosis [39]. In this study, both FVB/n and C57BL/6 mice expressed cleaved caspase 3 when treated with 9 mg/kg cisplatin, indicative of apoptosis. Surprisingly, C57BL/6 mice had apoptosis occurring with the development of fibrosis, whereas fibrosis developed with a lower dose in FVB/n mice and was less pronounced when there were

higher levels of the cell death marker cleaved caspase 3. This may be key in explaining why development of a fibrosis model with cisplatin in C57BL/6 mice is often met with decreased overall survival.

ER stress is another major component of kidney injury. We found that expression of CHOP, an indicator of ER stress, corresponded to the development of fibrosis in both strains of mice. While CHOP and ER stress are classically associated with apoptosis, they also play a role in renal fibrosis [120]. Several studies have found that CHOP deficient mice subjected to unilateral ureteral obstruction or ischemia reperfusion injury have lower levels of fibrosis, inflammatory cell infiltration, and lipid peroxidation compared to wild-type mice [68, 71, 121]. Thus, CHOP is important for the progression of CKD and should be examined in the repeated low-dose cisplatin model.

A surprising outcome in this study was the loss of fibrotic phenotype in FVB/n mice given 9 mg/kg cisplatin. Our rationale for this result is based on the fact that cisplatin induces kidney injury on a spectrum from AKI to CKD pathologies. We hypothesize that at 9 mg/kg, FVB/n mice develop more of an AKI phenotype. These mice have higher levels of BUN, NGAL, structural damage, and cell death, indicating greater acute injury. We believe that this higher level of acute injury is causing injured cells to be cleared quickly by apoptosis or necrosis and preventing accumulation of senescent cells. CKD and fibrosis development are known to be promoted by processes of maladaptive repair, including cell cycle arrest of sublethally injured proximal tubule cells [25]. Literature also suggests that apoptotic clearance of injured cells may prevent

accumulation of senescent cells that may otherwise contribute to fibrosis development [11, 53, 122]. Future studies should evaluate pathways of cell death activated at different cisplatin dosing levels as well as ER stress induction and cellular senescence. We also need to re-evaluate the phenotype presented in FVB/n mice treated with 9 mg/kg cisplatin to assess if this higher dose increases group variability as in C57BL/6 mice.

While 9 mg/kg cisplatin treatment consistently induces fibrosis in C57BL/6 mice, we did observe variability in renal function and structural damage. We used this variability to identify correlations among different injury parameters in our C57BL/6 populations. We analyzed correlations among quantitative data sets of cisplatin treated mice and found that *Cc/2* mRNA levels were significantly correlated with increased body weight loss, BUN, NGAL, and *Kim-1* mRNA levels. These data suggest that variability in these markers correspond to susceptibility for developing cisplatin-induced kidney injury, as mice that score high in one category are likely to score high in others. To further assess this correlation, we measured *Cc/2* mRNA in FVB/n mice treated with 7 and 9 mg/kg cisplatin. We observed a dose-dependent increase in *Cc/2* mRNA levels (data not shown). *Cc/2* mRNA was also increased more in FVB/n mice at 7 mg/kg than in C57BL/6 mice. These trends follow the patterns of kidney injury markers like BUN and NGAL, but do not trend the same as markers of fibrosis. This could suggest a disconnect between kidney injury and fibrosis development, with *Cc/2* mRNA being more of an indicator of kidney injury than development of fibrosis.

We also observed a significant increase in urinary CCL2 protein in cisplatin treated mice. Urinary CCL2 did not correlate with injury parameters or immune cell infiltration. Although we were able to detect an increase in urinary CCL2, the protein was present in such low amounts we do not believe the ELISA used is sensitive enough to calculate exact quantities and may be the reason a correlation was not observed. Clinically, urinary CCL2 has been identified as an indicator of cisplatin-induced kidney injury in lung cancer patients treated with cisplatin [118]. The presence of CCL2 in the urine of the mice in this study provides support to the argument that it could be used as a more sensitive biomarker of cisplatin-induced kidney injury than BUN or serum creatinine. These results also suggest that our repeated dosing regimen of cisplatin induces pathological processes that are similar to what occurs in humans.

The increase in CCL2 in this model could also hint at mechanisms promoting cisplatin-induced renal fibrosis. CCL2 is known to play a role in immune cell trafficking. It has been demonstrated that *Ccl2* mRNA levels increase in different models of renal injury, indicating the CCL2 protein may play a role in orchestrating development of renal fibrosis [123, 124]. Kitagawa et. al. demonstrated that pharmacologic inhibition and genetic knockdown of *Ccr2*, the receptor of CCL2, protects mice from renal fibrosis in the unilateral ureteral obstruction model. They also observe a significant decrease in infiltrating F4/80 macrophages [125]. Furuichi et. al. found similar results using the ischemia-reperfusion model, with *Ccr2*-deficient mice showing resistance to injury and fibrosis [126]. Pharmacologic inhibition of CCL2 also provides protection in a

model of diabetic nephropathy [127]. These studies attribute the protective effects of CCR2 and CCL2 inhibition to modulation of immune response following renal injury.

In light of these studies, we evaluated renal immune cell infiltration following repeated low dose (9 mg/kg) cisplatin treatment in C57BL/6 mice. Black et. al. recently published results indicating that repeated 9 mg/kg cisplatin doses in C57BL/6 mice did not lead to immune cell infiltration in the kidneys [44]. Interestingly, this group also reported only mild levels of fibrosis. In contrast, we found a significant increase in renal CD45+ immune cells, specifically macrophage and monocyte populations. This variability could be due to several factors. In discussion with this group, we have noted differences in the type of cisplatin given (our lab uses pharmaceutical grade pre-dissolved cisplatin while their lab uses cisplatin purchased as a powder and then dissolved in-house) as well as time of day of cisplatin injections. Administration of cisplatin at different times of day does alter its impact on kidney function and fibrosis (unpublished data in the Siskind laboratory). As displayed in this study, there is also inherent variability in different cohorts of C57BL/6 mice which could explain the different responses. Despite this inherent variability, Fu et. al. recently published findings similar to ours using repeated 8 mg/kg cisplatin doses in C57BL/6 mice, indicating there is reproducibility across some settings [45].

Macrophages have been studied in many different models of renal fibrosis. As in other organs, renal inflammation following an insult is a common precursor to fibrosis development [34, 128, 129]. In models of ischemia-

reperfusion, depletion of macrophages and monocytes with liposome encapsulated clodronate attenuates renal fibrosis [93, 130-132]. Similar results were also noted in models of unilateral ureteral obstruction [95, 133]. The role of macrophages in CKD is complex due to the diverse activity and heterogeneity of cell types [134]. Some studies suggest persistent “M2” macrophage activity could be a driver of renal fibrosis [93, 133]. We hypothesize that the repeated nature of injury in our repeated dosing model likely leads to sustained renal inflammation and persistent repair-like activities with M2-polarization. Future studies will determine if macrophage subsets are major drivers of fibrosis development in this model.

Taken together, this study indicates the importance of choosing the correct mouse strain and dosing regimen for renal studies. We have observed that group variability, in terms of renal function and structural damage, is inherent in the cisplatin model of injury, but our repeated dosing regimen of cisplatin consistently induces fibrosis in C57BL/6 mice with an increased cisplatin dose of 9 mg/kg. Administration of subcutaneous saline may also be used to prevent weight loss. This dosing regimen also has a low rate of animal death. This study demonstrates C57BL/6 mice are a viable option to use as a model of repeated low dose cisplatin-induced fibrosis. We also demonstrate the importance of using littermate control mice in this model due to population variability in renal function and tubular damage.

CHAPTER 3: RESIDENT AND INFILTRATING MACROPHAGES HAVE DIFFERENT ROLES IN CISPLATIN-INDUCED FIBROSIS

INTRODUCTION

Cisplatin (cis-diamminedichloroplatinum(II)) has become a widely used chemotherapeutic for the treatment of many solid-organ cancers since its FDA approval in 1978. Unfortunately, the success in treating these cancers with cisplatin is still hindered by dose-limiting nephrotoxicity. 30% of patients treated with cisplatin develop acute kidney injury (AKI) [2, 5, 9]. AKI not only warrants suspension of cisplatin treatment, but also puts patients at risk for long term declines in renal function, fibrosis development, and chronic kidney disease (CKD) [22-24, 36, 110]. The development of fibrosis following AKI has only recently begun to be modeled in rodents [47, 135]. Cisplatin-induced renal fibrosis is now modeled using a repeated low dose cisplatin (RLDC) regimen in mice [39, 86]. In this model, 4 weekly doses of 7-9 mg/kg cisplatin leads to development of renal fibrosis accompanied by renal immune cell infiltration [86]. Comparing the traditional, high-dose cisplatin model and the RLDC model highlights the biological differences occurring in acute and chronic injury processes [136]. These differences necessitate more studies on the mechanisms of AKI-to-CKD transition following cisplatin treatment.

Fibrosis development is a hallmark of the progression of AKI to CKD. Processes of maladaptive repair such as tubule G2/M cell cycle arrest, cellular senescence, chronic inflammation, and chronic vascular impairment drive the development of fibrosis following AKI [25]. With repeated insults, these maladaptive processes become more and more likely as normal repair processes are interrupted and immune cells are chronically recruited to sites of injury [25, 58, 81]. Macrophages respond to episodes of AKI and play important roles in clearing cellular debris and orchestrating proper immune responses [33]. Chronic macrophage activity, however, can lead to excessive myofibroblast activation and collagen deposition promoting progression of renal fibrosis [34, 128].

Macrophages constitute a diverse group of cells with various origins and functions. Resident macrophages are seeded in the kidney during embryonic development [137]. These macrophages help maintain renal homeostasis by silently clearing cellular debris and aiding in tissue remodeling. They can be distinguished by high expression of F4/80 in mice [138-140]. Infiltrating macrophages differentiate from monocytes that are recruited to the kidney following injury [34]. The C-C motif chemokine receptor 2 (CCR2)/C-C motif chemokine ligand 2 (CCL2) (also known as monocyte chemoattractant protein 1 (MCP-1)) axis plays a major role in inflammatory monocyte recruitment and accumulation of infiltrating macrophages [125, 141, 142]. These macrophages can be distinguished by low expression of F4/80 in mice [140]. Both resident and infiltrating macrophages can adopt different phenotypes to perform a variety of functions. For simplicity, we will refer to the extreme ends of the functional

spectrum as M1 and M2 macrophages. M1 macrophages appear in the kidney rapidly following injury and are considered “pro-inflammatory.” M2 macrophages appear later in kidney injury and have a “pro-repair” and “anti-inflammatory” phenotype. Although M1 macrophages may still be present in chronic injury, development of renal fibrosis is associated with an M1 to M2 phenotype transition [34, 94].

Although macrophages have been implicated in development of fibrosis in other models of kidney injury, their role in the AKI-to-CKD progression following RLDC treatment remains unknown. In this study, we examine the response of resident and infiltrating macrophages in the kidney after RLDC treatment. We also evaluate development of fibrosis and injury in the RLDC model following depletion of macrophages via liposome encapsulated clodronate treatment or Ccr2 genetic knockout. Our results suggest that F4/80^{hi} resident macrophages contribute to fibrosis development and M2 polarization following RLDC treatment. These data suggest targeting resident macrophages could ameliorate the AKI-to-CKD transition following cisplatin treatment.

MATERIALS & METHODS

Animal Experiments. Eight-week-old male Ccr2 knockout (Ccr2^{-/-}) mice on a C57BL/6 background were purchased from The Jackson Laboratory (stock #004999) and bred with eight-week-old female C57BL/6 wild type (WT) mice also purchased from The Jackson Laboratory (stock 000664). Heterozygous offspring were then aged to eight-weeks-old and cross-bred to produce littermate WT and Ccr2^{-/-} mice. WT, eight-week-old male C57BL/6 mice were purchased from The

Jackson Laboratory (stock 000664) for liposome encapsulated clodronate experiments. All mice were maintained on a 12:12 hour light-dark cycle and provided food and water *ad libitum*. Animals were maintained under standard laboratory conditions. All animal procedures were approved by the Institutional Animal Care and Use Committee of the University of Louisville (Protocol ID 19568) and followed the guidelines of the American Veterinary Medical Association. Mice were intraperitoneally (i.p.) injected with either 0.9% N saline vehicle or cisplatin at 9 mg/kg at 8:00 AM once a week for four weeks and euthanized three days after the last dose. Pharmaceutical grade cisplatin purchased from the University of Louisville hospital pharmacy (1 mg/ml in 0.9% N saline from Intas Pharmaceuticals) was used for all experiments. Standard Macrophage Depletion Kit (Clodrosome + Encapsome) was purchased from Encapsula Nanosciences (CLD-8901). 200 μ L of either liposome encapsulated clodronate (Clodrosome) or empty liposomes (Encapsome) was intravenously (i.v.) administered one day before the third and fourth dose of cisplatin. 100 μ L of either Clodrosome or Encapsome was i.v. administered the day after the third and fourth dose of cisplatin, as well as four days after the third dose of cisplatin. Mice were monitored for weight loss or evidence of high levels of discomfort/stress. Upon euthanasia, plasma was prepared and stored at -80°C. One kidney was divided into sections to be flash-frozen in liquid nitrogen or fixed in 10% neutral buffered formalin. The other kidney was taken for immune cell analysis by flow cytometry.

Blood urea nitrogen (BUN) and neutrophil gelatinase associated lipocalin (NGAL) determination. BUN was measured in the plasma of mice using a kit from AMS Diagnostics (80146, AMS Diagnostics) per the manufacturer's instructions, and as previously published [39]. ELISA for NGAL (DY1857, R&D Systems) was performed on mouse urine as previously published [39].

Gene expression. Total RNA was isolated from kidney cortex, and cDNA was made as previously published [39]. The following pre-designed TAQman primers (Life Technologies) were used: *Tnfa* (Mm00443258_m1), *Il-6* (Mm00446190_m1), *Cxcl1* (Mm04207460_m1), *Ccl2* (Mm00441242_m1), *B2m* (Mm00437762_m1), and *Arg-1* (Mm00475988_m1). The following self-designed primers were used: *Kim-1* forward AGATCCACACATGTACCAACATCAA and reverse CAGTGCCATTCCAGTCTGGTTT; *Col1a1* forward CGATGGATTCCCGTTTCGAGTA and reverse GTGGACATTAGGCGCAGGAA; *Tgfb* forward CAACATGTGGA ACTCTACCAGAAATATAG and reverse ACAACTCCAGTGACGTCAAAGAC; *Timp-1* forward GCAACTCGGACCTGGTCATAA and reverse TTAGTCATCTTGATCTTATAACGCTGGTA. Real-time qRT-PCR was performed using iTaq Universal Probes Supermix (172-5134, Bio-Rad) or iTaq Universal SYBR Green Supermix (172-5124, Bio-Rad).

Immunohistochemistry, Sirius Red/Fast Green (SR/FG), and Masson's trichrome staining. Alpha smooth muscle actin (α SMA) immunohistochemistry for myofibroblasts and SR/FG stain for total collagen deposition was performed on paraffin embedded kidney sections as previously published [39]. Masson's

trichrome staining was performed using the Trichrome Stain (Masson) Kit (HT15, Sigma-Aldrich). Paraffin-embedded tissue was deparaffinized, rehydrated, and placed in Bouin's solution (HT10132, Sigma-Aldrich) at 56°C for 15 minutes under chemical hood. Sections were washed in running tap water for 10 minutes. Sections were then stained with Weigert's iron hematoxylin solution (HT1079, Sigma-Aldrich) for 5 minutes, washed in running tap water for 5 minutes, and stained in Biebrich Scarlet-Acid Fuschin for 5 minutes. Sections were rinsed briefly in distilled water then stained with Phosphotungstic/Phosphomolybdic Acid solution for 15 minutes before being directly placed into Aniline Blue solution for 10 minutes. Lastly, sections were rinsed briefly in distilled water before dehydrating and clearing sections for mounting.

Flow Cytometry. Whole kidneys were homogenized into single cell suspensions and prepared for staining as previously described [86]. Cells were blocked with CD16/32 (101321, BioLegend) and extracellularly stained with: CD45-PerCP (103130, BioLegend), CD3e-PE-Cy7 (552774, BD Biosciences), CD19-PE-CF594 (562329, BD Biosciences), CD4-FITC (100406, BioLegend), CD8a-BUV737 (612759, BD Biosciences), Ly-6G-Alexa Fluor 700 (561236, BD Biosciences) Ly-6C-APC-Cy7 (560596, BD Biosciences), F4/80-BV421 (565411, BD Biosciences), CD11b-BV650 (563402, BD Biosciences), and PDGFR α -BUV737 (741789, BD Biosciences). After staining, cells were fixed and permeabilized with FoxP3/Transcription Factor Staining Buffer Set (00-5523-00, Invitrogen). Intracellular staining was done with CD206-PE (141705, BioLegend). Flow cytometry was done using a BD LSRFortessa, collecting 1 million events

per sample. Hierarchical gating was performed as depicted in Figure 15. Data are represented as the percentage of positively stained cells for the indicated population from the total number of single cells observed in that sample.

Resident macrophages are identified as CD45+CD3-CD19-CD11b+F4/80^{hi}.

Infiltrating macrophages are identified as CD45+CD3-CD19-CD11b+F4/80^{lo}.

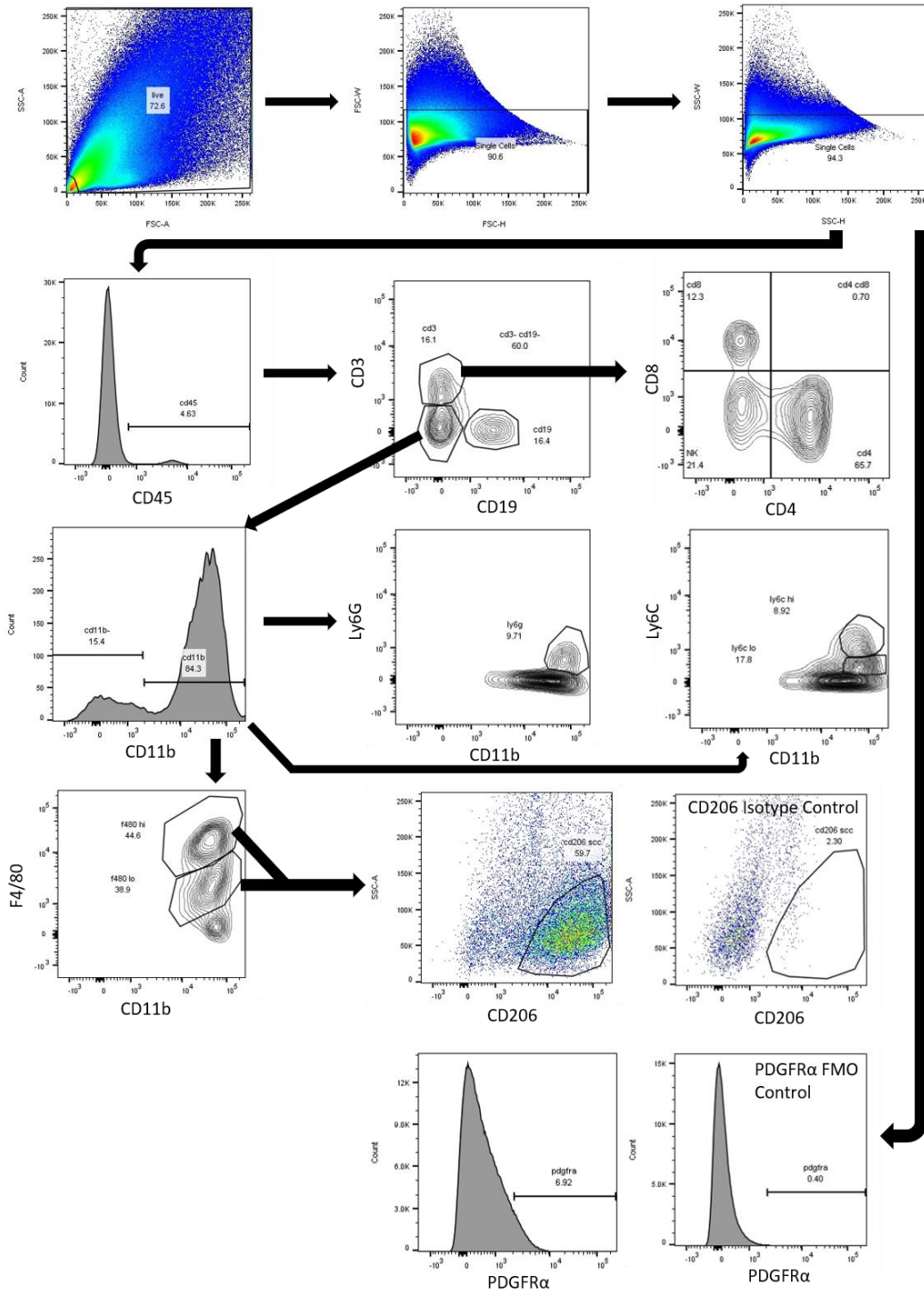


Figure 15. Hierarchical gating strategy for flow cytometry. Debris was gated out based on FSC-A x SSC-A plot. Doublet exclusion was performed. CD45+ Immune cells were selected. CD3+ T cells and CD19+ B cells were excluded

from myeloid cell analysis. CD11b⁺ cells were selected. Ly6g, Ly6c^{hi}, and Ly6c^{lo} cells were identified from CD11b⁺ cells. F4/80^{hi} and F4/80^{lo} cells were identified from CD11b⁺ cells. CD206⁺ cells were selected from all F4/80⁺ cells. PDGFR α ⁺ cells were identified from single cell gate.

Statistical analysis. Data are expressed as means \pm standard error of the mean (SEM) for all experiments. Comparisons of normally distributed data sets were analyzed by either a one-way or two-way ANOVA as appropriate and group means were compared using Tukey post-tests. Correlations were determined using a linear regression model. The criteria for statistical differences were $p < 0.05$.

RESULTS

Renal macrophage infiltration correlates with kidney injury and fibrosis markers but not BUN elevation following RLDC. To determine if macrophages were playing a role in promoting the AKI-to-CKD transition following RLDC treatment, we first analyzed data from cisplatin treated C57BL/6 wild type male mice to compare the degree of macrophage infiltration with degree of functional loss, kidney injury, and fibrosis. Macrophage infiltration did not significantly correlate with BUN elevation, indicating no correlation with functional loss (Fig 16A). In contrast, macrophage infiltration did correlate with elevation of mRNA injury markers *Kim-1* and *Ccl2* (Fig 16B-C), as well as elevation of mRNA fibrotic markers *Timp-1* and *Col1a1* (Fig 16D-E). We further divided the data to assess how F4/80^{hi} resident macrophages and F4/80^{lo} infiltrating macrophages correlated with these markers. While only F4/80^{hi} resident macrophage accumulation correlated with elevation of mRNA injury markers *Kim-1* and *Ccl2* (Fig 17A-D), both macrophage populations correlated with elevation of fibrotic mRNA markers *Timp-1* and *Col1a1* (Fig 17E-H). These data suggest that

resident and infiltrating macrophages may be playing different roles in the AKI-to-CKD transition following RLDC.

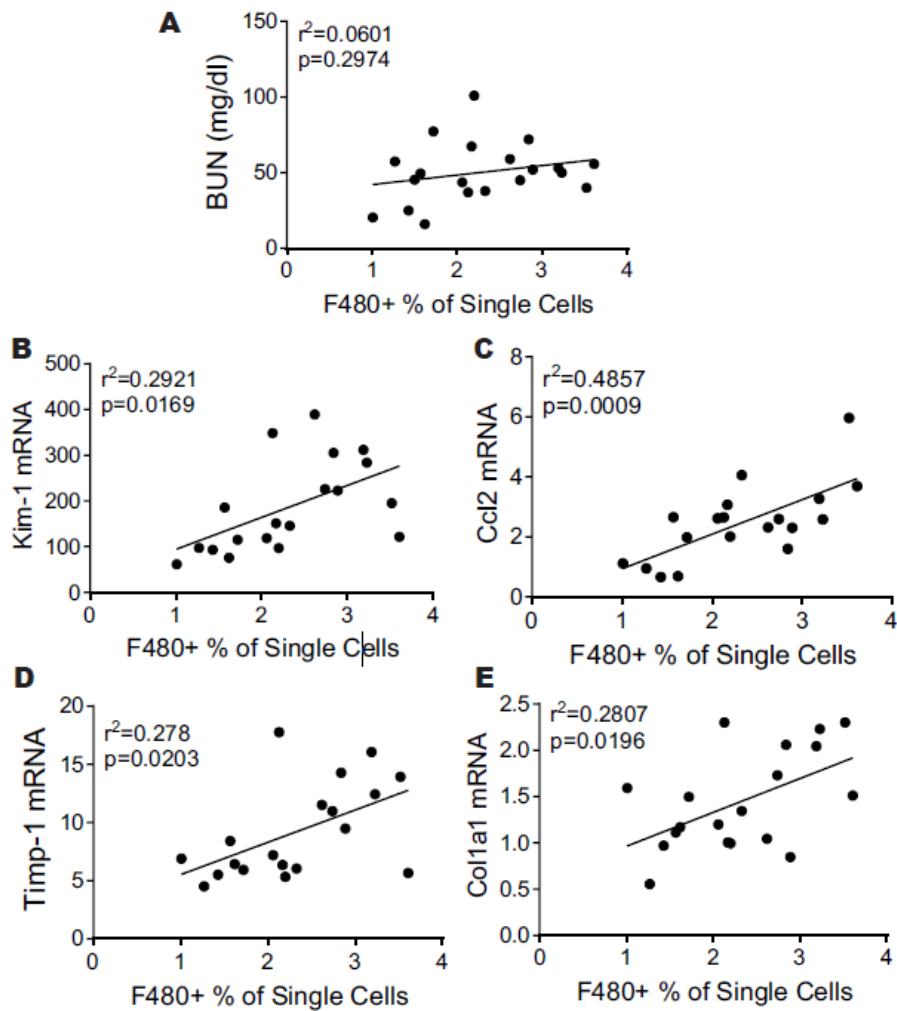


Figure 16. Macrophage infiltration correlates with kidney injury and fibrosis markers but not BUN following RLDC treatment. Renal infiltration of total F4/80 macrophages in cisplatin treated wild type C57BL/6 male mice was plotted against (A) BUN, (B-C) kidney injury mRNA makers, and (D-E) fibrotic mRNA markers following RLDC treatment. Significant correlations were determined as $p < 0.05$ using a linear regression model.

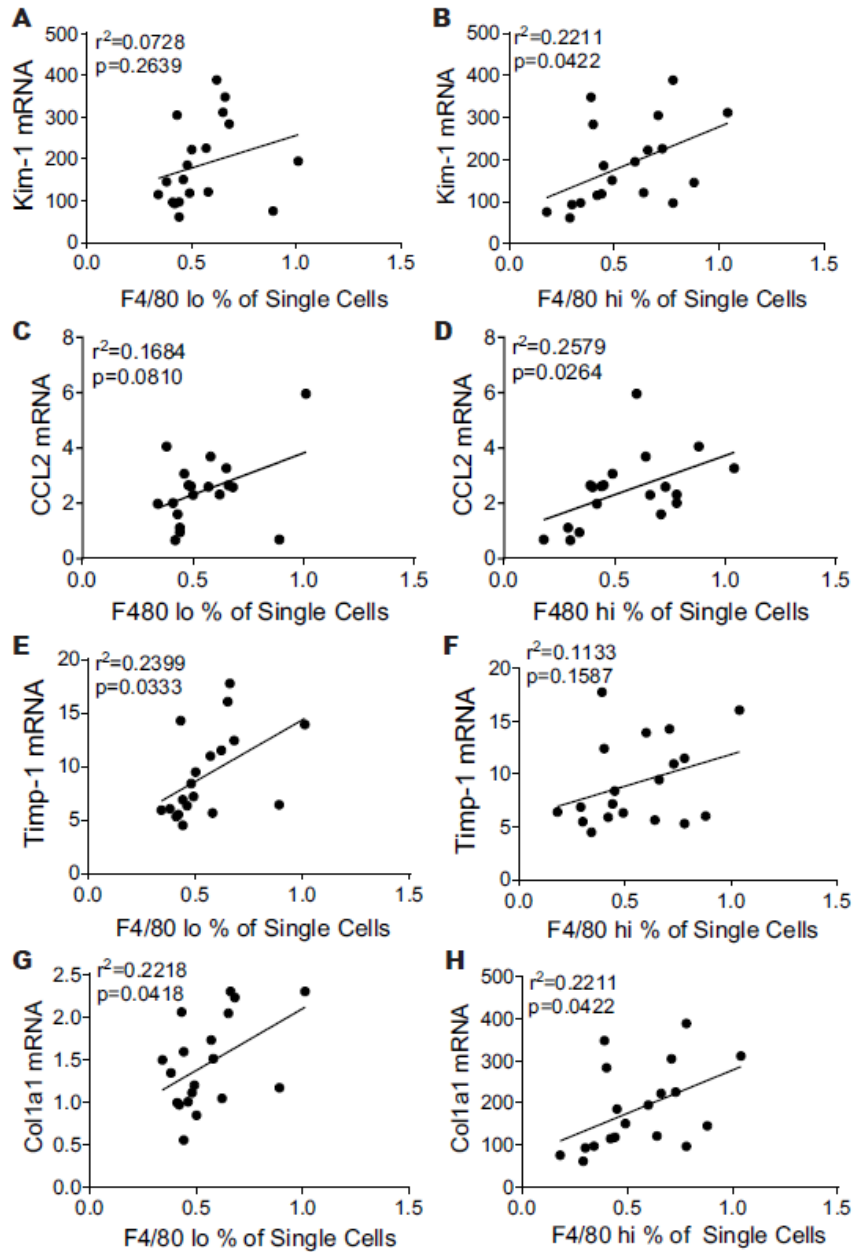


Figure 17. Resident macrophages correlate with kidney injury and fibrosis

markers following RLDC treatment. The percentage of F4/80^{hi} resident and F4/80^{lo} infiltrating macrophages in the kidney of cisplatin treated C57BL/6 male mice following RLDC treatment was plotted against (A-D) expression of kidney injury mRNA markers and (E-H) expression of fibrotic mRNA markers.

Significance was determined at $p < 0.05$ using a linear regression model.

Ccr2^{-/-} mice have reduced renal F4/80^{lo} infiltrating macrophages following RLDC. We assessed immune cell infiltration in kidneys of littermate C57BL/6 wild type and Ccr2^{-/-} mice following RLDC treatment. Cisplatin treated Ccr2^{-/-} mice had slightly less overall infiltration of CD45⁺ immune cells compared to cisplatin treated wild type mice although results were not significant (Fig 18A). F4/80^{hi} resident macrophage levels remained unchanged in all groups (Fig 18B). F4/80^{lo} infiltrating macrophages were significantly increased in cisplatin treated wild type mice compared to vehicle treated animals. Ccr2^{-/-} blocked this infiltration, keeping infiltrating macrophage populations at baseline levels (Fig 18C). CD206⁺ M2 macrophages were similarly elevated in cisplatin treated wild type and Ccr2^{-/-} mice compared to vehicle treated mice (Fig 18D). Cisplatin treated mice Ccr2^{-/-} mice also had impaired Ly6C^{hi} inflammatory monocyte recruitment compared to cisplatin treated wild type mice (Fig 18E). No changes in other immune cell populations in Ccr2^{-/-} cisplatin treated mice compared to wild type mice were observed (Fig 19A-H). Ccr2^{-/-} mice also had basally reduced circulating macrophages and inflammatory monocytes in the blood compared to wild type mice (Fig 20A-D). These data suggest that Ccr2^{-/-} mice have inhibited monocyte recruitment to the kidney following RLDC treatment, leading to decreased levels of F4/80^{lo} infiltrating macrophages. It also suggests CD206⁺ M2 macrophages accumulation can occur without significant contributions from the infiltrating macrophage population.

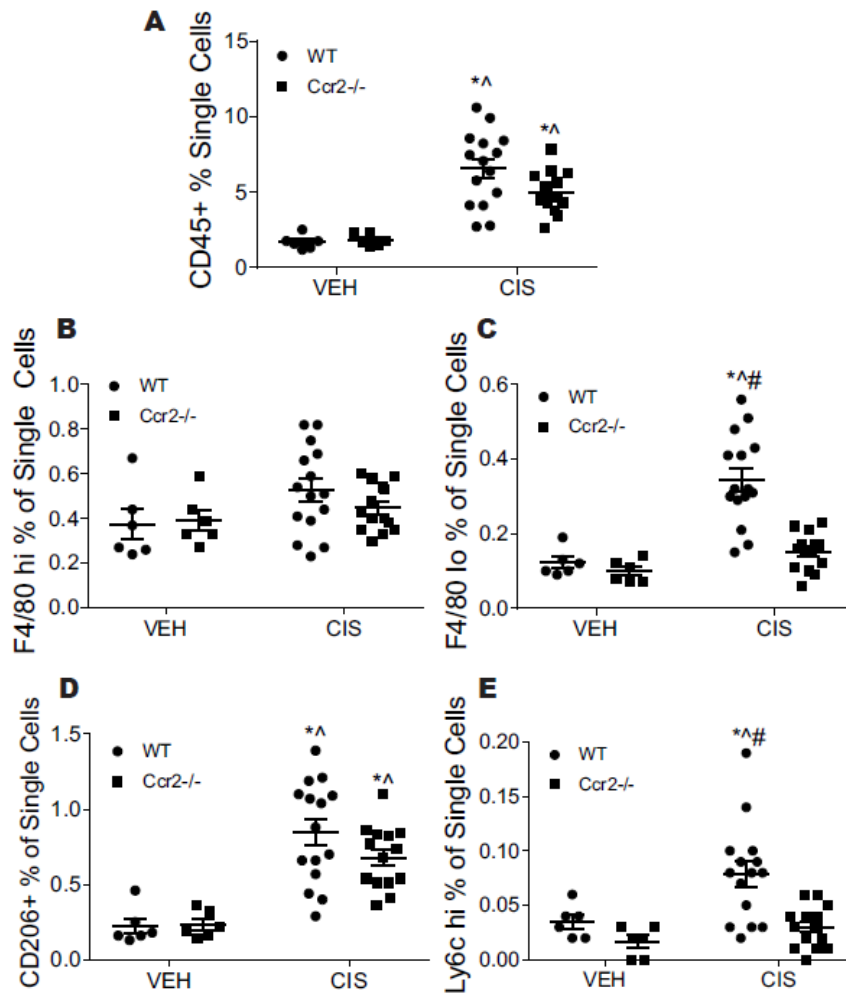


Figure 18. *Ccr2*^{-/-} blocks inflammatory monocyte and macrophage infiltration with no effect on resident or M2 macrophages. Whole kidneys were homogenized into a single cell suspension for flow cytometric analysis of immune cells. Hierarchical gating was performed to identify (A) CD45⁺ cells, (B) F4/80^{hi} resident macrophages, (C) F4/80^{lo} infiltrating macrophages, (D) CD206⁺ M2 macrophages, and (E) Ly6C^{hi} inflammatory monocytes present in the kidney following RLDC treatment. Data are presented as percentage of positively labeled cells from the total number of single cells counted for each sample. Statistical analysis was determined by two-way ANOVA followed by Tukey post-

test. Significance was determined at $p < 0.05$. VEH= vehicle, CIS= cisplatin, *= significantly different from WT VEH, ^= significantly different from $Ccr2^{-/-}$ VEH, #= significantly different from $Ccr2^{-/-}$ CIS.

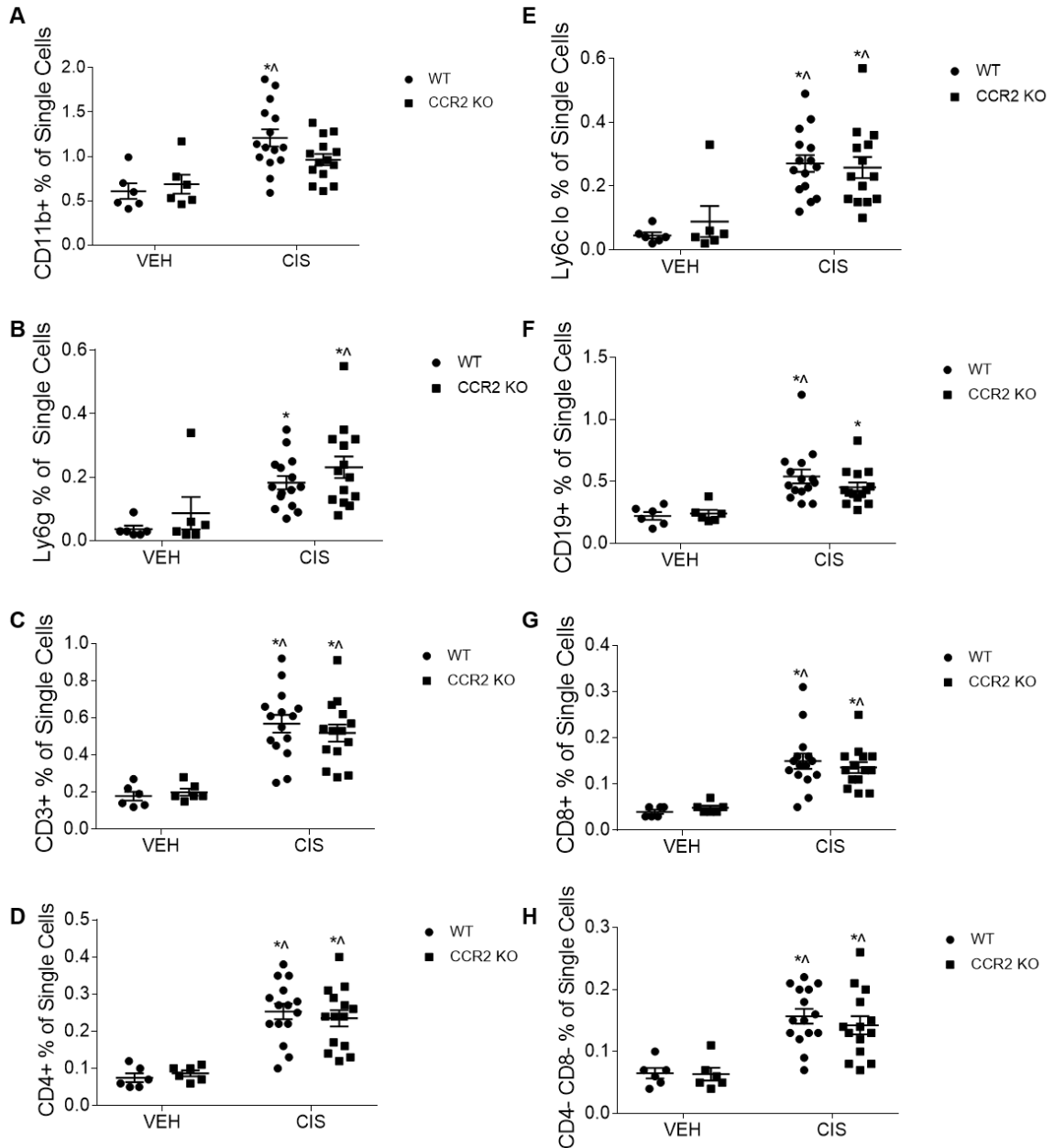


Figure 19. Immune cell alterations in *Ccr2*^{-/-} kidney. Whole kidneys were homogenized into a single cell suspension for flow cytometric analysis of immune cells. Hierarchical gating was performed to identify (A) CD11b+ cells, (B) Ly6g neutrophils, (C) CD3+ T cells, (D) CD3+CD4+ T cells, (E) Ly6c^{lo} patrolling monocytes, (F) CD19+ B cells, (G) CD3+CD8+ T cells, and (H) CD3+CD4-CD- cells present in the kidney following RLDC treatment. Data are presented as

percentage of positively labeled cells from the total number of single cells counted for each sample. Statistical analysis was determined by two-way ANOVA followed by Tukey post-test. Significance was determined at $p < 0.05$. VEH= vehicle, CIS= cisplatin. (A-D) *- significantly different from WT VEH, ^- significantly different from $Ccr2^{-/-}$ VEH, #- significantly different from $Ccr2^{-/-}$ CIS.

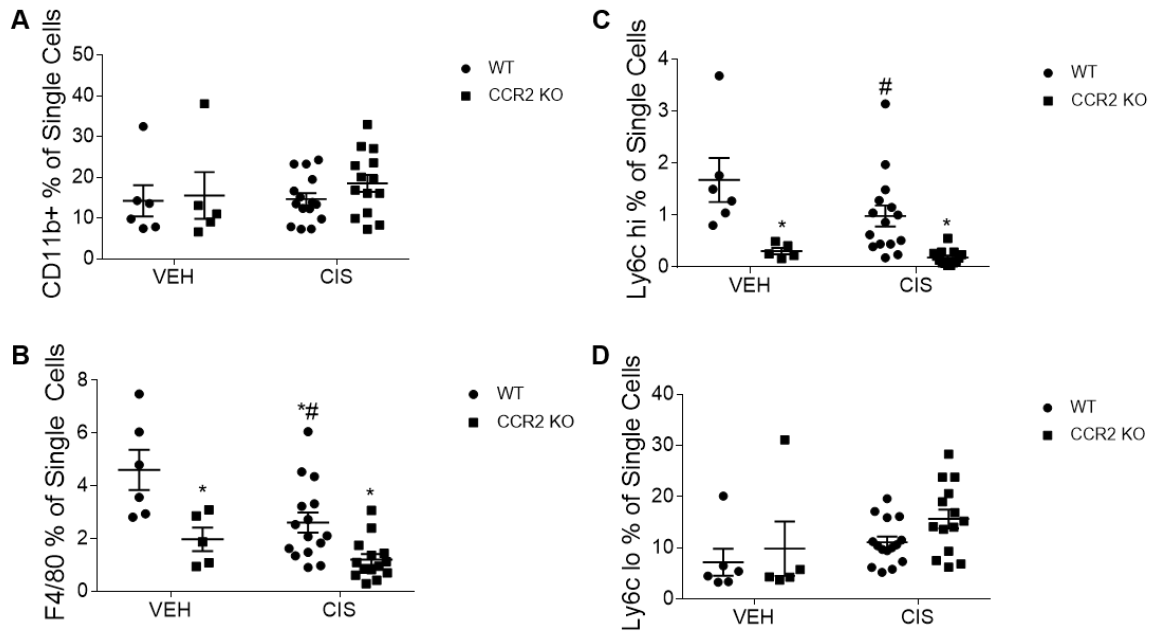


Figure 20. Immune cell alterations in *Ccr2*^{-/-} blood. Whole blood was stained for flow cytometric analysis of immune cells. Hierarchical gating was performed to identify (A) CD11b⁺ cells, (B) F4/80 macrophages, (C) Ly6c^{hi} inflammatory monocytes, and (D) Ly6c^{lo} patrolling monocytes present in the blood following RLDC treatment. Data are presented as percentage of positively labeled cells from the total number of single cells counted for each sample. Statistical analysis was determined by two-way ANOVA followed by Tukey post-test. Significance was determined at $p < 0.05$. VEH= vehicle, CIS= cisplatin. (A-D) *- significantly different from WT VEH, ^- significantly different from *Ccr2*^{-/-} VEH, #- significantly different from *Ccr2*^{-/-} CIS.

Clodrosome depletes renal F4/80^{hi} resident macrophages and CD206+ M2 macrophages following RLDC. Overall CD45+ immune cell infiltration was similarly elevated in all cisplatin treated groups compared to vehicle (Fig 21A). Interestingly, Clodrosome treatment led to a significant decrease in F4/80^{hi} resident macrophages compared to all other groups, including vehicle treated mice (Fig 21B). In contrast, F4/80^{lo} infiltrating macrophage populations were not affected by Clodrosome treatment among cisplatin treated groups at the timepoint observed (Fig 21C). CD206+ M2 macrophage accumulation following cisplatin treated was significantly reduced by Clodrosome (Fig 21D). This matched a decrease in *Arg-1* mRNA expression in the kidney of Clodrosome treated mice compared to other cisplatin treated groups (Fig 21E). We also observed a significant decrease in CD3+CD4-CD8- immune cells and an increase in inflammatory monocytes and neutrophils (Fig 22A-I). Clodrosome also increased circulating myeloid cells in the blood at the timepoint observed (Fig 23A-E). These data suggest that Clodrosome treatment reduces resident macrophage populations in the kidney, leading to reduced CD206+ M2 macrophage accumulation following RLDC.

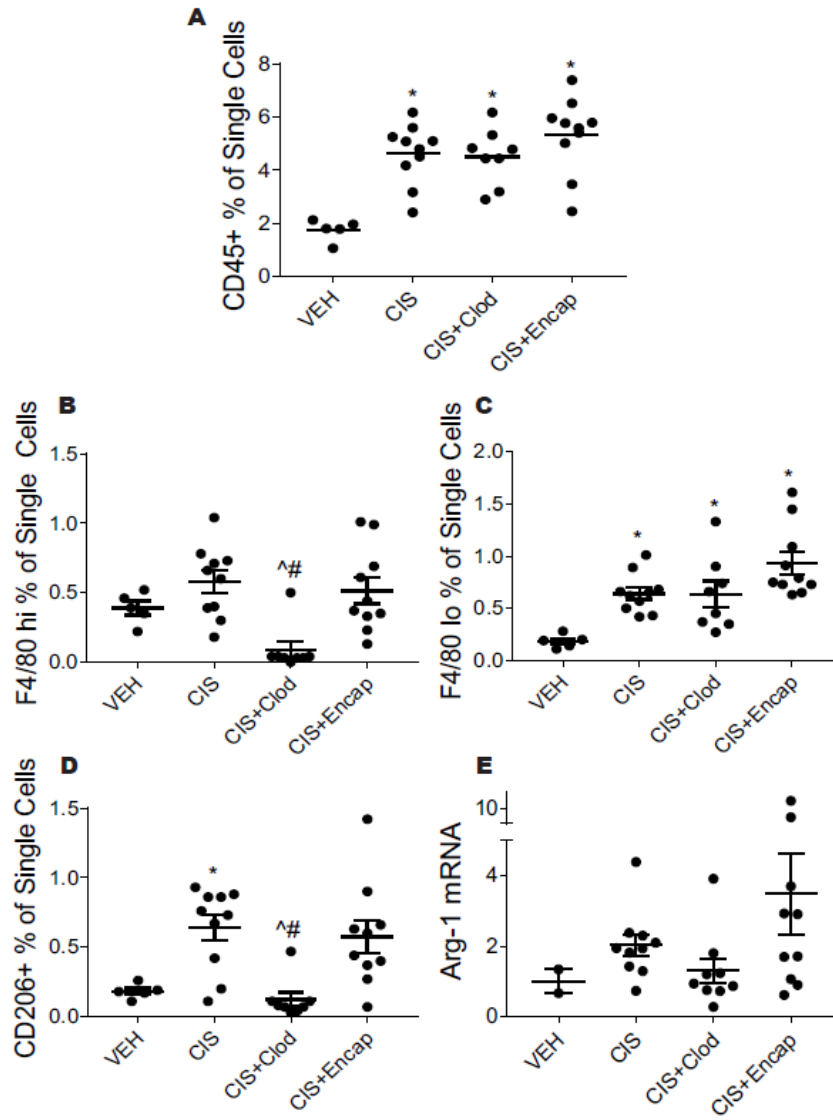


Figure 21. Clodrosome depletes renal resident and M2 macrophages with no effect on infiltrating macrophages. Whole kidneys were homogenized into a single cell suspension for flow cytometric analysis of immune cells. Hierarchical gating was performed to identify (A) CD45+ cells, (B) F4/80^{hi} resident macrophages, (C) F4/80^{lo} infiltrating macrophages, and (D) CD206+ M2 macrophages present in the kidney following RLDC treatment. Data are presented as percentage of positively labeled cells from the total number of

single cells counted for each sample. (D) mRNA expression of Arg-1 was measured relative to B2m in the kidney cortex. Statistical analysis was determined by one-way ANOVA followed by Tukey post-test. Significance was determined at $p < 0.05$. VEH= vehicle, CIS= cisplatin, CIS+Clod= cisplatin plus Clodosome, CIS+Encap= cisplatin plus Encapsome. *= significantly different from VEH, ^= significantly different from CIS, #= significantly different from CIS+Encap.

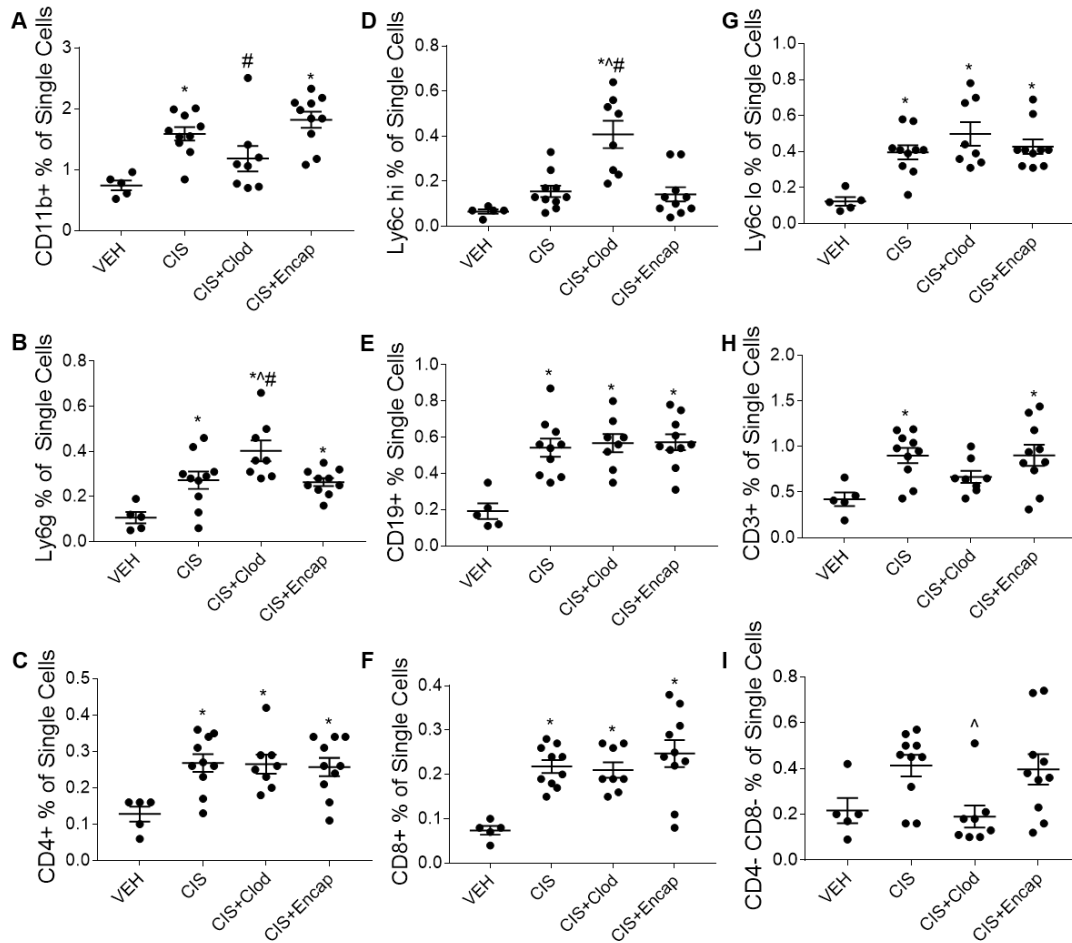


Figure 22. Immune cell depletion in the kidney following Clodrosome

treatment. Whole kidneys were homogenized into a single cell suspension for flow cytometric analysis of immune cells. Hierarchical gating was performed to identify (A) CD11b+ cells, (B) Ly6g neutrophils, (C) CD3+CD4+ T cells, (D) Ly6c^{hi} inflammatory monocytes, (E) CD19+ B cells, (F) CD3+CD8+ T cells, (G) Ly6c^{lo} patrolling monocytes, (H) CD3+ T cells, and (I) CD3+CD4-CD8- cells present in the kidney following RLDC treatment. Data are presented as percentage of positively labeled cells from the total number of single cells counted for each sample. Statistical analysis was determined by one-way ANOVA followed by Tukey post-test. Significance was determined at $p < 0.05$. VEH= vehicle, CIS=

cisplatin, CIS+Clod= cisplatin plus Clodrosome, CIS+Encap= cisplatin plus Encapsome. *= significantly different from VEH, ^= significantly different from CIS, #= significantly different from CIS+Encap.

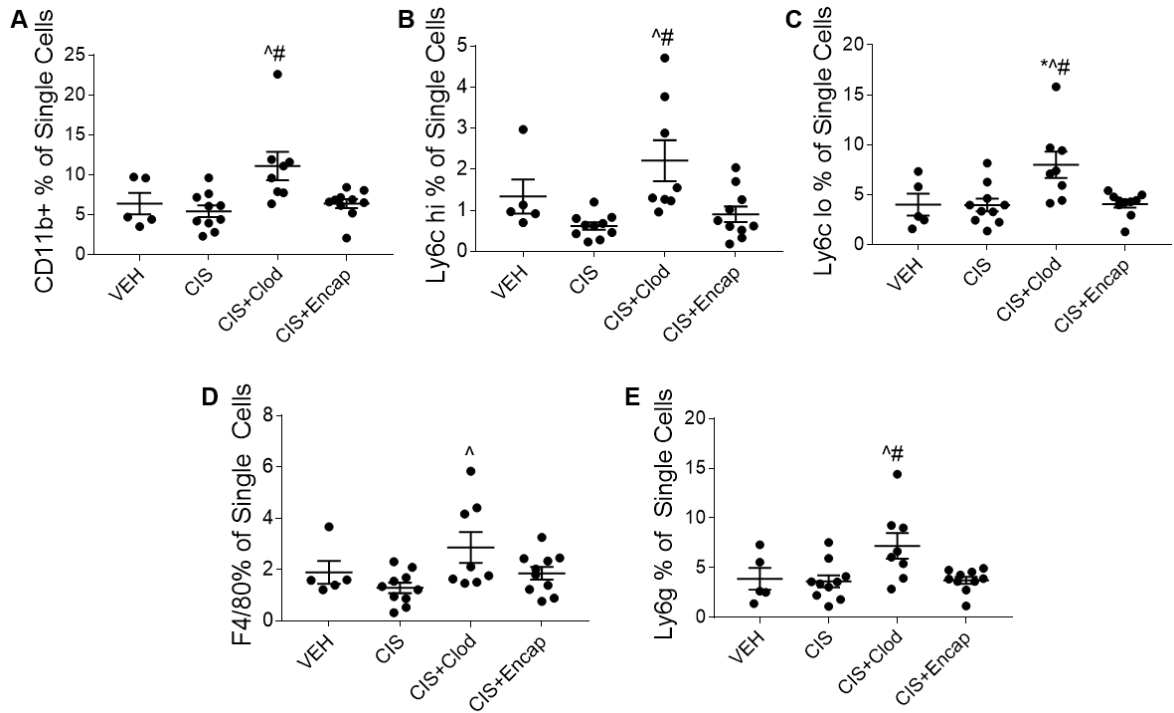


Figure 23. Immune cell depletion in the blood following Clodrosome

treatment. Whole blood was stained for flow cytometric analysis of immune cells.

Hierarchical gating was performed to identify (A) CD11b⁺ cells, (B) Ly6c^{hi}

inflammatory monocytes, (C) Ly6c^{lo} patrolling monocytes, (D) F4/80

macrophages, and (E) Ly6g neutrophils present in the kidney following RLDC

treatment. Data are presented as percentage of positively labeled cells from the

total number of single cells counted for each sample. Statistical analysis was

determined by one-way ANOVA followed by Tukey post-test. Significance was

determined at $p < 0.05$. VEH= vehicle, CIS= cisplatin, CIS+Clod= cisplatin plus

Clodrosome, CIS+Encap= cisplatin plus Encapsome. * = significantly different

from VEH, ^ = significantly different from CIS, # = significantly different from

CIS+Encap.

Inflammatory cytokine and chemokine production is reduced by

Clodrosome treatment but not *Ccr2*^{-/-}. We measured mRNA expression of

Tnfa, *Ccl2*, *Il6*, and *Cxcl1* in the kidney cortex following RLDC treatment. *Ccr2*^{-/-}

had no effect on cisplatin-induced elevation of *Tnfa* and *Ccl2* (Fig 24A-B).

Unexpectedly, cisplatin treated *Ccr2*^{-/-} mice had increased elevation of *Il6* and

Cxcl1 expression compared to cisplatin treated wild type mice (Fig 24C-D).

Clodrosome treatment reduced induction of *Tnfa*, *Ccl2*, and *Il6* compared to other

cisplatin treated groups, although results were not significant (Fig 24E-G). No

effect was observed on induction of *Cxcl1* with Clodrosome treatment (Fig 24H).

These data suggest that Clodrosome treatment and resident macrophage

depletion mildly blunts the inflammatory cytokine and chemokine response

induced by RLDC treatment, while *Ccr2*^{-/-} knockout and infiltrating macrophage

depletion has no effect.

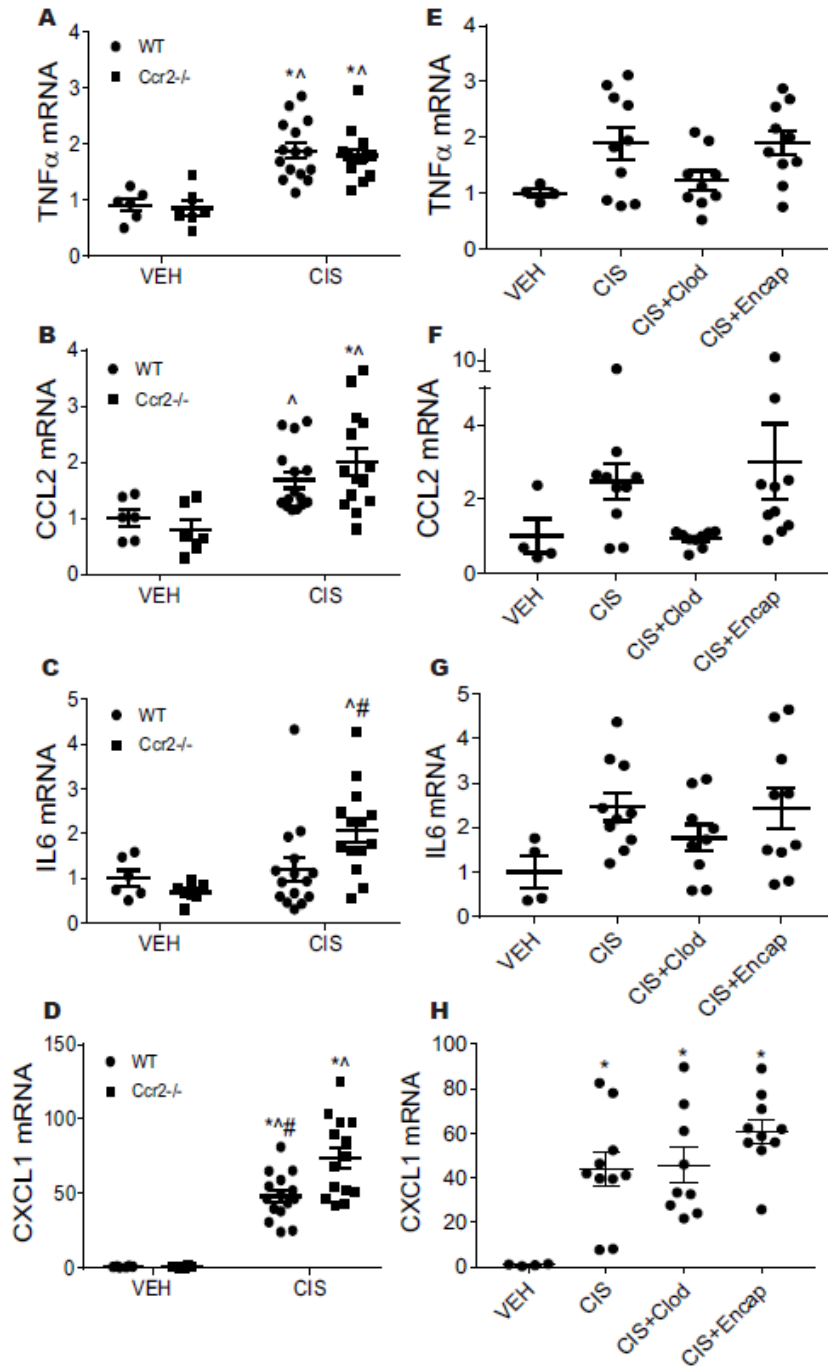


Figure 24. Clodrosome reduces inflammatory cytokine and chemokine induction following RLDC while *Ccr2*^{-/-} has no effect. RNA was isolated from kidney cortex tissue. mRNA expression of (A-B) *Tnfa*, (C-D) *Ccl2*, (E-F) *Il6*, and (G-H) *Cxcl1* was assessed relative to *B2m* expression. Statistical analysis was

determined by either one- or two-way ANOVA as appropriate followed by Tukey post-test. Significance was determined at $p < 0.05$. VEH= vehicle, CIS= cisplatin, CIS+Clod= cisplatin plus Clodrosome, CIS+Encap= cisplatin plus Encapsome. (A,C,E,G) *= significantly different from WT VEH, ^= significantly different from $Ccr2^{-/-}$ VEH, #= significantly different from $Ccr2^{-/-}$ CIS. (B,D,F,H) *= significantly different from VEH, ^= significantly different from CIS, #= significantly different from CIS+Encap.

Clodrosome treatment ameliorates cisplatin-induced renal fibrosis while

Ccr2^{-/-} has no effect. Collagen deposition was observed via SRFG and Masson trichrome staining. Both stains revealed decreased collagen deposition in Clodrosome treated mice compared to other cisplatin treated groups (Fig 25B and 25D). In contrast, cisplatin treated Ccr2^{-/-} mice had similar levels of collagen deposition compared to cisplatin treated wild type mice (Fig 25A and 25C). Myofibroblast accumulation was assessed using IHC staining for α SMA. RLDC treatment causes an increase in α SMA staining, typically observed in striated patterns through the corticomedullary region [39, 86]. Clodrosome treatment reduced α SMA staining compared to other cisplatin treated groups. α SMA staining in Clodrosome treated mice was also less striated and more scattered through the kidney (Fig 25F). In contrast, cisplatin treated Ccr2^{-/-} mice had a similar amount and pattern of α SMA staining compared to cisplatin treated wild type mice (Fig 25E). PDGFR α expression was also measured via flow cytometry to assess fibroblast and myofibroblast levels in the kidney following RLDC treatment. Clodrosome treatment caused a significant reduction in PDGFR α expression compared to Encapsome treated mice, but levels were the same as cisplatin only treated mice (Fig 25H). Cisplatin treated Ccr2^{-/-} mice had the same level of PDGFR α expression as cisplatin treated wild type mice (Fig 25G).

mRNA expression of *Timp-1*, *Col1a1*, *Tgf β* , and *Cdkn2a* in the kidney cortex was also used to assess fibrotic changes in the kidney following RLDC treatment. Clodrosome treatment significantly reduced *Timp-1* mRNA expression compared to other cisplatin treated groups (Fig 26B). Ccr2^{-/-} had no effect on

Timp-1 elevation following RLDC (Fig 26A). Similarly, Clodrosome treatment reduced expression of *Col1a1* and *Tgfβ* compared to other cisplatin treated groups, although results were not significant (Fig 26D and 26F). *Ccr2*^{-/-} had no effect on elevation of these fibrotic markers following RLDC treatment (Fig 26C and 26E). These data indicate that Clodrosome treatment reduced collagen deposition, myofibroblast accumulation, and induction of fibrotic mRNA expression in the kidney following RLDC while *Ccr2*^{-/-} had no effect.

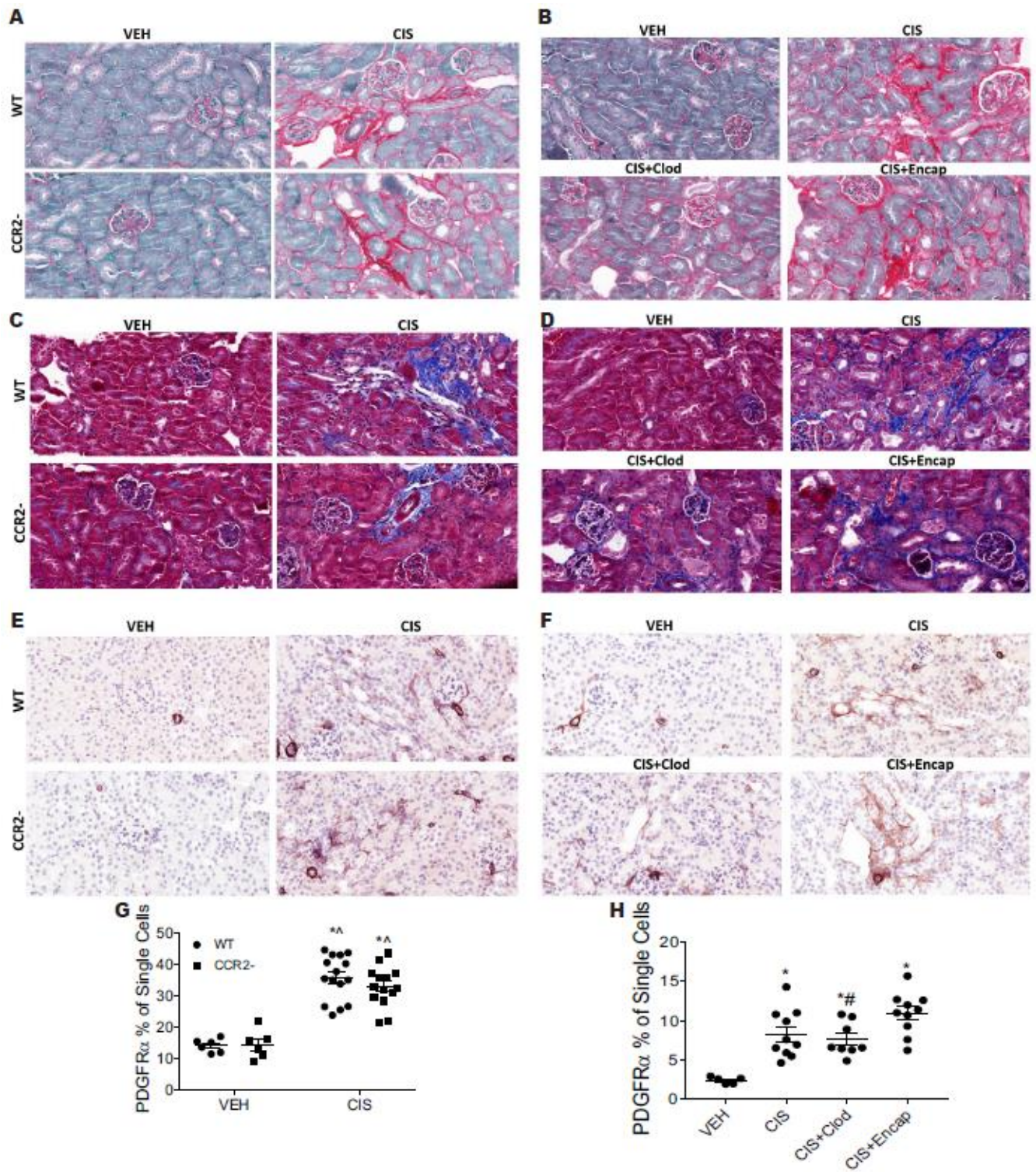


Figure 25. Clodrosome ameliorates RLDC induced renal fibrosis while *Ccr2*^{-/-} has no effect. (A-B) Sirius red/fast green, (C-D) Masson trichrome, and (E-F)

aSMA IHC staining of paraffin embedded kidney sections. (G-H) percent PDGFRa expressing cells of single cells counted in each sample run on flow cytometer. Statistical analysis was determined by one- or two-way ANOVA as appropriate followed by Tukey post-test. Significance was determined at $p < 0.05$. VEH= vehicle, CIS= cisplatin, CIS+Clod= cisplatin plus Clodrosome, CIS+Encap= cisplatin plus Encapsome. (G) *= significantly different from WT VEH, ^= significantly different from $Ccr2^{-/-}$ VEH, #= significantly different from $Ccr2^{-/-}$ CIS. (H) *= significantly different from VEH, ^= significantly different from CIS, #= significantly different from CIS+Encap.

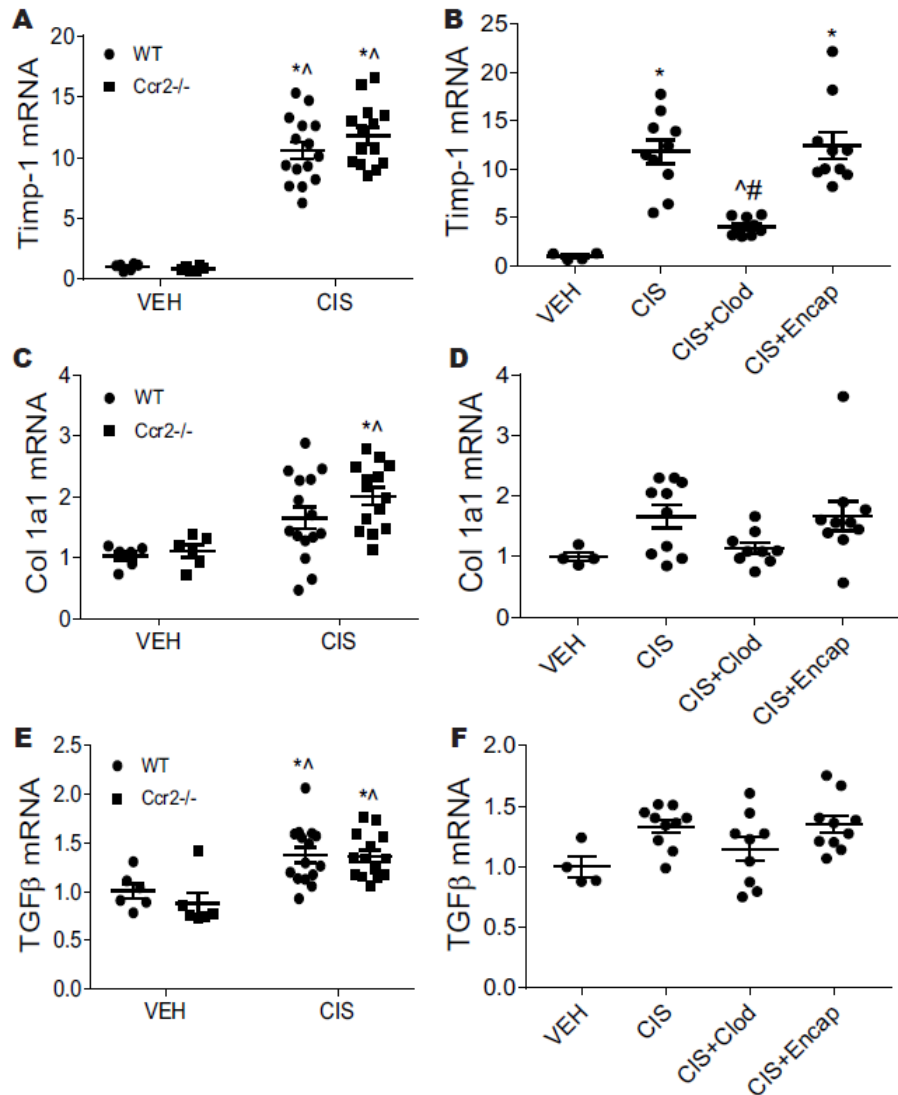


Figure 26. Clodrosome blunts RLDC induced fibrotic mRNA markers while *Ccr2*^{-/-} has no effect. RNA was extracted from kidney cortex tissue. mRNA expression of (A-B) Timp-1, (C-D) Col 1a1, and (E-F) Tgfb was assessed relative to B2m expression. Statistical analysis was determined by either one- or two-way ANOVA as appropriate followed by Tukey post-test. Significance was determined at $p < 0.05$. VEH= vehicle, CIS= cisplatin, CIS+Clod= cisplatin plus Clodrosome, CIS+Encap= cisplatin plus Encapsome. (A,C,E) *= significantly different from WT VEH, ^= significantly different from *Ccr2*^{-/-} VEH, #= significantly different from

Ccr2^{-/-} CIS.(B,D,F) *= significantly different from VEH, ^= significantly different from CIS, #= significantly different from CIS+Encap.

Clodrosome treatment reduces *Kim-1* mRNA expression following RLDC with no effect on BUN or NGAL. Surprisingly, neither Clodrosome treatment nor *Ccr2*^{-/-} prevented loss of kidney function following RLDC as measured by BUN (Fig 27A-B). Injury, as assessed by the AKI-biomarker NGAL, was also unchanged by Clodrosome and *Ccr2*^{-/-} (Fig 27C-D). *Kim-1* mRNA expression in the kidney cortex was significantly reduced in Clodrosome treated mice compared to other cisplatin treated groups (Fig 27F). This indicates less proximal tubule injury in mice receiving Clodrosome along with RLDC. *Ccr2*^{-/-} had no effect on *Kim-1* elevation following RLDC (Fig 27E). These data suggest that macrophage depletion does not impact development of AKI following cisplatin treatment by traditional markers but may prevent development of subclinical pathological changes.

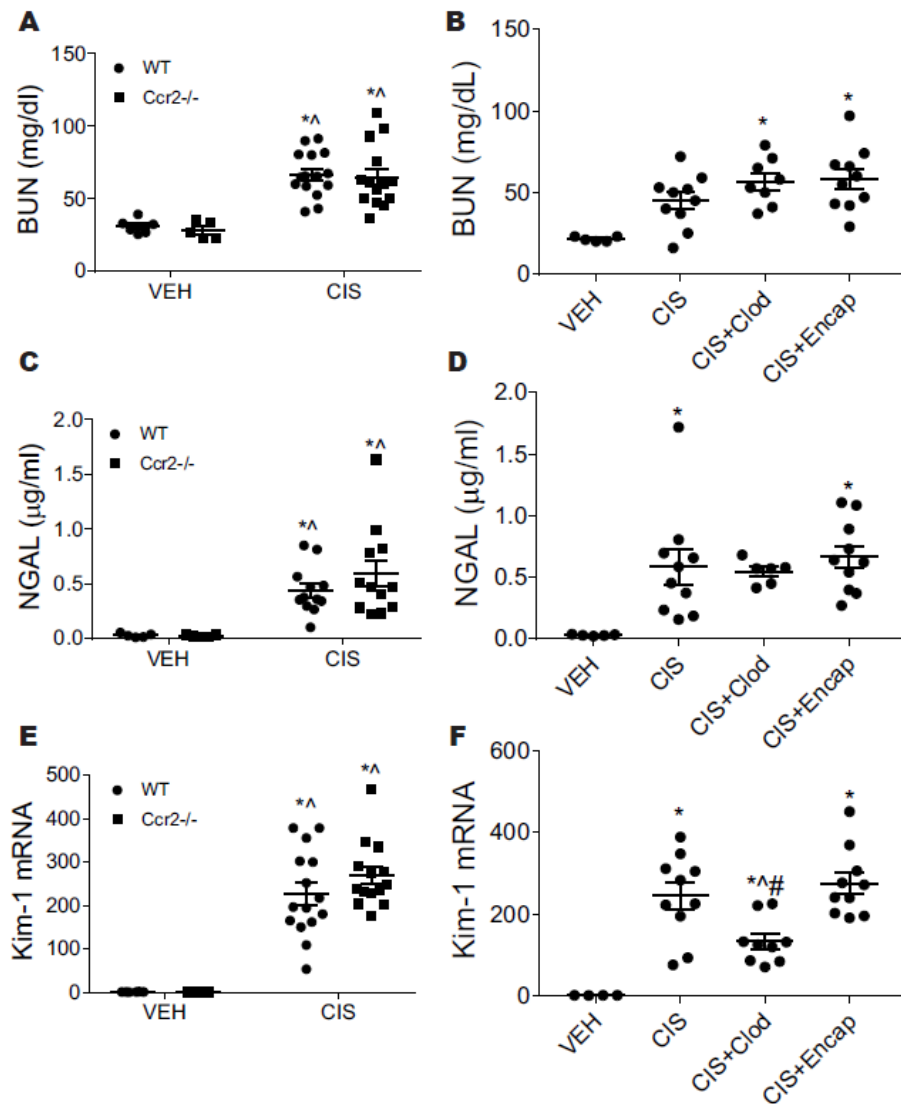


Figure 27. Clodrosome reduces Kim-1 expression but neither Clodrosome or *Ccr2*^{-/-} altered BUN or NGAL. (A-B) BUN was measured from plasma. (C-D) NGAL was measured from urine. (E-F) Kim-1 mRNA expression in the kidney cortex was assessed relative to B2m expression. Statistical analysis was determined by either one- or two-way ANOVA as appropriate followed by Tukey post-test. Significance was determined at $p < 0.05$. VEH= vehicle, CIS= cisplatin, CIS+Clod= cisplatin plus Clodrosome, CIS+Encap= cisplatin plus Encapsome.

(A,C,E) *= significantly different from WT VEH, ^= significantly different from Ccr2^{-/-} VEH, #= significantly different from Ccr2^{-/-} CIS.(B,D,F) *= significantly different from VEH, ^= significantly different from CIS, #= significantly different from CIS+Encap.

DISCUSSION

In this study, we examined how depletion of macrophage populations using either liposome encapsulated clodronate (Clodrosome) or Ccr2 genetic knockout impacted development of renal fibrosis following RLDC treatment. The differential effects these conditions had on immune cell populations allowed us to assess potential roles of F4/80^{hi} resident and F4/80^{lo} infiltrating macrophages separately in the development of fibrosis. We observed that Clodrosome depleted F4/80^{hi} renal resident and M2 macrophages following RLDC treatment with no effect on influx of F4/80^{lo} infiltrating macrophages at the timepoint observed. This depletion was accompanied by reduced fibrosis following RLDC treatment. In contrast, Ccr2 genetic knockout reduced F4/80^{lo} macrophage infiltration following RLDC treatment with no effect on resident or M2 macrophage accumulation. Ccr2 genetic knockout also had no effect on fibrosis development following RLDC treatment.

Other studies using liposome encapsulated clodronate have observed varied effects on macrophage populations in the kidney. These studies often report global depletion of macrophages, but do not differentiate between populations of resident and infiltrating macrophages [93, 95, 130-132, 143-145]. Interestingly, Yang et. al. utilized liposome encapsulated clodronate to deplete Ly6C⁺ tissue resident macrophages that were not depleted in the kidney of Ccr2^{-/-} mice [130]. These results indicated Ccr2 genetic knockout and liposome encapsulated clodronate alter different populations of macrophages. Additionally, Puranik et. al. reported that a single high dose of liposome encapsulated

clodronate depleted blood monocytes, but populations were recovering by 48 hours and were fully replenished by 72 hours. This single high dose of liposome encapsulated clodronate was also unsuccessful in depleting kidney resident macrophages. To achieve depletion of kidney resident macrophages, repeated low doses of clodronate were used [145].

These studies suggest that the dosing schedule and time of observation play a role in determining immune populations altered by clodronate encapsulated liposomes. In our study, we observed macrophage populations 48 hours after Clodrosome treatment. Bone-marrow derived immune cells may have had time to repopulate, causing an observed surge in inflammatory monocytes and neutrophils. Similar results have been reported [145]. It is important to consider that Clodrosome may be depleting F4/80^{lo} infiltrating macrophage populations at earlier unobserved timepoints. It is also important to note that Clodrosome treatment also depleted CD3+CD4-CD8- cells. Therefore, the protective effects observed with Clodrosome treatment in this study cannot be solely attributed to F4/80^{hi} resident macrophage depletion.

In other models of renal fibrosis, liposome encapsulated clodronate depletion of macrophages has been protective [93-96, 130-132, 143-145]. Our study supports these findings, indicating liposome encapsulated clodronate treatment targets immune cell populations that are pathogenic in processes of renal fibrosis. We believe the depletion of F4/80^{hi} resident and M2 macrophages by Clodrosome in our study is key to the protective effects observed. Kidney resident macrophages have been specifically implicated in fibrotic development

following ureteral obstruction and ischemia reperfusion [130, 141]. Additionally, M2 macrophage depletion by repeated administration of liposome encapsulated clodronate attenuated development of fibrosis following ureteral obstruction [133], and adoptive transfer of M2 macrophages to liposome encapsulated clodronate treated mice reversed protection from ischemia reperfusion induced fibrosis [93]. In this study, we observed that Clodrosome treatment reduced F4/80^{hi} resident and M2 macrophages while Ccr2 genetic knockout reduced F4/80^{lo} infiltrating macrophages with no effect on M2 macrophage accumulation. These data suggest that F4/80^{hi} kidney resident macrophages may be more susceptible to M2 polarization than F4/80^{lo} infiltrating macrophages. Although more studies are needed to examine this relationship, a predisposition towards M2 polarization could explain why kidney resident macrophages are more likely to promote development of fibrosis.

This study diverges from the literature in observations regarding Ccr2 genetic knockout effects on renal fibrosis development. Ccr2 genetic knockout has been shown to be protective in some models of renal fibrosis [125, 142, 146-148]. In contrast, Yang et. al. demonstrated that Ccr2 genetic knockout alleviated ischemia reperfusion induced AKI, but worsened subsequent development of fibrosis [130]. Our study demonstrated that Ccr2^{-/-} had no effect on development of fibrosis following RLDC treatment. We hypothesize that the CCR2/CCL2 signaling axis plays a role in cisplatin induced AKI, as indicated by its correlation with other markers of kidney injury [86], but this signaling axis may not be as important in the AKI-to-CKD transition following RLDC treatment. The

CCR2/CCL2 independence of RLDC-induced fibrosis highlights unique mechanisms of fibrosis development compared to ischemia-reperfusion and ureteral obstruction models of fibrosis.

The diverse activity of macrophages in the kidney leads to differential roles in injury development. In the high dose model of cisplatin-induced AKI, macrophage depletion with liposome encapsulated clodronate had no effect on development of AKI [89]. Importantly, liposome encapsulated clodronate depletion of macrophages after development of ischemia reperfusion induced AKI led to incomplete recovery, indicating essential roles for macrophages in the healing process [94]. In our study, macrophage depletion had no effect on BUN or NGAL elevation, which are used as markers of AKI development. This indicates that macrophages are not a viable target to prevent cisplatin-induced AKI; however, AKI-to-CKD transition processes may be prevented with macrophage depletion.

CHAPTER 4: OVERALL DISCUSSION

SUMMARY

Cisplatin is a commonly used chemotherapeutic agent with dose limiting nephrotoxicity. 10-20% of cancer patients will receive cisplatin as part of their treatment regimen [107]. 30% of these patients will develop acute kidney injury (AKI), or a rapid decline in renal function [2]. Even patients that do not develop AKI by clinical standards are still at risk for long term declines in renal function. Development of kidney injury greatly increases risk of mortality and development of chronic kidney disease (CKD) [22-24, 108, 109].

AKI is associated with high levels of tubule cell death, robust inflammation, and vascular damage [11]. This type of injury has been experimentally modeled by giving mice a single, high dose of cisplatin. Mice do not survive longer than 3-4 days after treatment [35]. CKD is associated with interstitial fibrosis, chronic inflammation, and vascular rarefaction [25]. Recent studies have brought to light the interconnectedness of AKI and CKD through processes of maladaptive repair [25]. In order to develop better nephroprotective agents we must use models that allow for study of this progression following cisplatin treatment. Our repeated low dose cisplatin (RLDC) model utilizes 4 weekly low doses of cisplatin that enable

mice to survive up to 6 months after treatment. This allows for evaluation of long-term progression to CKD [38, 39, 86].

Aim one of this dissertation expands the use of this new RLDC model of nephrotoxicity to C57BL/6 mice. C57BL/6 mice have been known to be resistant to development of interstitial fibrosis and glomerular sclerosis [114]. We found that increasing the dose of cisplatin from 7 mg/kg to 9 mg/kg was sufficient to induce renal fibrosis following four weekly doses of cisplatin. Although induction of fibrosis was consistent, this increased dose was met with increased animal variability in markers of AKI development and inflammation. We utilized this intra-animal variability to identify Ccl2 mRNA as a consistent marker of injury. Furthermore, we observed increases in M2 macrophages in the kidney following four doses of cisplatin. These results supported examining the role of macrophages in development of RLDC-induced kidney fibrosis.

In aim two of this dissertation, we explored how infiltrating and resident macrophages affected cisplatin-induced kidney injury in the RLDC model. Ccr2^{-/-} mice had reduced F4/80^{lo} infiltrating macrophages compared to wild type mice following cisplatin treatment, but development of kidney injury and fibrosis was unchanged. In contrast, liposome encapsulated clodronate (LEC) depleted F4/80^{hi} resident and M2 macrophages in the kidney of cisplatin treated mice at the timepoint observed. LEC treated mice also had reduced collagen deposition, myofibroblast accumulation, and inflammatory cytokine and chemokine production following cisplatin treatment compared to mice treated with cisplatin alone. Interestingly, BUN and NGAL levels were unaffected by LEC indicating a

disconnect between classical AKI markers and markers of RLDC-induced fibrosis.

The results of this dissertation indicate the importance of testing potential nephroprotective agents in both models of AKI and CKD. Macrophage depletion was shown to have no effect on AKI development following high dose cisplatin treatment [89]. Here, we show that LEC-macrophage depletion ameliorates development of RLDC-induced kidney fibrosis. Evaluating the success of different therapeutic strategies in both acute and chronic models of kidney injury will help shed light on the different nephrotoxic mechanisms employed by high-dose cisplatin and RLDC treatment. Patients exhibit a wide range of responses to cisplatin in the clinic. Some develop AKI after a single low dose while others may receive multiple doses without displaying signs of clinical AKI. Developing an understanding of the biological processes occurring in both the high-dose cisplatin and RLDC models will help us understand the pathological processes occurring in all categories of patients. This will lead to better treatment of AKI and prevention of CKD.

STRENGTHS & LIMITATIONS

The major limitations of this work lie in the fact that all of these studies were done in mice. While the RLDC model improves on clinical relevancy compared to the high-dose model of cisplatin-induced kidney injury, there are still issues with human relevance. One major factor to consider is that only humans with cancer are given cisplatin. None of the mice in these studies had cancer as

a comorbidity. Preliminary studies suggest that cancer alone can induce some kidney pathology and may even alter the immune response to cisplatin treatment.

Another factor to consider is that cancer patients are treated with cisplatin following many different dosing regimens and in conjunction with many other chemotherapeutics. Different dosing schedules and the addition of other treatments may alter the nephrotoxic activity of cisplatin. While we have tried to design a model of kidney injury that matches the pathology observed in humans, the lack of sensitive AKI biomarkers and patient biopsies make it difficult to understand all of the intricate processes occurring in the human kidney after cisplatin treatment.

Another limitation to consider is the lack of specificity of LEC. While we did see a depletion of F4/80^{hi} resident and M2 macrophages with LEC treatment, other populations of immune cells were also altered. Additionally, we must consider that LEC treatment may be depleting populations of circulating immune cells that have repopulated by the time of observation. The conclusions that can be made from this work are therefore limited, but, based on what we observed, these studies warrant future experiments examining the role of kidney resident macrophages in RLDC-induced fibrosis in more depth.

The strengths of this dissertation lie in the novelty of the RLDC model, and the wide range of outcomes observed. This study addresses a major current problem in the field regarding reproducibility of different measured endpoints characterizing kidney injury following RLDC treatment. This study not only provides support to the development of CCL2 as a biomarker of cisplatin-induced

kidney injury, but also highlights the limitations of using markers like BUN and SCr as the sole indicators of kidney injury. This study demonstrates that cisplatin-induced kidney injury is a complex disease that requires analysis of many endpoints to truly understand what is going on.

This study is also the first to evaluate the inflammatory response in the kidney to RLDC treatment. We identified myeloid and lymphoid infiltrates in the kidney following RLDC treatment. Furthermore, we established that altering this immune response can ameliorate RLDC-induced fibrosis. This assessment presents inflammation as an important player in cisplatin-induced AKI and transition to CKD.

Lastly, this study highlights a unique role of the CCL2/CCR2 signaling axis in RLDC-induced kidney fibrosis. Other models of renal fibrosis have shown that inhibiting this signaling axis could lessen ischemic and urinary blockage induced fibrosis. This study demonstrated that *Ccr2*^{-/-} had no effect on fibrosis development following RLDC treatment. These results suggest that there may be a key difference in the progression of nephrotoxic induced AKI to fibrosis compared to other types of insults. This further supports the need for development of injury-type specific biomarkers of kidney disease and progression.

FUTURE DIRECTIONS

This dissertation provides evidence to support further analysis of how different macrophage populations contribute to cisplatin-induced kidney injury. It

also raises the need to explore other biological processes in both the high dose and RLDC injury models. These goals can be met with the following future directions:

1. Explore how the comorbidity of cancer alters the role of macrophages in development of RLDC-induced fibrosis. To increase the clinical relevance of this work, it would be meaningful to assess if cancer impacts the results observed in this study. Preliminary studies show that cancer alone induces some renal pathology and sensitizes mice to RLDC-induced fibrosis. It has also been demonstrated by others that cancer cells can reprogram immune cells, altering their response to stimuli. Future studies should therefore examine the effect of LEC treatment on RLDC-induced fibrosis in mice with cancer as a comorbidity. These studies must also examine the ability of cisplatin to reduce tumor size. We hypothesize that depletion of macrophages could both prevent cisplatin-induced fibrosis and enhance the ability of cisplatin to kill cancer cells by removing tumor-associated macrophages. These studies would also need to incorporate several methods to deplete macrophages beyond LEC treatment. Inducible CX3CR1 knockout mice could be utilized as an alternative method to target tissue resident macrophages with greater specificity. Additionally, inhibition of M2 macrophage polarization could shed light on the effects of macrophage phenotypes in cisplatin-induced kidney injury and cancer treatment. All these studies would increase our understanding of how the immune system regulates patient response to cisplatin treatment in the context of cancer.

2. Increase the human relevance of the RLDC model by utilizing *Sus scrofa*.

Interestingly, pig kidneys are much more anatomically and physiologically similar to human kidneys than mice kidneys are. Pigs also appear to have similar sensitivity levels to cisplatin as a nephrotoxin, while mice need to be given a much higher dose of cisplatin to produce effects in the kidney. For these reasons, pigs are gaining attention as better models of many types of kidney injury [149]. We have done preliminary studies giving pigs doses of cisplatin equivalent to what humans are given. Evaluation of several markers of injury indicated development of AKI after one or two doses of cisplatin in two different pigs. Aging these pigs several months after treatment then lead to development of CKD as indicated by development of fibrosis and SCr levels. Flow cytometric evaluation of immune cells also revealed increased macrophage and monocyte populations in the kidney of cisplatin treated pigs compared to untreated pigs. Further study is needed to optimize the dosing regimen in pigs, as only two pigs were utilized, and neither was able to receive more than two doses of cisplatin. Optimization of this model would allow for testing of therapeutic agents in a more physiologically relevant model, increasing clinical relevancy.

3. Explore the role of autophagy in RLDC-induced kidney fibrosis. As

previously mentioned, many biological processes are speculated to have differential effects in the contexts of acute and chronic kidney injury. To further characterize RLDC-induced kidney pathologies we have begun exploring the role of autophagy in development of cisplatin-induced fibrosis. Inhibition of autophagy has been shown to exacerbate AKI development in the high dose model of

cisplatin-induced kidney injury [75]. In contrast, our preliminary studies have revealed that inhibition of autophagy with both a late and early-stage autophagy inhibitor ameliorates development of fibrosis while also reducing BUN and NGAL levels following cisplatin treatment. Autophagy inhibition was also accompanied by decreased infiltration of immune cells in the kidney following cisplatin treatment. Future studies will explore this further by utilizing mice with a cell-type specific genetic deficiency of autophagy. Furthermore, we hope to explore the relationship between autophagy and macrophage activity in the context of cisplatin-induced kidney injury. We hypothesize that global autophagy inhibition is altering the immune response to cisplatin treatment in a way that prevents kidney injury. These studies could lead to additional therapeutic targets to prevent cisplatin-induced kidney injury and provide mechanistic understanding of the relationship between autophagy and immune cell activity.

REFERENCES

1. Kelland, L., *The resurgence of platinum-based cancer chemotherapy*. Nat Rev Cancer, 2007. **7**(8): p. 573-84.
2. Miller, R.P., et al., *Mechanisms of Cisplatin nephrotoxicity*. Toxins (Basel), 2010. **2**(11): p. 2490-518.
3. Kelland, L., *The resurgence of platinum-based cancer chemotherapy*. Nature Reviews Cancer, 2007. **7**: p. 573.
4. Oun, R., Y.E. Moussa, and N.J. Wheate, *The side effects of platinum-based chemotherapy drugs: a review for chemists*. Dalton Trans, 2018. **47**(19): p. 6645-6653.
5. Pabla, N. and Z. Dong, *Cisplatin nephrotoxicity: mechanisms and renoprotective strategies*. Kidney Int, 2008. **73**(9): p. 994-1007.
6. Nakamura, T., et al., *Disruption of multidrug and toxin extrusion MATE1 potentiates cisplatin-induced nephrotoxicity*. Biochem Pharmacol, 2010. **80**(11): p. 1762-7.
7. Oh, G.-S., et al., *Cisplatin-induced Kidney Dysfunction and Perspectives on Improving Treatment Strategies*. Electrolyte & blood pressure : E & BP, 2014. **12**(2): p. 55-65.
8. Townsend, D.M., et al., *Metabolism of Cisplatin to a nephrotoxin in proximal tubule cells*. J Am Soc Nephrol, 2003. **14**(1): p. 1-10.

9. Ozkok, A. and C.L. Edelstein, *Pathophysiology of cisplatin-induced acute kidney injury*. Biomed Res Int, 2014. **2014**: p. 967826.
10. Levey, A.S. and M.T. James, *Acute Kidney Injury*. Ann Intern Med, 2017. **167**(9): p. ITC66-ITC80.
11. Basile, D.P., M.D. Anderson, and T.A. Sutton, *Pathophysiology of acute kidney injury*. Compr Physiol, 2012. **2**(2): p. 1303-53.
12. Lopes, J.A. and S. Jorge, *The RIFLE and AKIN classifications for acute kidney injury: a critical and comprehensive review*. Clin Kidney J, 2013. **6**(1): p. 8-14.
13. Martensson, J. and R. Bellomo, *The rise and fall of NGAL in acute kidney injury*. Blood Purif, 2014. **37**(4): p. 304-10.
14. Castillo-Rodriguez, E., et al., *Kidney Injury Marker 1 and Neutrophil Gelatinase-Associated Lipocalin in Chronic Kidney Disease*. Nephron, 2017. **136**(4): p. 263-267.
15. Sabbisetti, V.S., et al., *Blood kidney injury molecule-1 is a biomarker of acute and chronic kidney injury and predicts progression to ESRD in type I diabetes*. J Am Soc Nephrol, 2014. **25**(10): p. 2177-86.
16. Rizvi, M.S. and K.B. Kashani, *Biomarkers for Early Detection of Acute Kidney Injury*. The Journal of Applied Laboratory Medicine: An AACC Publication, 2017. **2**(3): p. 386-399.
17. Negi, S., et al., *Acute kidney injury: Epidemiology, outcomes, complications, and therapeutic strategies*. Semin Dial, 2018. **31**(5): p. 519-527.

18. Doyle, J.F. and L.G. Forni, *Acute kidney injury: short-term and long-term effects*. Crit Care, 2016. **20**(1): p. 188.
19. Naughton, C.A., *Drug-induced nephrotoxicity*. Am Fam Physician, 2008. **78**(6): p. 743-50.
20. Rahman, M., F. Shad, and M.C. Smith, *Acute kidney injury: a guide to diagnosis and management*. Am Fam Physician, 2012. **86**(7): p. 631-9.
21. Bonventre, J.V. and L. Yang, *Cellular pathophysiology of ischemic acute kidney injury*. J Clin Invest, 2011. **121**(11): p. 4210-21.
22. Chawla, L.S., et al., *Acute kidney injury and chronic kidney disease as interconnected syndromes*. N Engl J Med, 2014. **371**(1): p. 58-66.
23. Chawla, L.S., et al., *The severity of acute kidney injury predicts progression to chronic kidney disease*. Kidney Int, 2011. **79**(12): p. 1361-9.
24. Coca, S.G., S. Singanamala, and C.R. Parikh, *Chronic kidney disease after acute kidney injury: a systematic review and meta-analysis*. Kidney Int, 2012. **81**(5): p. 442-8.
25. Ferenbach, D.A. and J.V. Bonventre, *Mechanisms of maladaptive repair after AKI leading to accelerated kidney ageing and CKD*. Nat Rev Nephrol, 2015. **11**(5): p. 264-76.
26. Levey, A.S. and J. Coresh, *Chronic kidney disease*. Lancet, 2012. **379**(9811): p. 165-80.
27. Coresh, J., et al., *Prevalence of chronic kidney disease in the United States*. JAMA, 2007. **298**(17): p. 2038-47.

28. Coresh, J., et al., *Action plan for determining and monitoring the prevalence of chronic kidney disease*. *Kidney Int Suppl* (2011), 2017. **7**(2): p. 63-70.
29. Thakar, C.V., et al., *Acute kidney injury episodes and chronic kidney disease risk in diabetes mellitus*. *Clin J Am Soc Nephrol*, 2011. **6**(11): p. 2567-72.
30. Price, P.M., J. Megyesi, and R.L. Safirstein, *Cell cycle regulation: repair and regeneration in acute renal failure*. *Kidney Int*, 2004. **66**(2): p. 509-14.
31. Falke, L.L., et al., *Diverse origins of the myofibroblast—implications for kidney fibrosis*. *Nature Reviews Nephrology*, 2015. **11**: p. 233.
32. Jun, J.I. and L.F. Lau, *Resolution of organ fibrosis*. *J Clin Invest*, 2018. **128**(1): p. 97-107.
33. Han, H.I., et al., *The role of macrophages during acute kidney injury: destruction and repair*. *Pediatr Nephrol*, 2019. **34**(4): p. 561-569.
34. Tang, P.M., D.J. Nikolic-Paterson, and H.Y. Lan, *Macrophages: versatile players in renal inflammation and fibrosis*. *Nat Rev Nephrol*, 2019. **15**(3): p. 144-158.
35. Sharp, C.N. and L.J. Siskind, *Developing better mouse models to study cisplatin-induced kidney injury*. *Am J Physiol Renal Physiol*, 2017. **313**(4): p. F835-F841.
36. Skinner, R., et al., *Persistent nephrotoxicity during 10-year follow-up after cisplatin or carboplatin treatment in childhood: relevance of age and dose as risk factors*. *Eur J Cancer*, 2009. **45**(18): p. 3213-9.

37. Sharp, C.N., et al., *Moderate aging does not exacerbate cisplatin-induced kidney injury or fibrosis despite altered inflammatory cytokine expression and immune cell infiltration*. Am J Physiol Renal Physiol, 2019. **316**(1): p. F162-F172.
38. Sharp, C.N., et al., *Repeated administration of low-dose cisplatin in mice induces fibrosis*. Am J Physiol Renal Physiol, 2016. **310**(6): p. F560-8.
39. Sharp, C.N., et al., *Subclinical kidney injury induced by repeated cisplatin administration results in progressive chronic kidney disease*. Am J Physiol Renal Physiol, 2018. **315**(1): p. F161-F172.
40. Sears, S.M., et al., *C57BL/6 mice require a higher dose of cisplatin to induce renal fibrosis and CCL2 correlates with cisplatin-induced kidney injury*. American Journal of Physiology-Renal Physiology, 2020.
41. Katagiri, D., et al., *Interstitial renal fibrosis due to multiple cisplatin treatments is ameliorated by semicarbazide-sensitive amine oxidase inhibition*. Kidney Int, 2016. **89**(2): p. 374-85.
42. Landau, S.I., et al., *Regulated necrosis and failed repair in cisplatin-induced chronic kidney disease*. Kidney Int, 2019. **95**(4): p. 797-814.
43. Shi, M., et al., *Cisplatin nephrotoxicity as a model of chronic kidney disease*. Lab Invest, 2018.
44. Black, L.M., et al., *Divergent effects of AKI to CKD models on inflammation and fibrosis*. Am J Physiol Renal Physiol, 2018. **315**(4): p. F1107-F1118.

45. Fu, Y., et al., *Chronic effects of repeated low dose cisplatin treatment in mouse kidneys and renal tubular cells*. Am J Physiol Renal Physiol, 2019.
46. Torres, R., et al., *Three-Dimensional Morphology by Multiphoton Microscopy with Clearing in a Model of Cisplatin-Induced CKD*. J Am Soc Nephrol, 2016. **27**(4): p. 1102-12.
47. Fu, Y., et al., *Rodent models of AKI-CKD transition*. Am J Physiol Renal Physiol, 2018. **315**(4): p. F1098-F1106.
48. Wei, Q., et al., *The pathological role of Bax in cisplatin nephrotoxicity*. Kidney Int, 2007. **72**(1): p. 53-62.
49. Wei, Q., et al., *Activation and involvement of p53 in cisplatin-induced nephrotoxicity*. Am J Physiol Renal Physiol, 2007. **293**(4): p. F1282-91.
50. Bhatia, D. and M.E. Choi, *The Emerging Role of Mitophagy in Kidney Diseases*. Journal of life sciences (Westlake Village, Calif.), 2019. **1**(3): p. 13-22.
51. Bronze-da-Rocha, E. and A. Santos-Silva, *Neutrophil Elastase Inhibitors and Chronic Kidney Disease*. International journal of biological sciences, 2018. **14**(10): p. 1343-1360.
52. Hu, Z., et al., *Emerging Role of Ferroptosis in Acute Kidney Injury*. Oxidative Medicine and Cellular Longevity, 2019. **2019**: p. 8010614.
53. Priante, G., et al., *Cell Death in the Kidney*. International journal of molecular sciences, 2019. **20**(14): p. 3598.

54. Mei, S., et al., *Double knockout of Bax and Bak from kidney proximal tubules reduces unilateral urethral obstruction associated apoptosis and renal interstitial fibrosis*. Scientific Reports, 2017. **7**: p. 44892.
55. Ying, Y., et al., *Targeted deletion of p53 in the proximal tubule prevents ischemic renal injury*. J Am Soc Nephrol, 2014. **25**(12): p. 2707-16.
56. CHOI, Y.-J., et al., *Role of p53-Dependent Activation of Caspases in Chronic Obstructive Uropathy: Evidence from p53 Null Mutant Mice*. Journal of the American Society of Nephrology, 2001. **12**(5): p. 983-992.
57. Liu, L., et al., *p53 upregulated by HIF-1alpha promotes hypoxia-induced G2/M arrest and renal fibrosis in vitro and in vivo*. J Mol Cell Biol, 2019. **11**(5): p. 371-382.
58. Grgic, I., et al., *Targeted proximal tubule injury triggers interstitial fibrosis and glomerulosclerosis*. Kidney Int, 2012. **82**(2): p. 172-83.
59. Yang, L., et al., *Epithelial cell cycle arrest in G2/M mediates kidney fibrosis after injury*. Nat Med, 2010. **16**(5): p. 535-43, 1p following 143.
60. Francescato, H.D.C., et al., *Effect of JNK inhibition on cisplatin-induced renal damage*. Nephrology Dialysis Transplantation, 2007. **22**(8): p. 2138-2148.
61. Grynberg, K., F.Y. Ma, and D.J. Nikolic-Paterson, *The JNK Signaling Pathway in Renal Fibrosis*. Frontiers in physiology, 2017. **8**: p. 829-829.
62. Rutkowski, D.T. and R.J. Kaufman, *That which does not kill me makes me stronger: adapting to chronic ER stress*. Trends Biochem Sci, 2007. **32**(10): p. 469-76.

63. Rashid, H.O., et al., *ER stress: Autophagy induction, inhibition and selection*. *Autophagy*, 2015. **11**(11): p. 1956-1977.
64. Cybulsky, A.V., *Endoplasmic reticulum stress, the unfolded protein response and autophagy in kidney diseases*. *Nature Reviews Nephrology*, 2017. **13**(11): p. 681-696.
65. Hu, H., et al., *The C/EBP Homologous Protein (CHOP) Transcription Factor Functions in Endoplasmic Reticulum Stress-Induced Apoptosis and Microbial Infection*. *Frontiers in Immunology*, 2019. **9**(3083).
66. Chai, Y., et al., *Dexmedetomidine alleviates cisplatin-induced acute kidney injury by attenuating endoplasmic reticulum stress-induced apoptosis via the alpha2AR/PI3K/AKT pathway*. *Mol Med Rep*, 2020. **21**(3): p. 1597-1605.
67. Huang, Z., et al., *Activation of GPR120 by TUG891 ameliorated cisplatin-induced acute kidney injury via repressing ER stress and apoptosis*. *Biomedicine & Pharmacotherapy*, 2020. **126**: p. 110056.
68. Shu, S., et al., *Endoplasmic reticulum stress is activated in post-ischemic kidneys to promote chronic kidney disease*. *EBioMedicine*, 2018. **37**: p. 269-280.
69. Noh, M.R., et al., *C/EBP homologous protein (CHOP) gene deficiency attenuates renal ischemia/reperfusion injury in mice*. *Biochimica et Biophysica Acta (BBA) - Molecular Basis of Disease*, 2015. **1852**(9): p. 1895-1901.

70. Noh, M.R., et al., *Ablation of C/EBP homologous protein attenuates renal fibrosis after ureteral obstruction by reducing autophagy and microtubule disruption*. *Biochimica et Biophysica Acta (BBA) - Molecular Basis of Disease*, 2018. **1864**(5, Part A): p. 1634-1641.
71. Liu, S.H., et al., *C/EBP homologous protein (CHOP) deficiency ameliorates renal fibrosis in unilateral ureteral obstructive kidney disease*. *Oncotarget*, 2016. **7**(16): p. 21900-12.
72. Lin, T.A., V.C. Wu, and C.Y. Wang, *Autophagy in Chronic Kidney Diseases*. *Cells*, 2019. **8**(1).
73. Wang, Z. and M.E. Choi, *Autophagy in kidney health and disease*. *Antioxid Redox Signal*, 2014. **20**(3): p. 519-37.
74. Takahashi, A., et al., *Autophagy guards against cisplatin-induced acute kidney injury*. *Am J Pathol*, 2012. **180**(2): p. 517-25.
75. Jiang, M., et al., *Autophagy in proximal tubules protects against acute kidney injury*. *Kidney Int*, 2012. **82**(12): p. 1271-83.
76. Baisantry, A., et al., *Autophagy Induces Prosenescent Changes in Proximal Tubular S3 Segments*. *Journal of the American Society of Nephrology : JASN*, 2016. **27**(6): p. 1609-1616.
77. Nam, S.A., et al., *Autophagy attenuates tubulointerstitial fibrosis through regulating transforming growth factor- β and NLRP3 inflammasome signaling pathway*. *Cell Death & Disease*, 2019. **10**(2): p. 78.

78. Livingston, M.J., et al., *Persistent activation of autophagy in kidney tubular cells promotes renal interstitial fibrosis during unilateral ureteral obstruction*. *Autophagy*, 2016. **12**(6): p. 976-98.
79. Baisantry, A., et al., *The impact of autophagy on the development of senescence in primary tubular epithelial cells*. *Cell cycle (Georgetown, Tex.)*, 2016. **15**(21): p. 2973-2979.
80. Tang, C., et al., *Autophagy in kidney homeostasis and disease*. *Nature Reviews Nephrology*, 2020. **16**(9): p. 489-508.
81. Black, L.M., J.M. Lever, and A. Agarwal, *Renal Inflammation and Fibrosis: A Double-edged Sword*. *J Histochem Cytochem*, 2019: p. 22155419852932.
82. Ramesh, G. and W.B. Reeves, *TNF-alpha mediates chemokine and cytokine expression and renal injury in cisplatin nephrotoxicity*. *J Clin Invest*, 2002. **110**(6): p. 835-42.
83. Zhang, B., et al., *Cisplatin-induced nephrotoxicity is mediated by tumor necrosis factor- α produced by renal parenchymal cells*. *Kidney International*, 2007. **72**(1): p. 37-44.
84. Morimoto, Y., et al., *TNF-alpha deficiency accelerates renal tubular interstitial fibrosis in the late stage of ureteral obstruction*. *Exp Mol Pathol*, 2008. **85**(3): p. 207-13.
85. Meldrum, K.K., et al., *TNF-alpha neutralization ameliorates obstruction-induced renal fibrosis and dysfunction*. *Am J Physiol Regul Integr Comp Physiol*, 2007. **292**(4): p. R1456-64.

86. Sears, S.M., et al., *C57BL/6 mice require a higher dose of cisplatin to induce renal fibrosis and CCL2 correlates with cisplatin-induced kidney injury*. American Journal of Physiology-Renal Physiology, 2020. **319**(4): p. F674-F685.
87. Liu, M., et al., *A pathophysiologic role for T lymphocytes in murine acute cisplatin nephrotoxicity*. J Am Soc Nephrol, 2006. **17**(3): p. 765-74.
88. Tadagavadi, R.K. and W.B. Reeves, *Renal dendritic cells ameliorate nephrotoxic acute kidney injury*. J Am Soc Nephrol, 2010. **21**(1): p. 53-63.
89. Lu, L.H., et al., *Increased macrophage infiltration and fractalkine expression in cisplatin-induced acute renal failure in mice*. J Pharmacol Exp Ther, 2008. **324**(1): p. 111-7.
90. Tapmeier, T.T., et al., *Pivotal role of CD4+ T cells in renal fibrosis following ureteric obstruction*. Kidney Int, 2010. **78**(4): p. 351-62.
91. Dong, Y., et al., *Depletion of CD8+ T Cells Exacerbates CD4+ T Cell-Induced Monocyte-to-Fibroblast Transition in Renal Fibrosis*. J Immunol, 2016. **196**(4): p. 1874-81.
92. Ravichandran, K., et al., *CD4 T cell knockout does not protect against kidney injury and worsens cancer*. J Mol Med (Berl), 2016. **94**(4): p. 443-55.
93. Kim, M.G., et al., *The Role of M2 Macrophages in the Progression of Chronic Kidney Disease following Acute Kidney Injury*. PLoS One, 2015. **10**(12): p. e0143961.

94. Lee, S., et al., *Distinct macrophage phenotypes contribute to kidney injury and repair*. J Am Soc Nephrol, 2011. **22**(2): p. 317-26.
95. Kitamoto, K., et al., *Effects of liposome clodronate on renal leukocyte populations and renal fibrosis in murine obstructive nephropathy*. J Pharmacol Sci, 2009. **111**(3): p. 285-92.
96. Liu, Y., et al., *Complement C3 Produced by Macrophages Promotes Renal Fibrosis via IL-17A Secretion*. Front Immunol, 2018. **9**: p. 2385.
97. van Hennik, M.B., et al., *Comparative pharmacokinetics of cisplatin and three analogues in mice and humans*. Cancer Res, 1987. **47**(23): p. 6297-301.
98. Oronsky, B., et al., *Electrolyte disorders with platinum-based chemotherapy: mechanisms, manifestations and management*. Cancer chemotherapy and pharmacology, 2017. **80**(5): p. 895-907.
99. van Angelen, A.A., et al., *Cisplatin-induced injury of the renal distal convoluted tubule is associated with hypomagnesaemia in mice*. Nephrology Dialysis Transplantation, 2012. **28**(4): p. 879-889.
100. Chen, W.-Y., et al., *Cisplatin Nephrotoxicity Might Have a Sex Difference. An analysis Based on Women's Sex Hormone Changes*. Journal of Cancer, 2017. **8**(19): p. 3939-3944.
101. Holditch, S.J., et al., *Recent Advances in Models, Mechanisms, Biomarkers, and Interventions in Cisplatin-Induced Acute Kidney Injury*. International journal of molecular sciences, 2019. **20**(12): p. 3011.

102. Zazuli, Z., et al., *Genetic Variations and Cisplatin Nephrotoxicity: A Systematic Review*. *Frontiers in pharmacology*, 2018. **9**: p. 1111-1111.
103. Garcia, S.L., et al., *Prediction of Nephrotoxicity Associated With Cisplatin-Based Chemotherapy in Testicular Cancer Patients*. *JNCI Cancer Spectrum*, 2020. **4**(3).
104. Filipski, K.K., et al., *Contribution of organic cation transporter 2 (OCT2) to cisplatin-induced nephrotoxicity*. *Clin Pharmacol Ther*, 2009. **86**(4): p. 396-402.
105. Katsuda, H., et al., *Protecting Cisplatin-Induced Nephrotoxicity with Cimetidine Does Not Affect Antitumor Activity*. *Biological and Pharmaceutical Bulletin*, 2010. **33**(11): p. 1867-1871.
106. Sprowl, J.A., et al., *Cisplatin-Induced Renal Injury Is Independently Mediated by OCT2 and p53*. *Clinical Cancer Research*, 2014. **20**(15): p. 4026-4035.
107. *The "Accidental" Cure—Platinum-based Treatment for Cancer: The Discovery of Cisplatin*. 2014.
108. Amdur, R.L., et al., *Outcomes following diagnosis of acute renal failure in U.S. veterans: focus on acute tubular necrosis*. *Kidney Int*, 2009. **76**(10): p. 1089-97.
109. Ishani, A., et al., *Acute kidney injury increases risk of ESRD among elderly*. *J Am Soc Nephrol*, 2009. **20**(1): p. 223-8.
110. Latcha, S., et al., *Long-Term Renal Outcomes after Cisplatin Treatment*. *Clin J Am Soc Nephrol*, 2016. **11**(7): p. 1173-9.

111. *Cancer Statistics*. 2018.
112. Xue, J.L., et al., *Incidence and mortality of acute renal failure in Medicare beneficiaries, 1992 to 2001*. *J Am Soc Nephrol*, 2006. **17**(4): p. 1135-42.
113. Hsu, C.Y., et al., *Community-based incidence of acute renal failure*. *Kidney Int*, 2007. **72**(2): p. 208-12.
114. Rabe, M. and F. Schaefer, *Non-Transgenic Mouse Models of Kidney Disease*. *Nephron*, 2016. **133**(1): p. 53-61.
115. Volarevic, V., et al., *Molecular mechanisms of cisplatin-induced nephrotoxicity: a balance on the knife edge between renoprotection and tumor toxicity*. *Journal of Biomedical Science*, 2019. **26**(1): p. 25.
116. Xu, Y., et al., *A Role for Tubular Necroptosis in Cisplatin-Induced AKI*. *Journal of the American Society of Nephrology*, 2015. **26**(11): p. 2647-2658.
117. Nishihara, K., et al., *Urinary chemokine (C-C motif) ligand 2 (monocyte chemoattractant protein-1) as a tubular injury marker for early detection of cisplatin-induced nephrotoxicity*. *Biochemical pharmacology*, 2013. **85**(4): p. 570-582.
118. Shinke, H., et al., *Urinary kidney injury molecule-1 and monocyte chemoattractant protein-1 are noninvasive biomarkers of cisplatin-induced nephrotoxicity in lung cancer patients*. *Cancer Chemother Pharmacol*, 2015. **76**(5): p. 989-96.

119. Anders, H.-J., V. Vielhauer, and D. Schlöndorff, *Chemokines and chemokine receptors are involved in the resolution or progression of renal disease*. *Kidney International*, 2003. **63**(2): p. 401-415.
120. Maekawa, H. and R. Inagi, *Stress Signal Network between Hypoxia and ER Stress in Chronic Kidney Disease*. *Front Physiol*, 2017. **8**: p. 74.
121. Zhang, M., et al., *Chop deficiency prevents UUO-induced renal fibrosis by attenuating fibrotic signals originated from Hmgb1/TLR4/NFκB/IL-1β signaling*. *Cell Death & Disease*, 2015. **6**(8): p. e1847-e1847.
122. Gewin, L.S., *Renal fibrosis: Primacy of the proximal tubule*. *Matrix biology : journal of the International Society for Matrix Biology*, 2018. **68-69**: p. 248-262.
123. Sahin, H. and H.E. Wasmuth, *Chemokines in tissue fibrosis*. *Biochimica et Biophysica Acta (BBA) - Molecular Basis of Disease*, 2013. **1832**(7): p. 1041-1048.
124. Stroo, I., et al., *Chemokine expression in renal ischemia/reperfusion injury is most profound during the reparative phase*. *International Immunology*, 2010. **22**(6): p. 433-442.
125. Kitagawa, K., et al., *Blockade of CCR2 ameliorates progressive fibrosis in kidney*. *The American journal of pathology*, 2004. **165**(1): p. 237-246.
126. Furuichi, K., et al., *CCR2 Signaling Contributes to Ischemia-Reperfusion Injury in Kidney*. *Journal of the American Society of Nephrology*, 2003. **14**(10): p. 2503-2515.

127. Boels, M.G.S., et al., *Systemic Monocyte Chemotactic Protein-1 Inhibition Modifies Renal Macrophages and Restores Glomerular Endothelial Glycocalyx and Barrier Function in Diabetic Nephropathy*. *The American Journal of Pathology*, 2017. **187**(11): p. 2430-2440.
128. Cao, Q., D.C.H. Harris, and Y. Wang, *Macrophages in Kidney Injury, Inflammation, and Fibrosis*. *Physiology*, 2015. **30**(3): p. 183-194.
129. Nikolic-Paterson, D.J., S. Wang, and H.Y. Lan, *Macrophages promote renal fibrosis through direct and indirect mechanisms*. *Kidney Int Suppl* (2011), 2014. **4**(1): p. 34-38.
130. Yang, Q., et al., *Bone marrow-derived Ly6C⁻ macrophages promote ischemia-induced chronic kidney disease*. *Cell Death & Disease*, 2019. **10**(4): p. 291.
131. Lu, L., et al., *Depletion of macrophages and dendritic cells in ischemic acute kidney injury*. *American journal of nephrology*, 2012. **35**(2): p. 181-190.
132. Ferenbach, D.A., et al., *Macrophage/monocyte depletion by clodronate, but not diphtheria toxin, improves renal ischemia/reperfusion injury in mice*. *Kidney International*, 2012. **82**(8): p. 928-933.
133. Pan, B., et al., *Regulation of Renal Fibrosis by Macrophage Polarization*. *Cellular Physiology and Biochemistry*, 2015. **35**(3): p. 1062-1069.
134. Guiteras, R., M. Flaquer, and J.M. Cruzado, *Macrophage in chronic kidney disease*. *Clin Kidney J*, 2016. **9**(6): p. 765-771.

135. Silver, S.A. and C. Gerarduzzi, *Found in Translation: Reasons for Optimism in the Pursuit to Prevent Chronic Kidney Disease After Acute Kidney Injury*. Can J Kidney Health Dis, 2019. **6**: p. 2054358119868740.
136. Sears, S. and L. Siskind, *Potential Therapeutic Targets for Cisplatin-Induced Kidney Injury: Lessons from Other Models of AKI and Fibrosis*. Journal of the American Society of Nephrology, 2021: p. ASN.2020101455.
137. Schulz, C., et al., *A Lineage of Myeloid Cells Independent of Myb and Hematopoietic Stem Cells*. Science, 2012. **336**(6077): p. 86-90.
138. Lever, J.M., et al., *Resident macrophages reprogram toward a developmental state after acute kidney injury*. JCI Insight, 2019. **4**(2).
139. Munro, D.A.D. and J. Hughes, *The Origins and Functions of Tissue-Resident Macrophages in Kidney Development*. Frontiers in physiology, 2017. **8**: p. 837-837.
140. Liu, F., et al., *Distinct fate, dynamics and niches of renal macrophages of bone marrow or embryonic origins*. Nature Communications, 2020. **11**(1): p. 2280.
141. Peng, X., et al., *CX3CL1-CX3CR1 Interaction Increases the Population of Ly6C(-)CX3CR1(hi) Macrophages Contributing to Unilateral Ureteral Obstruction-Induced Fibrosis*. J Immunol, 2015. **195**(6): p. 2797-805.
142. Braga, T.T., et al., *CCR2 contributes to the recruitment of monocytes and leads to kidney inflammation and fibrosis development*. Inflammopharmacology, 2018. **26**(2): p. 403-411.

143. Oh, D.-J., et al., *Fractalkine receptor (CX3CR1) inhibition is protective against ischemic acute renal failure in mice*. American Journal of Physiology-Renal Physiology, 2008. **294**(1): p. F264-F271.
144. Sung, S.A., et al., *Reduction of Renal Fibrosis as a Result of Liposome Encapsulated Clodronate Induced Macrophage Depletion after Unilateral Ureteral Obstruction in Rats*. Nephron Experimental Nephrology, 2007. **105**(1): p. e1-e9.
145. Puranik, A.S., et al., *Kidney-resident macrophages promote a proangiogenic environment in the normal and chronically ischemic mouse kidney*. Scientific Reports, 2018. **8**(1): p. 13948.
146. Xia, Y., M.L. Entman, and Y. Wang, *CCR2 regulates the uptake of bone marrow-derived fibroblasts in renal fibrosis*. PLoS One, 2013. **8**(10): p. e77493.
147. Kashyap, S., et al., *Ccl2 deficiency protects against chronic renal injury in murine renovascular hypertension*. Scientific Reports, 2018. **8**(1): p. 8598.
148. Xu, L., D. Sharkey, and L.G. Cantley, *Tubular GM-CSF Promotes Late MCP-1/CCR2-Mediated Fibrosis and Inflammation after Ischemia/Reperfusion Injury*. Journal of the American Society of Nephrology : JASN, 2019. **30**(10): p. 1825-1840.
149. Huang, J., G. Bayliss, and S. Zhuang, *Porcine models of acute kidney injury*. American Journal of Physiology-Renal Physiology, 2021. **320**(6): p. F1030-F1044.

CURRICULUM VITAE

Sophia M. Sears
University of Louisville
School of Medicine
505 S Hancock St, CTRB 252G
Louisville KY, 40202
Phone: (812) 653-9691
Email: smsear03@louisville.edu

EDUCATION

- 2019-2021 Ph.D. Pharmacology & Toxicology
University of Louisville, Louisville, KY
Dissertation: Role of macrophages in cisplatin-induced kidney injury
and progression to chronic kidney disease
Anticipated completion: September 2021
- 2017-2019 M.S. Pharmacology & Toxicology
University of Louisville, Louisville, KY
Thesis: Characterizing the roles of neutral ceramidase in cisplatin-
induced kidney injury
- 2013-2017 B.A. Molecular Biology & Biochemistry
Goshen College, Goshen, IN

PROFESSIONAL APPOINTMENTS

- 2019-2021 **NIH F31 Predoctoral Fellow**
Department of Pharmacology & Toxicology
University of Louisville School of Medicine, Louisville, KY
- 2017-2019 **Graduate Student Researcher**
Department of Pharmacology & Toxicology
University of Louisville School of Medicine, Louisville, KY
- 2015-2017 **Research Assistant**
Department of Biological Sciences
Goshen College, Goshen, IN

- 2015-2017 **Assistant Chemical Hygiene Officer & Stockroom Manager**
Goshen College, Goshen, IN
- 2016 **Research Intern**
R25 Cancer Education Program
University of Louisville School of Medicine, Louisville, KY
- 2014 **Teaching Assistant**
Department of Chemistry
Goshen College, Goshen, IN

HONORS AND AWARDS

- 2021 ASN Kidney STARS Award Recipient
- 2020 KC Huang Outstanding Graduate Student Award
- 2020 F31 Predoctoral Fellowship
NIH: NIDDK
- 2020 Graduate Student Spring Travel Award
University of Louisville
- 2017-2019 IPIBS Fellowship (full tuition and stipend)
University of Louisville
- 2017 Graduated Summa Cum Laude
Goshen College
- 2016 & 2017 NAIA DII Women's Basketball All American
- 2016 & 2017 NAIA Daktronics Scholar-Athlete Award
- 2015-2016 Alicia Showalter Reynolds Women in Science Scholarship
Goshen College
- 2013-2017 Dean's List
Goshen College
- 2013-2014 General Chemistry Award (Best GPA in class)
Goshen College

PROFESSIONAL AFFILIATIONS

- 2017-Present American Society of Nephrology Student Member
- 2019-Present American Physiological Society Student Member
- 2019 American Heart Association Student Member: Council on Kidney in
Cardiovascular Disease
- 2018-2019 Society of Toxicologic Pathology Student Member

PEER REVIEWED PUBLICATIONS

1. **Sears SM**, Vega AA, Kurlawala Z, Oropilla GB, Krueger A, Shah PP, Doll MA, Miller R, Beverly LJ, Siskind LJ. (2021, in preparation) F4/80^{hi} resident

macrophages contribute to cisplatin-induced renal fibrosis. Target journal: *Journal of the American Society of Nephrology*.

2. Kurlawala Z, McMillan JD, Singhal R, Morehouse J, **Sears SM**, Duregon E, Burke D, Siskind LJ, Beverly LJ, Friedland RP. (2021, under revision) Curli-producing *E. coli* enhances the disease phenotype in an hSOD1 G93A mouse model of ALS. Submitted to *Nature Neuroscience*.
3. **Sears SM**, Dupre TV, Sharp CN, Vega AA, Krueger A, Megyesi J, Shah PP, Doll MA, Beverly LJ, Siskind LJ. (2021, under revision) Neutral ceramidase deficiency protects from cisplatin-induced acute kidney injury. Submitted to *Journal of Lipid Research*.
4. **Sears SM**, Siskind LJ. (2021) Potential Therapeutic Targets for Cisplatin-Induced Kidney Injury: Lessons from Other Models of AKI and Fibrosis. *Journal of the American Society of Nephrology*; 32(7): 1559-1567. doi: 10.1681/ASN.2020101455
5. **Sears SM**, Sharp CN, Krueger A, Oropilla GB, Saforo D, Doll MA, Megyesi J, Beverly LJ, Siskind LJ. (2020). C57BL6 mice require a higher dose of cisplatin to induce renal fibrosis and CCL2 correlates with cisplatin-induced kidney injury. *American Journal of Physiology: Renal Physiology*; 319(4): 674-685. doi: 10.1152/ajprenal.00196.2020
6. Pal D, Suman S, Kolluru V, **Sears S**, Das TP, Alatassi PH, Ankem MK, Freedman JH, Damodaran C. (2017). Inhibition of autophagy prevents cadmium-induced prostate carcinogenesis. *British Journal of Cancer*; 117: 56-64. doi: 10.1038/bjc.2017.143

RESEARCH SUPPORT

- | | |
|-----------|--|
| 2020-2021 | Role of macrophages in cisplatin-induced kidney injury and progression to chronic kidney disease
Funder: National Institute of Diabetes and Digestive and Kidney Diseases (F31DK126400)
Role: PI (Sponsors: Siskind, Yaddanapudi) |
| 2019-2020 | The role of neutral ceramidase in acute kidney injury and its progression to chronic kidney disease
Funder: National Institute of Diabetes and Digestive and Kidney Diseases (R01DK124112)
Role: Research Assistant (PI: Siskind) |
| 2017-2019 | Integrated Programs in Biomedical Sciences Fellowship
Funder: University of Louisville School of Medicine |

TEACHING AND MENTORING

- 2021 **Mentoring Academy**
University of Louisville School of Medicine
Louisville, KY
- 2021 **Strategies/Tools for Effective Teaching, Mentoring, & Managing in Science**
University of Louisville School of Medicine
Louisville, KY
- 2020 **Guest Lecture**, PHTX 641: Pharmacology I,
University of Louisville School of Medicine
Louisville, KY
- 2019 **Peer Mentor**, Peer Mentorship Program
University of Louisville School of Medicine
Louisville, KY
- 2014 **Teaching Assistant**, Chemistry 101: Chemistry of Life, Goshen College,
Department of Chemistry
Goshen, IN

Student Mentees

- 2021 Joanna Feng
2020 Gabrielle Oropilla
2019-2020 Andrew Orwick
2019 Aggie Williams

SERVICE AND COMMUNITY OUTREACH

- 2019 **Science Fair Judge**, Meyzeek Middle School Science Fair
Meyzeek Middle School,
Louisville, KY
- 2018 **Bio-Rad Science Ambassadors Program**
Walden School
Louisville, KY

ADDITIONAL TRAINING

- 2020 Introduction to Medical Regulatory Affairs
2019 Risk Assessment

PEER-REVIEWED POSTER PRESENTATIONS

1. **Sears SM**, Dupre T, Doll MA, Shah P, Beverly LJ, Siskind LJ. (October 2020). Neutral ceramidase and autophagy play diverse roles in cisplatin-induced acute kidney injury and fibrosis. American Society of Nephrology Kidney Week, Virtual Event.
2. **Sears SM**, Doll MA, Beverly LJ, Siskind LJ. (October 2020). Renal macrophage infiltration precedes macrophage to myofibroblast transition and T cell recruitment following repeated low dose cisplatin treatment. American Society of Nephrology Kidney Week, Virtual Event.
3. **Sears SM**, Sharp CN, Doll MA, Beverly LJ, Siskind LJ. (February 2020). Renal macrophage infiltration and macrophage to myofibroblast transition accompanies fibrosis and CKD development following repeated low dose cisplatin treatment. Keystone Symposia Fibrosis and Tissue Repair: From Molecules and Mechanics to Therapeutic Approaches, Victoria, BC, Canada.
4. **Sears SM**, Dupre T, Sharp CN, Shah P, Doll MA, Beverly LJ, and Siskind LJ. (September 2019). Characterizing the role of neutral ceramidase in cisplatin-induced kidney injury. University of Louisville: Research!Louisville, Louisville, KY.
5. **Sears SM**, Sharp CN, Saforo D, Doll MA, and Siskind LJ. (October 2018). Neutral ceramidase inhibition as a potential treatment for cisplatin-induced kidney injury. University of Louisville: Research!Louisville, Louisville, KY.
6. **Sears SM**, Pal D, Kolluru V, Damodaran C, and Freedman J. (October 2016). Effects of therapeutic compounds on cadmium-induced prostate cancer. University of Louisville: Research!Louisville, Louisville, KY.